Biological mechanisms in respiratory and limb muscle dysfunction in chronic respiratory conditions: influence of disease severity and body composition

Ester Puig Vilanova

Director:

Dr. Esther Barreiro Portela

UPF Doctoral Thesis / 2014

Department of Experimental and Health Sciences

upf. Universitat Pompeu Fabra Barcelona

A vosaltres:

Eduard, Roser i Sergi

AGRAÏMENTS

Aquesta tesi no hauria estat possible sense la col·laboració de molta gent. Sens dubte, no puc agrair tota l'ajuda rebuda al llarg d'aquests 4 anys amb una simple pàgina! Per tant, aquest apartat només té la finalitat de fer un breu recull de totes les persones que, directament o indirectament, han fet possible aquesta tesi, i de deixar constància de com us estic d'agraïda.

Primer de tot, voldria donar les gràcies a tots aquells que hi han contribuït directament:

A la Dra. Esther Barreiro, per deixar-me formar part del seu grup de recerca i confiar en mi per tirar endavant un projecte i, finalment, tota una tesi! Donar-li gràcies també per tota la tutela rebuda, tant científica com personal, durant aquesta estada al grup.

Gràcies també a tots els membres de l'Hospital del Mar; entre ells el Dr. Lluis Molina i la Mireia així com d'altres companys que també han col·laborat amb part dels experiments de la tesi. Sense la seva contribució, de ben segur que aquest projecte no s'hauria pogut dur a terme.

Haig d'agrair immensament l'ajuda rebuda durant aquests 4 anys a les meves actuals "companyes" de treball: la Mònica, l'Alba i la Mercè; així com a les "excompanyes": la Lluïsa, la Marina, la Noèlia, l'Alba i la Cristina. Totes em vau ajudar en el seu moment i encara ara m'ajudeu en tot el que podeu! Gràcies a totes vosaltres, "companyes", tant per l'ajuda professional com per l'emocional, perquè no només m'heu facilitat el dia a dia, sinó que també m'heu donat una gran amistat que va començar en el seu dia com a "companyes" tot continuant, i de ben segur continuarà, com a grans amigues.

Vull agrair també tota l'ajuda rebuda per la Judith, la Clara, en Cisco i la Carme, els quals han dedicat molt del seu temps a compartir amb mi moltes tècniques i metodologies. Gràcies també als companys dels altres grups, en José Yelamos i la Coral, a la Judith del grup URIE, i a tots els membres de la URTEC, per l'ajuda rebuda sempre que ho he necessitat.

Per altra banda, vull donar les gràcies també a tots aquells que han contribuït d'una manera indirecta en aquesta tesi. La vostra contribució ha estat essencial:

Als companys del gimnàs, i especialment a l'Asún, per ser allà cada matí disposats a escoltar, i amb un somriure per ajudar-me a començar el dia amb plena energia.

Gràcies Ana, Xavier, Kathi, Marina, Ana, Laura, Lorena, Eva, Federico i Joana, pels retrobaments i pels bons moments compartits. Tots junts vam iniciar aquesta etapa amb un màster a Barcelona i de ben segur que continuarem compartint junts molts més bons moments.

Gràcies Rosa per les teves paraules i visió de la vida, sempre a punt fossis on fossis.

Vull donar les gràcies a l'Iris per tota l'ajuda rebuda de forma totalment desinteressada, i per estar sempre disposada a col·laborar en el que fes falta.

També vull agrair a tots els meus amics, en Sergi i la Vane, la Sílvia, tots els de la Conga Catalana, però sobretot a les Nenes, la confiança dipositada en mi. Per creure fermament en el que estava fent tot i no saber massa de què anava, però tot i així, sempre m'heu animat a continuar endavant!

I, finalment, vull donar gràcies a tota la meva família, però especialment a en Costa, i als meus pares, per la immensa paciència que heu tingut durant aquests 4 anys i per estar sempre disposats a fer i entendre el que fes falta!

A tots vosaltres, moltes gràcies!

TABLE OF CONTENTS

ABSTRACT

Skeletal muscle dysfunction and wasting are major comorbidities of chronic obstructive pulmonary disease (COPD) and lung cancer (LC). Despite that the lower limb muscles are usually more severely affected, the respiratory muscles may also experience structural and functional abnormalities in COPD. Muscle dysfunction negatively impacts on the patients' quality of life by impairing their exercise tolerance even of daily life activities. Several molecular mechanisms are involved in the etiology of COPD muscle dysfunction. **Hypothesis:** We hypothesized that oxidative stress may be a trigger of enhanced muscle proteolysis and dysfunction in the limb muscles of cachectic patients bearing two different respiratory conditions such as COPD and LC, and that epigenetic events may be involved in the pathophysiology of COPD muscle dysfunction. **Objectives:** 1) To assess the molecular mechanisms that contribute to muscle dysfunction and wasting in limb muscles of LC and COPD patients, 2) to explore the expression of a wide range of epigenetic events in the diaphragm muscle of COPD patients with a wide range of disease severity, 3) to analyze epigenetic markers in the vastus lateralis (VL) of patients with a wide range of airway obstruction and body composition, and 4) to assess epigenetic mechanisms in the VL of patients with mild–very mild COPD. **Methods:** Study #1: Redox balance, inflammation, cell signaling pathways, and the ATP-ubiquitin proteasome system were explored in VL of LC (N=10) and COPD (N=16) cachectic patients. Studies #2, #3, and #4: MicroRNA expression, levels of total acetylated proteins, histone acetyltransferases (HAT) and histone deacetylases (HDAC), and myocyte enhancer factors (MEF) were evaluated in diaphragm (N=18, study #2) and VL muscles of COPD patients with a wide range of airflow limitation and body composition (moderate, N=11; non-wasted severe, N=18; and muscle-wasted severe, N=12; study #3) (mild, N=13, study #4). Control subjects were also recruited in all studies. Patients and healthy controls were clinically and functionally evaluated before obtaining the muscle specimens. **Results:** Compared to controls; Study #1: limb muscles of LC and COPD cachectic patients showed increased levels of systemic superoxide anion production, muscle and blood protein oxidation, muscle antioxidant enzyme protein content and activity, muscle and blood cytokines and growth factors, redox-sensitive signaling pathways (NF-kB, FoxO-3), E3 ligases and total protein ubiquitination. Study #2: in diaphragm muscles of moderate COPD patients, the expression of myomiRs (miR-1, -133, and -206) was downregulated, while protein levels of HDAC4 and MEF2C were increased. Study #3:

in limb muscles of non-wasted severe COPD patients, the expression of muscle-enriched microRNAs was upregulated, whereas the expression of the same microRNAs was downregulated in muscle-wasted severe COPD patients compared to non-wasted patients. Additionally, in limb muscles of muscle-wasted patients total acetylation levels were increased, while levels of HDAC3 and SIRT-1 were decreased. Study #4: limb muscles of mild COPD patients showed a significant rise in miR-1 expression and increased protein levels of HDAC4. **Conclusions:** We conclude from the four studies that 1) oxidative stress, inflammation, and signaling pathways (NF-kB and FoxO-3) seem to be trigger of enhanced protein degradation in limb muscles of both LC and COPD cachectic patients, 2) in the diaphragm of COPD patients, epigenetic events may act as biological adaptive mechanisms to better overcome the continuous inspiratory loads imposed to the respiratory system in COPD, 3) in the vastus lateralis of patients with severe COPD, epigenetic mechanisms are differentially expressed regardless of the airflow limitation, suggesting that they may regulate muscle activity and mass maintenance, and 4) several epigenetic events are also differentially expressed in limb muscles of early COPD patients, probably as an attempt to counterbalance the underlying mechanisms that alter muscle function and mass.

RESUM

La disfunció muscular esquelètica i la pèrdua de massa muscular són dues manifestacions sistèmiques freqüents en malalties com la Malaltia Pulmonar Obstructiva Crònica (MPOC) i el Càncer de Pulmó (CP). Malgrat que en els malalts amb MPOC, els músculs perifèrics sovint es veuen més greument afectats, els músculs respiratoris també mostren alteracions estructurals i funcionals. La disfunció muscular que pateixen aquests pacients afecta negativament la seva qualitat de vida, no només reduint la seva tolerància a l'exercici físic sinó també a les seves activitats quotidianes. Diferents mecanismes moleculars estan implicats en la etiologia de la disfunció muscular en la MPOC. **Hipòtesi:** La nostra hipòtesi és que l'estrès oxidatiu podria ser un desencadenant de l'augment de proteòlisi i disfunció muscular en els músculs perifèrics de pacients amb caquèxia associada a processos respiratoris com ara la MPOC i el CP. Els mecanismes epigenètics podrien estar també implicats en la fisiopatologia de la disfunció muscular en la MPOC. **Objectius:** 1) Avaluar els mecanismes moleculars que contribueixen a la disfunció muscular i pèrdua de massa muscular en els músculs perifèrics de pacients amb MPOC i CP, 2) Explorar l'expressió de varis fenòmens epigenètics en el múscul diafragma de pacients amb MPOC d'un ampli rang d'obstrucció aèria, 3) Analitzar els marcadors epigenètics en el múscul vast extern (VE) del quàdriceps en pacients d'un ampli rang d'obstrucció aèria i composició corporal, i 4) Avaluar els mecanismes epigenètics en el VE de pacients amb MPOC lleu o molt lleu. **Mètodes:** Estudi #1: L'equilibri redox, la inflamació, les vies cel·lulars de senyalització, i el sistema de degradació proteica ATP-ubiquitina es van explorar en el VE de pacients amb caquèxia deguda al CP (N=10) o a la MPOC (N=16). Estudis #2, #3, i #4: L'expressió de MicroARNs, els nivells de proteïnes acetilades, les histones acetiltransferases (HATs) i les histones deacetilases (HDACs), i els factors potenciadors específics de miòcit (MEF)2 es van avaluar en els músculs diafragma (N=18, estudi #2) i VE de pacients amb MPOC d'un ampli rang de limitació aèria i composició corporal (moderat, N=11; greu sense pèrdua de massa muscular, N=18; i greu amb pèrdua de massa muscular, N=12; estudi #3) (lleu, N=13, estudi #4). En totes els estudis es van reclutar també subjectes control. Tant els pacients com els controls sans es van avaluar clínicament i funcionalment abans de obtenir-ne les mostres musculars. **Resultats:** Respecte dels subjectes control: Estudi #1: els músculs perifèrics dels pacients amb pèrdua de massa muscular deguda al CP o a la MPOC presentaren nivells sistèmics augmentats de producció d'anió superòxid, major

oxidació proteica, tant sistèmica com muscular, major contingut i activitat muscular d'enzims antioxidants, major nivells de citoquines i factors de creixement musculars, nivells augmentats de les vies de senyalització redox (NF-kB, FoxO-3), i un augment dels nivells d'enzims lligases E3 i de la ubiquitinació proteica total. Estudi #2: en el diafragma de pacients amb MPOC moderada, l'expressió de microARNs específics de múscul (miR-1, -133, i -206) estava disminuïda, mentre que els nivells proteics de HDAC4 i MEF2C estaven augmentats. Estudi #3: en els músculs perifèrics de pacients amb MPOC greu sense pèrdua de massa muscular, l'expressió de microARNs enriquits en el múscul estava augmentada, mentre que l'expressió dels mateixos microARNs estava disminuïda en els pacients amb MPOC greu i pèrdua de massa muscular en comparació amb aquells sense pèrdua muscular. A més, en els músculs perifèrics dels pacients amb pèrdua de massa muscular els nivells d'acetilació estaven augmentats, mentre que els nivells de la HDAC3 i el SIRT-1 estaven disminuïts. Estudi #4: Els músculs perifèrics de pacients amb MPOC lleu presentaren un augment en l'expressió de miR-1 i en els nivells proteics de la HDAC4. **Conclusions**: 1) L'estrès oxidatiu, la inflamació, i les vies de senyalització (NF-kB i FoxO-3) semblen ser desencadenants de l'augment de degradació proteica en els músculs perifèrics en pacients amb caquèxia deguda al CP o a la MPOC, 2) Els fenòmens epigenètics podrien actuar com a mecanismes biològics adaptatius en el diafragma de pacients amb MPOC per tal d'afrontar les continues carregues inspiratòries en què està sotmès el sistema respiratori en aquests pacients, 3) En el vast extern del quàdriceps de pacients amb MPOC greu, els mecanismes epigenètics estan diferencialment expressats amb independència de la seva limitació aèria, suggerint així que aquests fenòmens epigenètics podrien estar regulant l'activitat i el manteniment muscular dels pacients amb MPOC, i 4) Diversos mecanismes epigenètics estan també diferencialment expressats en els músculs perifèrics de pacients amb MPOC precoç, probablement com a mesura per a intentar contrarestar els mecanismes subjacents que alteren la funció i massa muscular.

PREFACE

Scientific collaborations

In the current thesis, the investigations have been conducted in the Muscle and Respiratory System Research Unit (URMAR), *IMIM-Hospital del Mar*, in collaboration with researchers from other departments and centers as described below.

Study #1 was in collaboration with the Pulmonology Department at *Hospital del Mar*, Barcelona, Spain, the Pathology Department at *Hospital del Mar*, Barcelona, Spain, and with the Pulmonology Department (ICT) at *Hospital Clinic-IDIBAPS*, Barcelona, Spain.
Study #2 was in collaboration with the Pulmonology Department at *Hospital del Mar*, Barcelona, Spain, and the Thoracic Surgery Department at *Hospital del Mar*, Barcelona, Spain.
Study #3 was in collaboration with the Pulmonology Department at *Hospital del Mar*, Barcelona, Spain, and with the Pulmonology Department (ICT) at *Hospital Clinic-IDIBAPS*, Barcelona, Spain.
Study #4 was in collaboration with the Pulmonology Department at *Hospital del Mar*, Barcelona, Spain.

Publications

The results of the investigation included in the current PhD thesis have been recently submitted in international journals. Additionally, during the four years in the Molecular Mechanisms of Lung Cancer predisposition group, under the supervision of Dr. Esther Barreiro, I had also the opportunity to participate in other studies apart from those that compose the current PhD thesis. Some of these studies have been already published in several international journals.

Study #1- Puig-Vilanova E, Rodriguez DA, Lloreta J, Ausín P, Pascual-Guardia S, Broquetas J, Roca J, Gea J, Barreiro E.
Oxidative stress and redox signaling pathways in cachectic muscles of patients with advanced COPD and lung cancer.
Submitted.

Study #2- Puig-Vilanova E, Aguilo R, Rodriguez-Fuster A, Martínez-Llorens J, Gea J, Barreiro E.
Epigenetic mechanisms in respiratory muscle dysfunction of patients with chronic obstructive pulmonary disease.
Submitted.

Study #3 - Puig-Vilanova E, Martínez-Llorens J, Ausín P, Roca J, Gea J, Barreiro E.
Epigenetic events in the vastus lateralis of patients with severe COPD and muscle atrophy.
Submitted.

Study #4 - Puig-Vilanova E, Ausín P, Martínez-Llorens J, Gea J, Barreiro E.
Do epigenetic events take place in the vastus lateralis of patients with mild chronic obstructive pulmonary disease?
Revised version submitted.

1- Fermoselle C, Garcia-Arumi E, Puig-Vilanova E, Andreu AL, Urtreger AJ, Bal de Kier Joffé ED, Tejedor A, Puente-Maestu L, Barreiro E.
Mitochondrial dysfunction and therapeutic approaches in respiratory and limb muscles of cancer cachectic mice.
Exp Physiol. 2013 Sep;98(9):1349-65. Epub 2013 Apr 26

2- Fermoselle C, Rabinovich R, Ausín P, Puig-Vilanova E, Coronell C, Sanchez F, Roca J, Gea J, Barreiro E.
Does oxidative stress modulate limb muscle atrophy in severe COPD patients?
Eur Respir J. 2012 Oct;40(4):851-62. Epub 2012 Mar 9.

3- Barreiro E, del Puerto-Nevado L, Puig-Vilanova E, Pérez-Rial S, Sánchez F, Martínez-Galán L, Rivera S, Gea J, González-Mangado N, Peces-Barba G.
Cigarette smoke-induced oxidative stress in skeletal muscles of mice.
Respir Physiol Neurobiol. 2012 Jun 15;182(1):9-17.

4- Rodriguez DA, Kalko S, Puig-Vilanova E, Perez-Olabarría M, Falciani F, Gea J, Cascante M, Barreiro E, Roca J.
Muscle and blood redox status after exercise training in severe COPD patients.
Free Radic Biol Med. 2012 Jan 1;52(1):88-94.

Communications

The results of the investigation included in the current PhD thesis as well as those from other studies, which are not included in the thesis, have been previously presented in the form of an abstract at several national and international conferences.

1- Barreiro E, Puig-Vilanova E, Martínez-Llorens M, Pascual-Guardia S, Casadevall C, Gea J.
Differential profile of epigenetic events in diaphragm and limb muscles of COPD patients.
American Thoracic Society (ATS) International Conference, San Diego, May 2014

2- Puig-Vilanova E, Busquets S, Toledo M, Sanchez F, Argiles JM, Gea J, Lopez-Soriano F, Barreiro E.
Redox balance and mitochondrial dysfunction in respiratory and limb muscles of cancer cachectic rats.
The 4th EMBO meeting (Abstract book, page 200), Nice, France, September 2012

3- Barreiro E, Puig-Vilanova E, Ausín P, Sánchez F, Martínez-Llorens J, Curull V, Broquetas J, Gea J.
Patrón diferencial de estrés oxidativo e inflamación muscular en la caquexia asociada al cáncer y a la EPOC.
XIII International Symposium on COPD, Barcelona, Spain, April 2012.

4- Barreiro E, del Puerto L, Puig-Vilanova E, Pérez-Rial S, Sánchez F, Martínez-Galán L, Gea J, González-Mangado N, Peces-Barba G.
Estrés oxidativo en los músculos respiratorios y periféricos en un modelo experimental de enfisema inducido por el humo del cigarrillo.
XIII International Symposium on COPD, Barcelona, Spain, April 2012.

5- Puig-Vilanova E, Marín-Corral J, Sabaté M, Sánchez F, Gea J, Molina L, Barreiro E.
Papel de los antioxidantes y de la inhibición de la proteólisis en la caquexia asociada al cor pulmonale en un modelo experimental.
XIII International Symposium on COPD, Barcelona, Spain, April 2012.

6- Puig-Vilanova E, Marín-Corral J, Sánchez F, Sabaté M, Gea J, Molina L, Barreiro E.
Efecto de los antioxidantes y el bortezomib sobre la proteólisis muscular en un modelo experimental de insuficiencia cardiaca derecha.
Cuartas Jornadas de Formación del CIBERES (Abstract book, page 22), Bunyola, Mallorca, Illes Balears, Spain, October 2011.

7- Barreiro E, Ausín P, Sánchez F, Puig-Vilanova E, Martinez-Llorens J, Curull V, Broquetas J, Gea J.
Role of systemic and muscle oxidative stress and cytokines in patients with lung cancer cachexia.
European Respiratory Society (ERS) Annual Congress. Eur Respir J 2011; 38 (suppl 55). Amsterdam, September 2011

8- Marín-Corral J, Fornaguera C, Sánchez F, Sabaté M, Puig-Vilanova E, Gea J, Molina L, Barreiro E.
Efecto de los antioxidantes y el bortezomib sobre la proteólisis muscular en un modelo experimental de insuficiencia cardiaca derecha.
Arch Bronconeumol 2011; 47 (especial congreso): 96.

9- Puig-Vilanova E, Busquets S, Toledo M, Sánchez F, Argilès JM, Gea J, López-Soriano F, Barreiro E.
Efectos del formoterol sobre el estrés oxidativo, la inflamación, la estructura y el daño muscular en los músculos respiratorios y periféricos de ratas con caquexia.
Terceras Jornadas de Formación del CIBERES (Abstract book, page 26), Bunyola, Mallorca, Illes Balears, Spain, October 2010.

Funding

The research studies included in the current PhD thesis have been supported by: CIBERES; FIS 11/02029; FIS 12/02534; SAF-2011-26908; 2009-SGR-393; SEPAR 2009; SEPAR 2014; FUCAP 2011; FUCAP 2012; and Marató TV3 (MTV3-07-1010) (Spain). Dr. Esther Barreiro was a recipient of the ERS COPD Research Award 2008.

ABBREVIATIONS

ActRIIB: activin receptor type-IIB
ADP: adenosine diphosphate
AIDS: acquired immunodeficiency syndrome
Akt: RAC-alpha serine/threonine-protein kinase
AMP: adenosine monophosphate
AMPK: adenosine monophosphate-activated protein kinase
APR: acute phase response
Atg: autophagy-related gene
ATP: adenosine triphosphate
bHLH: basic-helix-loop-helix
BMI: body mass index
BSA: bovine serum albumin
C8-20S: C8 alpha-subunit of the 20S proteasome
CAT: catalase
CBP: cAMP response element-binding protein
cDNA: complementary deoxyribonucleic acid
CHF: chronic heart failure
CKD: chronic kidney disease
CO_2: carbon dioxide
CoA: coenzyme A
COPD: chronic obstructive pulmonary diseases
CRP: C-reactive protein
CSA: cross-sectional area
CuZn-SOD: copper zinc superoxide dismutase
DLCo: diffusing capacity
DNA: deoxyribonucleic acid
DNP: dinitrophenol
E1: ubiqiutin-activating enzyme
E2: ubiquitin-conjugating enzyme
E3: ubiquitin-ligase enzyme
EDTA: ethylenediaminetetraacetic acid
ELISA: enzyme-linked immunosorbent assay
ERK: extracellular signal-regulated kinase

FEV_1: forced expiratory volume in one second
FFMI: fat free mass index
FoxO: forkhead box O class
FVC: forced vital capacity
GAPDH: glyceraldehyde-3-phosphate dehydrogenase
GDF-8: growth factor differentiation factor-8
GNAT: Gcn5-related N-acetyltransferase
GOLD: global initiative for chronic obstructive lung disease
GSV: globular sedimentation velocity
HAT: histone acetyltransferase
HDAC: histone deacetylase
HKMT: histone lysine methyltransferases
HNF4: hepatocyte nuclear factor 4
HNE: hydroxynonenal
H_2O: water
HRMT: histone arginine methyltransferases
HRP: horseradish peroxidase
IGF-1: insulin-like growth factor 1
IkB-α: nuclear factor kappa-light-chain-enhancer of activated B cells inhibitor-alpha
IKK: I kappaB kinase
IL-1β: interleukin-1-beta
IL-6: interleukin-6
IL-8: interleukin-8
INF-γ: interferon-gamma
JNK: c-Jun NH_2-terminal kinase
KAT: lysine acetyltransferase
K_{CO}: *Krough* transfer factor
LC: lung cancer
LDCL: lucigenin-derived chemiluminescence
MAFbx: muscle atrophy F box
MAPK: mitogen-activated protein kinase
MDA: malondialdehyde
MEF2: myocyte enhancer factor 2
miR: microRNA
miRNA: microRNA

Mn-SOD: manganese superoxide dismutase
MRF: myogenic regulatory factor
Mrf4: muscle regulatory factor 4
mRNA: messenger ribonucleic acid
mTOR: mammalian target of rapamycin
MuRF1: muscle ring finger protein 1
MyHC: myosin heavy chain
MyoD: myogenic differentiation
Myf5: myogenic factor 5
Myf6: myogenic factor 6
MIP: maximal inspiratory pressure
NAD: nicotinamide adenine dinucleotide
NF-kB: nuclear factor kappa-light-chain-enhancer of activated B cells
NT: nitrotyrosine
NSCL: non-small cell lung cancer
$O_2^{\cdot-}$: superoxide anion
p300: E1A binding protein p300
$PaCO_2$: arterial carbon dioxide partial pressure
PaO_2: arterial partial pressure of oxygen
PGC1-α: peroxisome proliferator-activated receptor-γ coactivator 1-alpha
PI3K: phosphoinositide 3-kinase
PRMT: protein arginine methylatransferases
Pdi max: maximal transdiaphragmatic pressure
PVDF: polyvinylidene difluoride
QMVC: quadriceps isometric maximum voluntary contraction
qRT-PCR: quantitative reverse transcription - polymerase chain reaction
RISC: ribonucleic acid-induced silencing complex
RNA: ribonucleic acid
RNS: reactive nitrogen species
ROS: reactive oxygen species
RV: residual volume
SDS-PAGE: sodium dodecyl sulfate – polyacrylamide gel electrophoresis
Sirt1: silent information regulator 1
SMAD: similar to mothers against decapentaplegic
SOD: superoxide dismutase

SR: sarcoplasmic reticulum

SUMO: small ubiquitin-related modifier

SCLC: small cell lung cancer

TGF-β: transforming growth factor-beta

TLC: total lung capacity

TNF-α: tumour necrosis factor-alpha

TNM: tumor, nodes, metastasis classification of malignant tumors

TV: tidal volume

UBL: ubiquitin-like protein

UTR: untranslated region

VEGF: vascular endothelial growth factor

VO_2 peak: peak exercise oxygen uptake

WR peak: peak work rate

XPO5: exportin-5

YY1: yin yang 1

INTRODUCTION

1- Skeletal muscles

The skeletal muscle accounts for approximately 40-50% of human body weight. It is a specialized tissue with the ability to contract and relax due to its internal organized arrangement that confers the characteristic striated appearance. This property of the muscle to contract and relax can be controlled either in a voluntary or involuntary manner depending on the muscle type, with the primarily function to assist to the maintenance of homeostasis and adapt to our needs (1-3).

1.1- Muscle formation, structure and organization

Each muscle of our body is composed for several muscle fascicles which in turn are formed by numerous muscle cells that lie parallel to each other (3). These muscle cells are named muscle fibers or also myofibers due to their elongated and cylindrical shape fiber like, which is usually long as the muscle fiber in which they are contained (4). Muscle fibers are formed by the process of myogenesis, which is divided into two main distinct phases: muscle growth and muscle differentiation. Initially, during the skeletal muscle development, muscle progenitor cells called myoblasts exclusively proliferate, but later on, in the absence of growth factors these myoblasts quits the cell cycle and starts to differentiate and fuse into multi-nucleated fibers called myotubes (3, 5). These two processes of the skeletal muscle development are strictly regulated by a family of transcription factors known as myogenic regulatory factors (MRFs), which are responsible for the regulation of downstream targets required for the terminal differentiation of a myoblast into a functional myofiber (6, 7). Myf5, MyoD, Myogenin and Mrf4, also known as Myf6, are members of the MRFs, which belong to the basic-helix-loop-helix (bHLH) class of transcription factors specifically expressed in the skeletal muscles (5, 6, 8). In order to accomplish their function, these proteins bind to the regulatory region of muscle specific genes and provide a cascade of gene expression (8) that results in a functional myotube (5, 6).

Each muscle fiber is attached to a membrane called Sarcolemma, and has a cytoplasm, which we referred to as Sarcoplasm. Within the sarcoplasm we found the main structures that can be seen under electron microscopy; myofibrils, mitochondria, nuclei and the tubular system (4). Several units of myofibrils composed the muscle

fibers. In turn, each myofibril is formed by two types of filaments; the thick and the thin filaments that correspond to clusters of the contractile proteins myosin and actin respectively (2, 4). The organized arrangement of these two contractile proteins along with the other cytoskeletal proteins confers to the skeletal muscle the characteristic repetitive pattern of light and dark striations appearance. This striated appearance of the myofibril is divided into sarcomeres of 2 um length which are the functional unit of skeletal muscles (3). Within the sarcomere, the pattern of overlap between the myosin and actin proteins creates a variety of zones and bands that can be identified under a microscope by the following characteristics (3, 4) (shown in figure 1):

The Z-line: which is a dense region of proteins that delimitates one sarcomere form the next.

The A-band: which corresponds to the dark stripe and is found in the middle part of the sarcomere thus extending the entire length of thick filament (myosin).

The I-band: which is a less dense area corresponding to the light stripe due to the presence of thin filament (actin) and non-thick filament.

The H-zone: which corresponds to the light area at the centre of a sarcomere, concretely in the middle of A-band. In this region there is no overlapping of the cytoskeletal proteins actin and myosin and only the thick filament is found. Particularly, the width of this zone is diminished during contraction.

The M-region: which is the dark line in the middle of H-zone, is located exactly in the centre of sarcomere and contains the myosin and other supporting proteins (myomesin and creatine kinase) that are critical for organization and alignment of the thick filament.

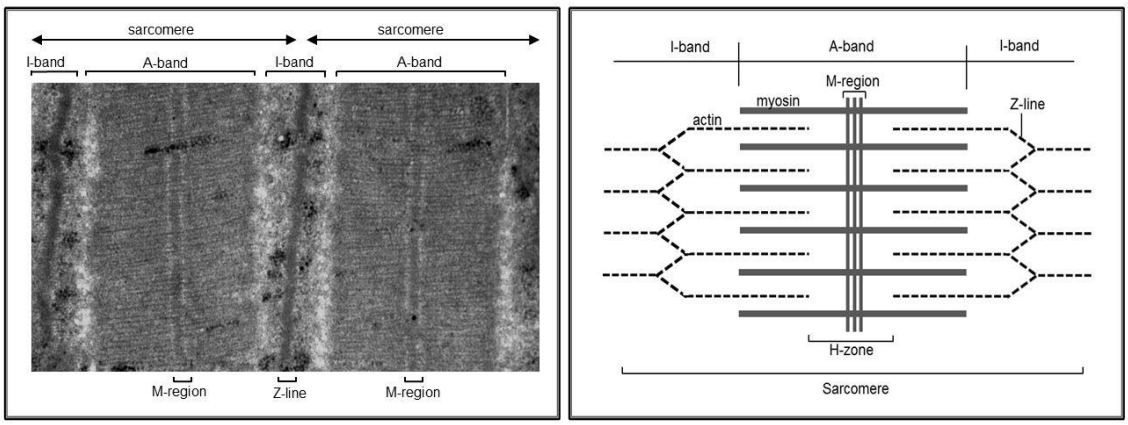

Figure 1: Sarcomere bands from a human vastus lateralis muscle. Image extracted from the *Unitat de Recerca en múscul i aparell respiratòri* (URMAR).

Apart from the presence of numerous myofibrils the muscle fiber is abundant in mitochondria. The mitochondria length is up to 1 to 2 um of diameters and adopts an oval shape within the muscle fibre. Mitochondria are found mainly between myofibrils and are the organelles responsible to form the ATP, the main energy of the living cells. Therefore, mitochondria are required for muscle contraction. Mitochondria produced the ATP from the krebs tricarboxylic acids cycle trough the cytochrom chain and the ATP-synthase by degrading two components that can be found in the cytoplasm of the cell; the glyocogen granules and the lipid droplets. However, mitochondria are also a major source of reactive oxygen species production inside skeletal muscle fibers (3, 9).
Each subunit of muscle is surrounded by connective tissue that adopts different names according to their localization. As shown in figure 2, there are three layers of muscle connective tissue: the epimysium, the perimysium and the endomyisium. While epimysium is the most outer layer surrounding the whole muscle, the perimysium is the sheat of connective tissue that surrounds the muscle fascicle being the endomysium the most indoor sheat of connective tissue surrounding the muscle cell. The role of the connective tissue is to transmit to the tendon and skeleton the action of the contractile proteins in order to effect the movement (2).

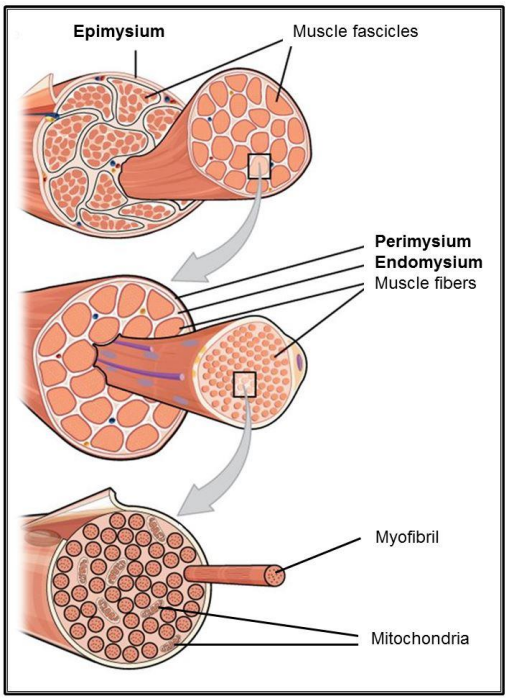

Figure 2: Skeletal muscle tissue organization and connective tissue layers. Image adapted from CNX Anatomy & Physiology (10).

1.2- Muscle function (Diaphragm and Vastus lateralis)

The interactions between myosin and actin filaments lead to the cross-bridge formation and the subsequently cross-bridge cycle or sliding filament theory, the mechanisms by which the myosin produces force causing the filaments to slide and shortens the sarcomere. This ability to contract and relax allows the skeletal muscles to perform three main functions: 1) support the skeleton, 2) allow movements such as locomotion and manipulation of objects, and 3) the vital function of ventilation through the movement of the respiratory muscles (4, 11, 12).

The diaphragm is the main respiratory muscle and a vital organ that trough the continuous involuntary contractions and relaxations assist to the function of adequate gas exchange through the movement of air into and out of the lungs (11, 13, 14).

In contrast, the vastus lateralis is a peripheral muscle exposed to voluntary manner that through contraction make possible movements of daily life such as rise from a position, walking, etc. Most studies focus on the analysis of the vastus lateralis, which is the largest and the most accessible muscle of the quadriceps femoris group of muscles composed by the rectus femoris, vastus medialis, vastus intermedius, and the vastus lateralis, located in the lateral side of the thigh (1, 11, 14).

1.3- Skeletal muscle fiber types

Each muscle can perform different tasks in order to adapt to our needs due to the different types of skeletal muscle fibers that coexist within the same muscle and differ one from another by their structural and functional properties (15, 16). Proportions of each muscle fiber type varies depending on the action of the muscle although in some muscles one or another type of muscle fiber predominates depending upon its requirements (17). In addition, due to its higher plasticity, muscle fiber can convert from one type to another and change its size in response to different stimuli such as exercise, training and environmental factors, which regulate muscle phenotype, both, fiber type composition and fiber size, in order to adapt to the different functional demands (15, 16).

Several muscle fiber classification systems exist due to the different techniques available. Classification can be based on their morphological (red or white colour), physiological (fast or slow speed of contraction), histochemical (mATPase staining and myosin heavy chain (MyHC) isoform) and biochemical characteristics (ATP generation through oxidative or glycolytic pathways) (1, 16). Therefore, human skeletal muscle

fibers are classified into three main types according to their histochemical and biochemical characteristics as illustrated in the following table (Table 1):

Properties	**Human skeletal muscle fiber types**		
MyHC isoform	Type I	Type IIa	Type IIx
Speed of contraction	Slow	Fast	Very fast
Metabolism	Oxidative	Oxidative glycolytic	Glycolytic
Myofibrillar ATPase activity (Force production)	Low	High	Very High
Resistance to fatigue	High	Intermediate	Low
Activity used for	Aerobic	Long term anaerobic	Short term anaerobic
Muscle colour	Red	Intermediate	White
Myoglobin content	High	Medium	Low
Number of mitochondria	High	Medium	Low
Capillary density	High	Intermediate	Low

Table1: Main characteristics of the three types of human skeletal muscle fibers (16, 18).

Type I muscle fibers are the slow-twitch oxidative fibers, characterized by being the smallest in diameter and red due to their large amounts of myoglobin content that confers them the red color. These fibers are supplied with many blood capillaries and mitochondria and generate ATP mainly by aerobic cellular respiration. That is the reason why they are called oxidative fibers. These fibers are also referred to as slow, since the ATP is hydrolysed by the ATPase relatively slowly and consequently the speed of contraction is slow. They are the least powerful type of muscle fibers but they are resistant to fatigue, thus being suitable to low intensity but sustained activities (16, 18).

The **type IIa** muscle fibers, also called fast-twitch oxidative-glycolytic fibers, contain large amounts of myoglobin and intracellular glycogen and many blood capilliaries. Therefore they can generate ATP by both, aerobic cellular respiration and anaerobic glycolysis. They have a faster speed of contraction since the ATPase hydrolizes the ATP three to five times faster than in the slow fibers and have a moderately high resistance to fatigue. These fibers are briefer in duration than slow fibers (16, 18).

The **type IIx** muscle fibers, also called fast-twitch glycolytic fibers, are the largest in diameter and have a white appearance since they have low myoglobin content and

relatively few blood capillaries and mitochondria. In contrast to other types, they contain large amounts of glycogen and generate the ATP mainly by glycolysis. These fibers have the ability to hydrolyze the ATP rapidly so they contract strongly and fast but they come quickly fatigue. This type of fibers is appropriate for intense exercise of short duration (16, 18).

2 – Muscle dysfunction and muscle mass loss

2.1- Definition of muscle dysfunction

Muscle dysfunction is defined by either the loss of at least one of the two main functional properties of the muscle: strength and endurance (11, 14). While **strength** is the capacity of the muscle to generate force through muscle contraction, **endurance** is the capacity of the muscle to maintain that force over time. Both properties depend on muscle characteristics: while strength depends on muscle mass, endurance depends on muscle composition, concretely on the proportion of type I fibers, those more resistant to fatigue. Therefore, the loss of these two properties leads to muscle weakness and fatigue respectively (11, 14, 19, 20).

Several respiratory diseases and malignant conditions including chronic obstructive pulmonary disease (COPD) and lung cancer (LC) are associated with muscle dysfunction and weakness of both respiratory and limb muscles, thus affecting the quality of life of these patients and aggravating the disease itself. Whereas peripheral muscle weakness limits the activities of daily life, leading to inactivity and loss of independence, the loss of respiratory muscle function is critical since implies respiratory muscle weakness and consequently a ventilator insufficiency that may lead to respiratory failure (13, 21-23).

2.2- Cachexia

Cachexia comes from the Greek *kakos hexis*, which literally means bad condition (23, 24). Cachexia is defined as a wasting syndrome commonly observed as a secondary phenomenon (24) that describes the involuntary loss of both adipose and skeletal muscle tissue in the context of chronic or end-stage malignant or infectious diseases (21). However, loss of muscle can occur either as a consequence of several chronic or end-staged diseases such as cancer, COPD, chronic heart failure (CHF), chronic kidney disease (CKD), acquired immunodeficiency syndrome (AIDS), sepsis among others as well as during normal aging (22-24). In the case of cancer, the loss of muscle

mass it is known as cachexia whereas when it is due to the process of normal aging it is known as sarcopenia (21, 22).

Cachexia is a highly prevalent condition ranging from 5 to 15% in COPD patients and 60 to 80% in patients with advanced cancer. These cachectic patients can reach a progressive weight loss, up to 80% along with alterations in body composition and disturbed homeostasis of fat and muscle tissues (23, 24).

In order to diagnose cachexia, the international consensus statement (25) defined that cachexia is present when at least one of the following clinical conditions are found in patients:

• Weight loss >5% over the past 6 months (in absence of simple starvation);

• Body mass index (BMI) <20 kg/m and any degree of weight loss >2%;

• Appendicular skeletal muscle index consistent sarcopenia (males <7.26 kg/m; females <5.45 kg/m; determined by dual energy x-ray absorptiometry and sex-specific defined reference values) and any degree of weight loss >2%

2.3- Conditions associated with muscle dysfunction

2.3.1- Chronic obstructive pulmonary disease (COPD)

Chronic obstructive pulmonary disease (COPD) is described by an airflow limitation that is usually progressive and is not fully reversible (11, 26). Cigarette smoke is the main risk factor for the development of the pathogenesis of COPD that causes a parenchymal destruction of the lungs along with extrapulmonary (systemic) effects that lead to other comorbid conditions, and contribute to the severity of the disease (26, 27). Different symptoms are present during the course of COPD. While chronic cough and sputum are preceded symptoms that can be present many years before of the development of the airflow limitation, progressive dyspnea appears once COPD is present. Throughout the advanced severity of COPD other symptoms such as weight loss, anorexia and other psychiatric morbidities such as depression or anxiety become evident (26).

COPD is a highly prevalent and costly disease (26) that ranks one of the most important causes of death worldwide either consequence of the disease itself of its complications, and is expected to become the third leading cause of death worldwide by 2020 (26, 28).

Several lung function parameters are used to evaluate and monitor disease progression in COPD patients: forced expiratory volume in 1 second (FEV_1), forced vital capacity (FVC), tidal volume (TV), total lung capacity (TLC), and diffusing capacity

(DLCO) (26, 29). Briefly, FEV_1 is the volume of air forcibly exhaled during the first second; FVC is the volume of air that can be forcibly exhaled in the point of maximal inspiration; TV is the volume of air inhaled and exhaled at rest; TLC is the maximum volume of air that can be present in the lungs; and DLCO is the carbon monoxide uptake from a single inspiration usually in 10 sec.

According to the Global Initiative for Chronic Obstructive Lung Disease (GOLD) guidelines (26), these parameters are used to classify the severity of COPD into four stages as follow (Table 2):

Stage I: mild	$FEV_1/FVC < 0.70$ FEV1 > 80% predicted
Stage II: moderate	$FEV_1/FVC < 0.70$ 50% < FEV1 , 80% predicted
Stage III: severe	$FEV_1/FVC < 0.70$ 30% < FEV1 , 50% predicted
Stage IV: very severe	$FEV_1/FVC < 0.70$ FEV_1 < 30% predicted *or* FEV_1 < 50% predicted plus chronic respiratory failure*

Table 2: Spirometric classification of COPD based on post-bronchodilator FEV_1 (26).

*Respiratory failure: arterial partial pressure of oxygen (Pa_{O2}) < 8.0 kPa (60 mm Hg) with or without arterial partial pressure of CO_2 (Pa_{CO2}) > 6.7 kPa (50 mm Hg) while breathing air at sea level.

As above mentioned, COPD is one of the diseases associated with muscle dysfunction and wasting (11). Muscle dysfunction is one of the most studied systemic manifestations of COPD since it affects both respiratory and peripheral muscles. Therefore, it reduces the exercise capacity of these patients and their quality of life (11, 30). Respiratory and peripheral muscles are differentially affected by the diseases severity. These phenotypic differences are due to the different activity pattern that these two groups of muscles perform. Respiratory muscles, and more specifically the diaphragm muscle, is continuously working and thus being overloaded in these patients (30). However, the assessment of quadriceps strength is a good reflector of the disease severity since large evidence has demonstrated that muscle weakness and wasting is a good predictor of mortality among patients with moderate to severe COPD (11, 14, 31, 32).

2.3.2- Cancer

Cancer is a major condition that among other things is also associated with muscle dysfunction and wasting. Unlike COPD, muscle mass loss in cancer is more strikingly evident and called cachexia, whereas in COPD is more frequently used the term wasting to describe the muscle mass loss. Patients with several types of cancer often develop cachexia with or without anorexia (33). However, in lung cancer, the cachexia syndrome is more evident than in other types of cancer (34, 35). Lung cancer is the leading cause of cancer-related deaths worldwide accounting for more than one million people deaths each year (27, 36). In addition, at the time of their diagnosis, approximately the 60% of patients have already experienced considerable body weight loss (33, 37).

Cachexia has been associated with reduce survival and estimated to be the responsible cause of death in 20 to 40% of cancer patients. However, it has also other negative implications; it also increases surgical risk and decreases the response to chemotherapy. Together with a decreased physical function, cachexia really impairs the quality of life of cancer patients (25, 33, 35).

2.4- Biological mechanisms involved in the process of muscle dysfunction and mass loss

2.4.1- Oxidative and nitrosative stress

Reactive oxygen and nitrogen species (ROS and RNS) are highly reactive free radicals containing an oxygen or nitrogen atoms respectively. Both ROS and RNS are products of the normal metabolism and low concentrations are beneficial and even necessary for muscle contraction and force production (9, 14, 38). In contrast, increased levels of ROS and RNS exert harmful effects on muscle by altering enzymes and damaging structural proteins as well as cellular lipids and/or DNA, inhibiting their normal function thus leading to a number of human diseases (11). Oxidative and nitrosative stress occurs when the increased levels of ROS and RNS can not be neutralized by the intracellular antioxidant defenses (9, 11, 14, 31, 39). Therefore, the levels of intracellular antioxidants are essential for health and survival of the organisms (9). The antioxidants enzymes catalase (CAT) and superoxide dismutase (SOD) both the cytosolic (CuZn-SOD) and the mitochondrial (Mn-SOD), are abundantly expressed inside skeletal muscle fibers and play an important role during the redox regulation by counterbalancing the excess of ROS and RNS (9).

Proteins and consequently the structural myofilament proteins of skeletal muscle are the major targets of oxidative stress. The posttranslational modification that they undergo makes them more susceptible to further degradation (40) suggesting a role of oxidative stress in muscle dysfunction and wasting (9, 40). Protein carbonylation along with the final products of lipidic peroxidation malondialdehyde (MDA), 4-hydroxy-2-nonenal (HNE), and 3-nitrotyrosine formation (NT) are important markers of oxidative stress (9, 39-42). The assessment of these markers has been widely studied in our group demonstrating a link between oxidative stress and skeletal muscle dysfunction and wasting of COPD patients (31, 43) in both respiratory (31) and limb muscles (9, 11, 14, 31, 40) as well as in cancer animal models (9, 38, 39).

2.4.2- Inflammation

Inflammation is a physiologic response mediated by different cells and molecules of the organism against aggressions of external agents. Inflammatory response have the objective to defend, aisle and destroy the damaging agents as well as repair the tissue or organ damaged. However, when this response is persistent or excessive, inflammation can become detrimental (44, 45).

During the inflammatory response, different cells become activated, attracted to the injured tissue and deliver different substances such as cytokines and growth factors that are essential for elimination of the detritus and repairing the damaged tissue (44, 45). Inflammation of skeletal muscle can be both a systemic and a local factor. Presence of inflammatory mediators can affect systemic circulation, reaching various organs and tissues, including muscles, and directly damage the muscle structure through affecting the contractile performance of muscle fibers and thus contributing to their dysfunction (11, 46).

Tumor necrosis factor-alpha (TNF-α), interleukin-1-beta (IL-1β), IL-6, IL-8, and interferon-gamma (INF-γ) are the main proinflammatory cytokines produced at the time of systemic inflammatory response. These cytokines have been found to play a role in COPD and cancer muscle wasting and dysfunction (11, 14, 23, 32, 34, 45, 47-50). These cytokines form a complex network that regulates throughout the inflammatory process by activating and removing the inflammatory cells as well as the production and action of other cytokines (45). In addition, they can also activate the acute phase response (APR) proteins such as C-reactive protein (CRP) and fibrinogen (51). Blood levels of CRP are considered a good reflection of systemic inflammation and in turn

can up-regulate the production of other proinflammatory substances (45). Most of these cytokines exert their function by binding to specific extracellular receptors that execute intracellular signaling pathways that results in muscle atrophy and dysfunction (14) through inducing increase protein degradation by the activation of catabolic pathways (11, 14, 45). In addition, evidence shown that oxidative/nitrosative stress and inflammation are related molecular mechanisms that could act cooperatively in the triggering of muscle dysfunction and muscle mass loss since oxidative stress can activate the expression of inflammatory mediators and in turn, inflammation can modulate oxidative stress through the regulation of ROS production levels (11, 14, 39, 48, 52).

However, contradictory results have also been reported regarding the role of proinflamamtory cytokines in muscle (45). Furthermore and probably due to the differences of activity and function of each muscle, the expression of proinflammatory cytokines seems to be differentially expressed between respiratory and limb muscles (32, 50).

2.4.3- Signaling pathways

Cell signaling pathways are responsible for the transmission of information within the cell and coordinate cellular activities. Cell signaling pathways are able to respond either to an external or internal stimulus and generate a cellular response. This signal transduction process usually involves several steps, which in turn; each step amplifies the signal response. Thus one signaling molecule can cause many cellular responses. Usually, the names of these signaling pathways receive the name of the major component of the pathway (53).

Oxidative stress and inflammation are among others, triggers to multiple intracellular signaling pathways that contribute to skeletal muscle atrophy by tipping the homeostatic balance of protein metabolism towards proteolysis (54, 55). The signaling pathways, p38 mitogen-activated protein kinase (MAPK), nuclear factor-KappaB (NF-kB), and forkhead box O class (FoxO) have been shown to be involved in several conditions of muscle wasting (54, 55).

2.4.3.1- Mitogen-activated protein kinase (MAPK) pathway

The MAPK pathway is consists of a complex family of proteins which are divided into four subclasses of signaling proteins: the extracellular signal-regulated kinases (ERKs) 1 and 2 (ERK1/2); the p38 MAPK, the c-Jun NH2-terminal kinase (JNK); and the ERK5

or big MAPK (54, 55). All of them are stimulated by cytokines, growth factors and cellular stress (54) and through a phosphorylation mechanism, they signal to either substrates or transcription factors which are involved in the processes of carbohydrate and fat metabolism, cell proliferation, hypertrophy, apoptosis, and inflammation (54).
Specifically, p38 MAPK subclass is formed by four isoforms (p38-α, p38-β, p38-γ, and p38-δ) of which only the p38-γ isoform, almost exclusively, is expressed in skeletal muscle (54, 55). p38 is mainly involved in inflammation, cell growth and differentiation, cell cycle regulation, cell death, glucose metabolism and energy expenditure (55). The activation of p38 MAPK pathway through oxidative stress stimuli has been shown to upregulate the downstream genes involved in protein degradation (E3 ligase MAFbx /Atrogin-1 and the autophagy-related gene Atg7) participating by this way in muscle wasting through both, the ubiquitin-proteasome and autophagy-lysosome dependent proteolytic mechanisms (56). However, MAPK has also shown to signals upregulation of antioxidant enzymes in order to neutralize free radicals and thus regulating the redox status of skeletal muscle (54). Together, these evidences suggest that there is a link between oxidative stress and proteolysis through the p38 MAPK pathway (55).

2.4.3.2- Nuclear Factor-KappaB (NF-κB) pathway

The Nuclear Factor kappaB (NF-kB) or Rel signaling pathway is composed for 5 proteins named: p50, p52, p65 (Rel A), Rel B and c-Rel. The dimerization of two of them either as homodimers or heterodimers makes them to be able to act as transcription factors by binding to DNA and regulate gene expression. However, each dimer regulate and function differentially depending on the stimulus received (54). In normal conditions, NF-kB is bound to the inhibitory proteins IkappaB-alpha (IkB-α). Various stimulus leads to the activation of Ikappa kinase (IKK), which in turn phosphorylates IkB-α leading them to degradation through the ubiquitin-proteasome system. Only then, the free NF-kB complexes can translocate into the nucleus and influence gene expression to consequently regulate multiple signaling pathways including apoptosis, inflammation and differentiation programs (54).
NF-kB pathway can be activated by ROS and inflammation and its activation is associated with muscle wasting (54, 56). Evidence shown that NF-kB activation up-regulate the expression of the E3 ligases (MuRF-1 and Atrogin-1), which are involved in the breakdown of myofibrillar proteins, as well as in the protein synthesis inhibition (56).

2.4.3.3- Forkhead box O class (FoxO) pathway

Forkhead box transcription factors (Fox) are a family of proteins, which are characterized by a DNA binding domain called Forkhead box (57). In mammals, there are four Fox O class subfamily of proteins: FoxO-1, FoxO-3, FoxO-4 and FoxO-6 (58). FoxO transcription factors regulate various cellular processes such as cell cycle progression, cell size, cell death, cell differentiation, cellular resistance and metabolism (57, 58).

As proteins, FoxO transcription factors can be post-translationally modified by phosphorylation or acetylation resulting in different signaling responses (58). These covalent modifications, as well as protein-protein interactions can modulate the transcription of specific target genes (58).

As a transcription factors, FoxO proteins also shuttle between nucleus and cytoplasm according to the changes in their phosphorylation status (58). Depending to the stimuli that trigger FoxO phosphorylation, it causes opposing effects on FoxO localization; In response to growth factors, the phosphorylation of FoxO proteins causes the exclusion from the nucleus, whereas in response to oxidative stress, FoxO phosphorylation results in a shuttle into the nucleus (58). However, when both stimuli are present, the effect of oxidative stress seems to prevail on the effect of growth factors resulting in a FoxO nuclear localization (58).

The activation of FoxO transcription factors, either FoxO-1 or FoxO-3, lead to the upregulation of the two major proteolytic systems, the ubiquitin-proteasome and the autophagy-lysosomal proteolytic systems through the increased expression of the muscle-specific ubiqutin ligases and the autophagy related genes respectively (55, 56).

2.4.3.4- Myostatin/Activin pathway

Myostatin, also called growth factor differentiation factor-8 (GDF-8), is an extracellular cytokine belonging to the transforming growth factor (TGF) family mostly expressed in skeletal muscle (59, 60). Myostatin regulates muscle growth and it is known to be a negative regulator of muscle mass since a role in the induction of muscle loss was observed in muscle wasting and cachexia (59-61). In addition, upregulation of myostatin was found in muscles of patients with cachexia of different illnesses including cancer and COPD (60, 61). Upon binding to activin receptors (ActRIIB), myostatin signaling regulates muscle growth through the phoshphorylation of transcription factors belonging to the Similar to Mothers Against Decapentaplegic (SMAD) family of proteins that translocate to the nucleus and blocks the transcription of

downstream target genes including MyoD, Myf5 and myogenin among others (61). Myostatin also signals through different pathways such as the p38 MAPK and the ERK1/2, which in turn also down-regulate the myogenesis-related genes (59, 61). A part from the SMAD family of transcription factors, the activation of others transcription factors such as the FoxO signaling pathway has also been found to be increased upon myostatin-activin binding leading to muscle mass loss through an upregulation of the components of the ubiquitin proteasome system (Murf-1 and atrogin-1) and autophagy-related genes (60, 61).

On the other hand, myostatin overexpression has also showed to inhibit the IGF-1-PI3k-Akt pathway in muscle wasting conditions, through the inhibition of the Insulin-growth factor 1 (IGF-1), the main positive regulator of muscle growth responsible for protein synthesis through the downstream kinase mammalian target of rapamycin (mTOR). Together, myostatin signaling involves activation and inhibition of several cellular signaling pathways that result in downregulation of myogenic factors, activation of the ubiquitin proteasome system and a decrease in protein synthesis (59-61).

2.4.3.5- Adenosine monophosphate (AMP)-activated protein kinase (AMPK) pathway

Muscle 5' adenosine monophosphate (AMP)-activated protein kinase (AMPK) is a heterotrimeric complex composed by a catalytic α-subunit and two regulatory β- and γ-subunits (62, 63). This latter has three sites of binding; two of them can bind either AMP or adenosine triphosphate (ATP) whereas the third site already contains a tightly bound AMP molecule (62, 63). Adenosine monophosphate-activated protein kinase is a protein kinase enzyme regulator of cellular energy homeostasis, which in turn also regulates protein synthesis (62, 63). Although increase protein degradation has been widely studied and demonstrated in several muscle wasting conditions, a reduction of protein synthesis has also been shown, thus accounting for the misbalance between protein synthesis and degradation that occurs during the process of muscle mass loss (64).

As a sensor of cellular energy, AMPK is regulated by the intracellular metabolism being activated when the cellular AMP to ATP ratio is increased due to either low ATP production such as glucose deprivation, or increase energy expenditure such as muscle contraction (63). In order to maintain the cellular energy store, AMPK perform their function through the phosphorylation of metabolic enzymes (62, 63).

AMPK increases ATP generation (fatty acid oxidation and glucose transport) while decreases others that consume ATP (lipid and protein synthesis, cell growth and proliferation) (63, 64). Therefore, under normal conditions of energy availability, the decreased levels of AMP inhibit AMPK activation, whereas during conditions of energy restriction, the ATP is hydrolyzed into adenosine diphosphate (ADP) being rapidly converted to AMP through the adenylate kinase reaction. The increased AMP levels lead to AMPK activation (58, 63) resulting in PI3K/Akt/mTOR signaling pathway inhibition and consequently protein synthesis suppression (64). However, if ATP remains depleted, AMPK can also phophsphorylate the transcription factors and co-activators FoxO-3, peroxisome proliferator-activated receptor-γ coactivator (PGC)1-α, E1A binding protein p300 (p300), and hepatocyte nuclear factor 4 (HNF4), that further regulate gene expression (62).

2.4.4- Proteolysis

The process of protein degradation or proteolysis is necessary to maintain the homeostasis through the continually hydrolyses of intracellular and many extracellular proteins, to their forming amino acids, in order to be used for a new synthesis (65). In addition, protein degradation is necessary for the removal of regulatory proteins. This is essential for the control of cell growth and metabolism (65, 66), and also as act of quality control, by selectively eliminating the abnormally folded or damaged proteins for example as consequence of oxygen radicals (65).

Mammalian cells contain multiple proteolytic systems in order to achieve the functions of proteolysis, and these systems need to be highly regulated and precisely balanced in order to prevent excessive breakdown of key proteins (65).

Enhanced protein degradation, has been shown to be the most important mechanism of muscle wasting in a range of catabolic processes including COPD and cancer (23, 48, 56, 65, 67-70). There are three main proteolytic pathways responsible for protein catabolism in skeletal muscle; 1) the calcium activated system, 2) the autophagy-lysosomal system, and 3) the ATP-ubiquitin dependent proteolytic pathway (23, 56, 68, 71). Although evidences show that these three pathways are involved in muscle mass loss, the calcium activated and autophagy-lysosomal systems seems to be principally involved in the cleavage of specific target proteins rather than in the bulk of protein degradation (23, 67); whereas the ATP-ubiquitin proteolytic system is the most relevant proteolotyic pathway involved in the process of muscle wasting and dysfunction through the proteolyisis of contractile proteins (23, 48, 71).

2.4.4.1- ATP ubiquitin dependent proteolytic pathway

The ATP-ubiquitin dependent proteolytic pathway, also shorten as ubiquitin-proteasome pathway, is the responsible to degradate the bulk of intracellular proteins found in the cytosol (65). An upregulation of this pathway has been widely associated with muscle wasting and cachexia (35, 65, 68). The initiation of the proteolytic pathway is the ubiquitination process in which proteins are marked for degradation by ubiquitin moieties and are subsequently recognized and processed in the catalytic core of the ubiquitin-proteasome pathway (48), where proteins are degraded to small peptides (65, 66, 68, 72).

Ubiquitination of proteins is summarized in a cascade of reactions involving at least three different enzymes: the ubiquitin-activating enzyme E1, the ubiquitin conjugating enzyme E2 and the ubiquitin ligase E3 (65, 68). This process detailed below and illustrated in figure 2, is finalized when the proteins marked by a polyubiquitin chain are recognized by the 26S proteasome proteolytic system and degraded in the catalytic core 20S which is a complex composed of four stacked rings surrounding a central cavity that forms a barrel shaped structure (65, 66, 68, 72).

Ubiquitination

The first step in the ubiqutination process of proteins requires the ubiquitin-activating enzyme E1 that utilizes ATP to generate a highly reactive form of ubiquitin, and consequently activate the ubiquitin molecule. The E1-activating enzyme, transfer this ubiquitin activated molecule to the ubiquitin conjugating enzyme E2. E1 is essential for the attachment of the protein substrate to the ubiquitin moieties during next reactions. E2, which is the ubiquitin carrier enzyme, accept the activated ubiquitin molecule and transfer it to the enzyme E3 that is linked to the protein substrate. The E3 enzymes are the determinants of substrate specificity and catalyse the formation of long ubiquitin chains (65) (Figure 3).

E3-ubiqutin protein ligases enzymes muscle atrophy F box (MAFbx) also called atrogin-1, and the muscle RING1 (MuRF1) also known as Trim63 are important for degradation of muscle proteins (68). These two ligases are strictly required for the process to occur (51). In addition, they have also been found to be highly expressed in several catabolic conditions (51, 56, 71). Further progressives rounds of ubiquitin ligation results in the attachment of a polyubiquitin chain in the substrate protein that is the mark for recognition and degradation by the 26S proteasome (23, 65, 68). In this last step, the hydrolysis of ATP is needed again for the proteolytic activity (66, 68).

Once the protein is completely degraded, deubiquitination process takes place resulting in the release of the ubiquitin molecule to further reuse in subsequent proteolytic cycles (23, 65, 68).

Sumoylation

Sumoylation is a highly dynamic and reversible modification similar to ubiquitination that involves a ubiquitin-like protein (UBLs) called small ubiquitin-related modifier (SUMO) protein (73). These proteins are structurally related to ubiquitin and are mainly involved in the regulation of transcription factors (74). There are four SUMO isoforms in mammals able to mediate the process of sumoylation: SUMO-1, SUMO-2, SUMO-3 and SUMO-4 (74). The small ubiquitin-related modifier 2 and 3 are highly related proteins, which differ from one another by only three N-terminal residues, and appear to be functionally redundant. In addition, SUMO2/3 are 50% identical in sequence to SUMO1 (73, 75, 76).

As ubiquitin moieties, SUMO is attached to lysine residues in target proteins (74) and the conjugation cycles can be repeated to produce polymeric chains (73). In an analogous way to ubiquitination, SUMO is activated by the E1-SUMO activation enzyme and transferred to the E2-SUMO conjugation enzyme, which mediates the further conjugation of SUMO to the substrate by a specific E3-SUMO ligase (74-77) (Figure 3).

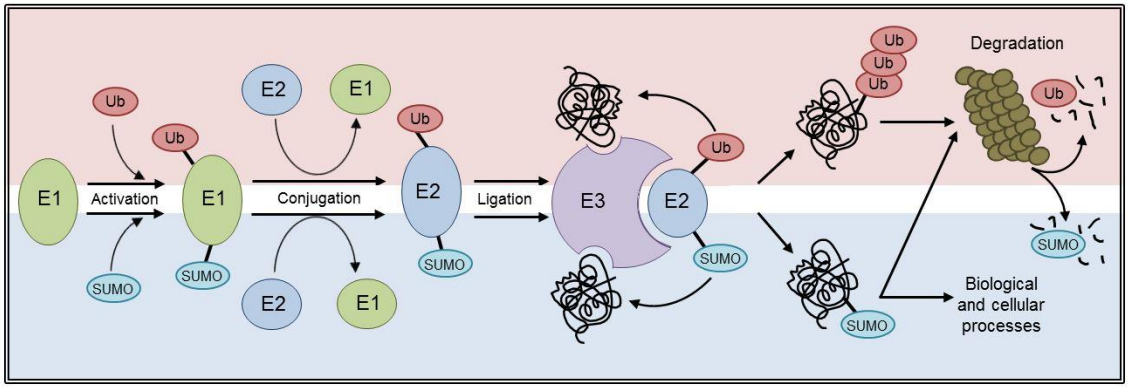

Figure 3: Steps of protein ubiquitination (top) and protein sumoylation (bottom).

Despite the similarities between the sumoylation and the ubiquitination process, the functional consequences of these two modifications are quite different. Unlike ubiquitination, whose primary function is to target proteins for degradation, sumoylation has been involved in many biological and cellular processes including; protein-protein

interactions, protein stability, cellular localization, DNA-binding, and control of gene expression (74-77). Target proteins of sumoylation are mainly transcription factors and it seems to have a negative effect on their expression thus promoting gene repression (74, 76). Members of the myocyte enhancer factor 2 (MEF2) family of transcription factors, MEF2C and MEF2D, are examples of target proteins which are repressed through sumoylation by SUMO-2 and SUMO-3. Consequently, the expression of muscle-specific genes required for myogenesis is also being repressed (74).

However, recent findings suggest that SUMO, like ubiquitination can target proteins to degradation through signaling for the recruitment of E3 ubiquitin ligases, which leads to the ubiquitination and degradation of the modified protein (75). It remains unclear, what is the signal that triggers ubiquitination of the SUMO modified protein. It was suggested that an important determinant could be the length of SUMO chains (75), which is regulated by SUMO-specific isopeptidases that are the responsible of deconjugating and remove the SUMO moieties (74, 77).

2.4.4.2- Autophagy-lysosomal pathway

The Autophagy-Lysosomal pathway is mainly responsible for the degradation of extracellular proteins and cell surface receptors that are taken up by endocytosis and completely degraded within lysosomes (78-80). These organelles contain several acid proteases including the cysteine proteases cathepsins (B,H,L and D) and many other hydrolases (carbohydrases, lipases, and nucleases) required for the digestion of macromolecules (56).

There are three types of autophagy; 1) the macroautophagy, 2) microautophagy and 3) chaperone-mediated autophagy. Nonetheless, the word “autophagy” is commonly used to refer to macroautophagy (79).The autophagy process consists in the sequestration of proteins into an autophagosome, the transport of these proteins to lysosomes and their degradation into amino acids or peptides for further re-utilization (78-80). Since autophagy is the engulf of a portion of cytoplasm through the autophagosomes, this degradation systems seems to be nonselective compared to the specificity of the ubiquitin-proteasome system, which specifically recognizes the ubiquitinated proteins (78-80). Although it remains unclear if the degradation activity of autophagy is harmful or in contrast a compensatory mechanism for cell survival, excessive autophagy triggered by nutrient starvation and insulin growth factor signals, has been reported to promote severe muscle wasting (78-80). However, several other factors such as ROS, calcium, and AMPK seem to be also involved in the induction of autophagy (79, 81).

2.4.4.3- Calcium activated system

The calcium-activated system is an ATP independent proteolytic process that is regulated by the cysteine proteases called calpains. There are two forms of calpains, I and II, which differ in their affinity for Ca^{2+} (65). Calpains are involved in tissue injury, necrosis and autolysis (23, 35, 48) and have been implicated in the initial degradation of myofibrillar proteins during muscle wasting together with the ATP-ubiquitin dependent proteolytic pathway (71).

Apart from these three main proteolytic systems detailed above, there are also other systems of protein degradation within the cell such as the cytosolic proteases called Caspases and mitochondrial proteases (65). On one hand, caspases are activated in response to a variety of toxic stimuli, and are involved in the apoptotic pathway leading to a programmed cell death (65). On the other hand, mitochondrial proteases are located within the mitochondrial matrix where, the protein turnover of these organelles is regulated by the ATP-dependent pathway (65). However, the calcium activated system does not involve the intermediate step process of ubiquitination (65).

2.4.5- Epigenetic mechanisms

Epigenetics are the heritable changes that regulate gene expression without affecting the DNA sequence (82). These changes may be induced spontaneously or in response to environmental factors and are maintained through meiosis and transmitted from one generation to the next (83-85). Our genome is packaged within the cell as chromatin. Chromatin is the complex of DNA and histones that forms the functional unit nucleosome which in turn, is composed by 147 base-pairs of DNA that are wrapped around an octamer of the two of each four core histones H2A, H2B, H3 and H4 (85, 86). Chromatin can be modified depending on the environment, thus regulating the tightness of the packing DNA to histones (83). Depending on this tightness, the chromatin can be divided into heterochromatin, which is a highly packed and condensed region, and euchromatin, which is a more relaxed genomic region (83, 85-87). While heterochromatin is usually associated with gene repression, due to their higher level of compactness that difficult the accessibility to the transcription factors, euchromatin contains principally the active genes since transcription factors are able to access it more easily and therefore activate transcription (87).

Epigenetic regulation of gene expression comprises several mechanisms: 1) modifications to DNA; of which DNA methylation is the most studied and stable DNA

modification of chromatin structure, associated with gene silencing (82, 83, 86); 2) modifications to histones, which comprehend: methylation, acetylation, phosphorylation, ubiquitylation, sumoylation, deamination, ADP ribosylation and proline isomerization; despite, the highly abundance of histone tail modifications that make easier the crosstalk between them, histone methylation and acetylation are the best known post translational chromatin modifications and the central mechanisms in the control of skeletal muscle development and gene expression that seems to act synergistically to either activate or repress transcription of muscle genes (83, 85, 88); 3) noncoding RNAs such as microRNAs; and 4) histone variants (82). These modifications are very dynamically controlled by chromatin-modyifing enzymes that act through two main mechanisms to accomplish the modification (85, 86): i) through the alteration of chromatin structure and thereby chromatin accessibility to transcription factors, or ii) by recruiting additional DNA interacting proteins with enzymatic activities (chromatin modifiers and remodelling enzymes) which further modify the chromatin (83, 85, 86, 89, 90).

Recent evidence suggests that these epigenetic mechanisms could play a relevant role in the process of muscle wasting and dysfunction (82).

2.4.5.1- Histone modifications

Histone methylation

Histone methylation can occur at the side chain of both lysine and arginine residues, which can accept up to two and three methyl groups respectively (82, 87). The addition of these methyl groups does not directly alter the chromatin folding since they do not modify the charge of amino acid; however, it can mediate the recruitment of proteins to chromatin that can either activate or repress gene transcription (82, 83, 87, 91). Histone lysine methyltransferases (HKMT) and Histone arginine methyltransferases called protein arginine methylatransferases (PRMT) are the enzymes responsible to mediate lysine and arginine methylation respectively (85, 87). Their output can be either activation or repression of transcription. However, some specific methylation sites are associated with one or other (85). Among them, the best-known histone methylation marks of muscle cells are: methylation of H3K4, H3K36 and H3K79 which are implicated in activation of transcription and methylation of H3K9, H3K27 and H4K20 which in contrast are associated with transcriptional repression (83, 85, 92).

In contrast, demethylases are the opposing enzymes whose function is to remove the methyl groups having important roles in various cellular processes in which a switch in gene expression is required (85, 87).

Histone acetylation

Histone acetylation is the most frequently found post translational modification of histones, in which an acetyl group from the acetyl-CoA is transferred to an epsilon-amino group of a lysine residue within a histone tail (82, 87, 93). The addition of this acetyl group, can act through two different mechanisms that lead to the same final scenario: an increase in gene expression. The first mechanism of action is through the weakening of interactions between histones and DNA with nucleasomes that result from the neutralization of the positive charge of the lysine residue as a consequence of the acetyl group addition. Such alteration results in a conformational change in the structure of the histone towards a more open chromatin (euchromatin) as well as in the recruitment of remodelling enzymes to specific regions of the chromatin (82, 83, 85, 94, 95). In contrast, deacetylation reverses this process, through the restoration of the positive charge of lyisine, hence resulting in a close chromatin structure (heterochromatin) that is transcriptionally blocked (82, 83, 85, 92).
Two families of enzymes; the histone acetyltransferases (HATs) and histone deactylases (HDACs) control the modulation of these opposing processes (82, 87, 88).The interplay between these two families of enzymes, ensure that acetylation is a transient and a dynamic alteration (83, 88).

Histone acetyltransferases (HATs) which are also referred to as lysine acetyltransferases (KATs) are the responsible to mediate the addition of the acetyl group into the lysine target residue. They are divided into three main families; GNAT, MYST and CBP/p300 (85). These enzymes are often associated with large mutliprotein complexes that play an important role in controlling enzyme recruitment, activity and specificity (87). For example, the nuclear cofactor p300 has been implicated in the development of muscle wasting through the acetylation of histone and non-histone proteins such as the transcription factors NF-kB and FoxO which are involved in the degradation of proteins (94).

Histone deacetylases (HDACs) are the enzymes that carry out the opposing effect, thus blocking transcription and promoting gene repression by removing the acetyl group of the lysine residues. To date, there are 18 HDACs classified into four classes (82, 85, 87, 92): Class I comprises the HDAC members 1,2,3 and 8 which are located primarily in the nucleus and are ubiquitously expressed (88). Class IIa is formed by the HDAC members 4,5,7 and 9, which are able to shuttle in and out of the nucleus and are found to be expressed in high levels in heart, skeletal muscle and brain tissues (88). Class IIb includes the members HDAC6 and 10 which are located in the cytoplasm and distributed primarily in liver and kidney tissues (88). Class III or also called Sirtuins is constitued by the members silent information regulator (Sirt)1,2,3,4,5,6 and 7 which are nicotinamide adenine dinucleotide (NAD)-dependent enzymes that requires NAD^+ as specific cofactor for their activity (88, 96). Lastly, class IV, only formed by HDAC11, is able to shuttle in and out of the nucleus and it is also found in various tissues including skeletal muscle (88, 96).

These enzymes have low substrate specificity, being capable of deacetylating multiple sites within histones (87). Therefore, they are involved in multiple signaling pathways by repressing chromatin complexes (82, 85). One member of the Class III, silent information regulator 1 (Sirt1), is an important master enzyme involved in controlling gene expression of active metabolic tissues and regulates multiple cellular functions and biological processes such as differentiation of cultured skeletal muscle cells, satellite cell proliferation, and senescence among others (62). Sirt1 acts through the deacetylation of transcription factors that can either increase or decrease their transcriptional activity depending on the target gene. Therefore it has been shown to inhibit muscle atrophy and promoting muscle growth through blocking the activity of the transcription factors FoxO-1 and 3 (97, 98). In this regard, the HDAC activity of Sirt1 along with the other HDAC members, 3 and 6, have been found downregulated in muscle wasting conditions (99).

Furthermore, HATs and HDACs also act cooperatively with the families of transcription factors myogenic bHLH and MEF2 in order to either activate or repress the expression of skeletal muscle genes (83, 88, 100, 101). The transcription factors MEF2C and MEF2D, which participate in muscle differentiation, are found downregulated in muscle wasting conditions. In contrast, the transcription factor Yin Yang 1 (YY1), which is a repressor of gene expression implicated in the muscle regeneration and in the shift of muscle fiber type, is found upregulated in muscle wasting conditions (102).

2.4.5.2- MicroRNAs

MicroRNAs (miRNAs) are noncoding single-stranded ribonucleic acids of approximately 22 nucleotides long, that play a role in gene expression through transcriptional and translational regulation through targeting the transcripts in the cytoplasm (82, 103). miRNAs inhibit protein translation or enhance mRNA degradation through base-pairing with complementary sequences of targets mRNAs (82, 103, 104). The efficacy of miRNA on mRNA degradation depends on its binding capacity which is usually located in the 3 untranslated region (UTR) of the target mRNA. The binding between miRNA-mRNA target molecules can be perfectly paired leading to degradation or imperfectly paired promoting gene repression of the target transcript (103, 105). The process of gene regulation through miRNA is complex since miRNAs have multiple gene targets (mRNA) which in turn can be regulated by multiple miRNAs (103). Thereby miRNAs are implicated in numerous processes including the control of muscle mass and in the regulation of muscle phenotype (82, 103, 104).

The process of miRNAs formation (see figure 4), involves the action of several enzyme activities (105); miRNAs are firstly transcribed in the nucleus by the RNA polymerase II. These primary transcripts have several kilobases long and are known as pri-miRNAs. Further cleaved by the RNAse III endonuclease Drosha, pri-miRNAs are called pre-miRNAs, which are the intermediate precursor of approximately 60-70 nucleotides long. Once the pre-miRNA is processed, the protein Exportin-5 (XPO5) transports the pre-miRNA from the nucleous to the cytoplasm where a second RNAse III endonuclease known as Dicer, cleaves the pre-miRNA into the double stranded RNA of 22 nucleotides miRNA. This double strand miRNA is further separated by RNA helicases and the single-stranded mature miRNA is then incorporated into the RNA-induced silencing complex (RISC) and further binding to the 3 or 5’ UTR of the complementary target mRNA (103-106).

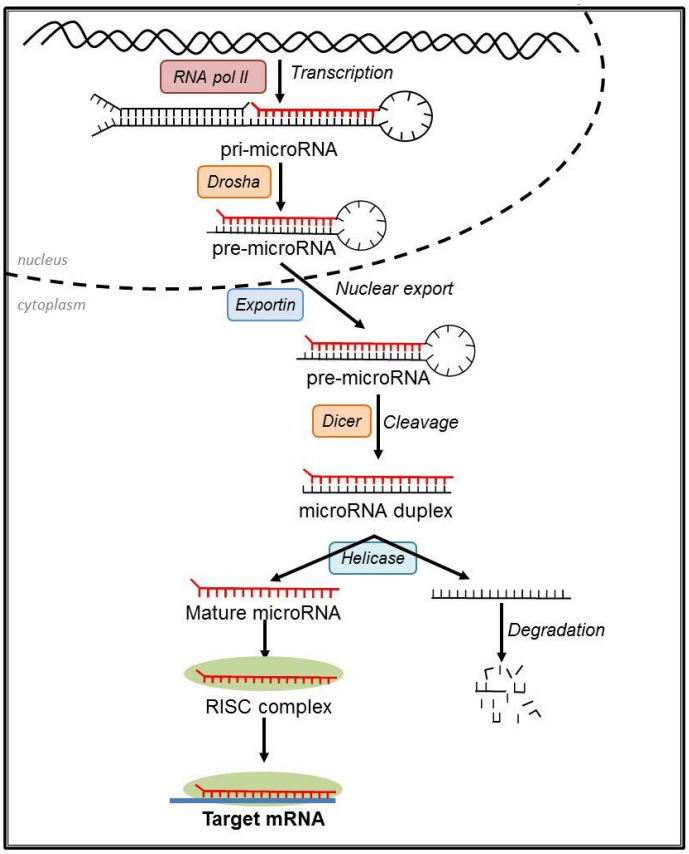

Figure 4: Formation of miRNAs.

Some miRNAs are tissue specific and those abundantly expressed in skeletal muscles are known as muscle-specific miRNAs or also named myomiRs (82, 103, 105). miR-1, miR-133a, miR-133b, miR-206, miR-208, miR-486 and miR-499 are these muscle-specific miRNAs and among them, miR-1, miR-133 and miR-206 are the most widely studied myomiRs which in turn are arranged from biscistronic clusters and transcribed together (103, 105, 107). Other miRNAs, such as miR-27, miR-29 and miR-181 are considered non-specific muscle miRNAs besides are also found to be expressed in skeletal muscle tissue (103, 105).

The regulation of these miRNAs is controlled by the myogenic regulatory factors (MRFs) as well as the family of transcription factors myocyte enhancer factor 2 (MEF2) (103, 105). Due to their regulatory relationship with MRFs, miRNAs have been involved in myogenesis as well as in many other cellular and molecular processes such as muscle fiber type, muscle atrophy and hypertrophy, muscle regeneration and muscle disease and dysfunction (82, 103). During the myogenic process, miR-1, miR-206, miR-181, miR-27, and miR-29 participate in the differentiation program. In contrast the miR-133 expression inhibits the myotube formation and promotes myoblast

proliferation (103). In addition, all except miR-29 also participate in muscle regeneration (103). Other aspects of muscle phenotype are also controlled by these myomiRs; miR-1, 133 and 206 contribute to regulation of muscle hypertrophy and atrophy while the miR-208 and 499 controlled the muscle fiber type and muscle performance (103).

There are multitude of possible interactions between transcription factors, miRNAs and their target genes (104). Consequently, an aberrant regulation of some of these myomiRs can disrupt intracellular signalling networks, which may result in pathological conditions (103). Recent studies shown that miRNA dysregulation appears to have a role in the pathogenesis of LC and COPD associated with muscle wasting (105, 108). Specifically, the expression of miR-1 has been found reduced in the quadriceps muscle of COPD patients (109). Since miRNA are essential regulators of skeletal muscle health, their implications in chronic diseases associated with muscle wasting and dysfunction are primordial (105).

HYPOTHESIS

Skeletal muscle dysfunction and/or muscle mass loss are common systemic manifestations associated with different conditions such as COPD and cancer. Muscle mass loss as a consequence of enhanced proteolysis may be triggered by different molecular events, namely oxidative stress and inflammation. Evidence shows that ATP-ubiquitin proteasome system is a major proteolytic pathway responsible for the degradation of muscle contractile proteins. Signaling pathways such as MAPK, NF-kB, FoxO, and AMPK may participate in the enhanced proteolysis of skeletal muscle proteins.

A variety of transcription factors such as the myogenic myocyte enhancer factor 2 (MEF2) family of proteins participate in the control of muscle formation (myogenesis) and repair after injury. Moreover, epigenetic mechanisms such as microRNAs and histone acetylation and deacetylation may regulate skeletal muscle phenotype as well as muscle mass maintenance. A reduction in muscle-enriched microRNA expression and an imbalance of histone acetylation/deacetylation towards hyperacetylation have been demonstrated in different animal models of muscle dysfunction and atrophy. Additionally, SUMOylation, a reversible post-translational modification whereby SUMO peptides are conjugated to protein substrates, seems to have a role in premature senescence of muscle satellite cells. Therefore, SUMOylation could also be involved in the process of muscle dysfunction and wasting in patients with chronic conditions such as in COPD, as in most of instances, they are elderly subjects.

In the current thesis, we hypothesized that oxidative stress may also be a trigger of enhanced muscle proteolysis and dysfunction in the limb muscles of patients with muscle wasting bearing two different respiratory conditions: COPD and lung cancer (LC). Moreover, we also hypothesized that epigenetic mechanisms may regulate muscle mass and function in patients with COPD of a wide range of body composition and disease severity (airway obstruction, from mild to advanced COPD). Finally, we also hypothesized that the expression of epigenetic events may also differ between respiratory (diaphragm) and limb muscles (vastus lateralis of the quadriceps) in patients with COPD of different disease severity.

OBJECTIVES

The current thesis is divided into four different studies, in which we focused on different aspects of the process of muscle dysfunction and wasting in patients with different respiratory conditions. Specifically, in the first study the objectives were to identify in the lower limb muscles of patients with two different respiratory conditions (COPD and LC), molecular mechanisms such as redox balance, inflammation, ATP-ubiquitin proteasome system, and myostatin, which have already been shown to contribute to muscle dysfunction and mass loss in other models. We also aimed to explore the similarities and/or differences in these molecular mechanisms between the two different types of patients. The second, third, and fourth studies were designed to evaluate several relevant epigenetic mechanisms: microRNAs, acetylation and deacetylation of histones, and total acetylated proteins in the diaphragm and vastus lateralis of COPD patients with different degrees of COPD severity and body composition. Moreover, muscle-specific transcription factors, and SUMOylation events were also assessed in the muscles of the same patients.

In this regard, the specific objectives of each study were as follows:

1- Specific objectives of study #1:

In control subjects and patients with COPD cachexia and LC cachexia:

1) To evaluate the patient characteristics: clinical, analytical, and both lung and muscle functions

In the vastus lateralis of healthy controls and in both groups of patients:

2) To assess muscle phenotype:
    a. Size and composition of the different muscle fiber types
    b. Muscle structure abnormalities
    c. Ultrastructural abnormalities of the sarcomere
3) To explore the expression of molecular mechanisms involved in muscle wasting and dysfunction:
    a. Oxidative stress and antioxidant markers
    b. Inflammatory cytokines and growth factors
    c. Signaling pathways: MAPK, NF-kB, FoXO, and AMPK
    d. ATP-ubiquitin-proteasome system: E3-ligases (Atrogin-1 and MuRF-1), C8-20S, and total ubiquitinated proteins
    e. Myostatin and myogenin proteins

In the blood of healthy controls and both groups of patients:

4) To determine:
    a. Oxidative stress and antioxidant mechanisms
    b. Inflammatory cytokines and growth factors

5) In both groups of patients: to analyze the potential correlations between clinical, analytical, functional, and structural parameters, and the different molecular markers analyzed in both compartments

2- Specific objectives of study #2:

In control subjects and COPD patients with different degrees of airflow obstruction:

1) To evaluate the patient characteristics: clinical, analytical, and both lung and muscle functions

In the diaphragm muscle of both patients and control subjects:

2) To determine the muscle phenotype (fiber type composition and size)
3) To analyze the following epigenetic mechanisms:
    a. microRNAs
    b. Histone acetylation and deacetylation and total acetylated proteins
4) To assess the levels of muscle-specific transcription factors
5) To explore the expression of SUMOylation events
6) In the COPD patients: to explore the potential correlations between clinical, analytical, functional, and structural parameters, epigenetic markers, muscle-specific transcription factors, and SUMOylation events

3- Specific objectives of study #3:

In control subjects and patients with moderate and severe COPD and different body composition:

1) To assess the patients characteristics: clinical, analytical, and both lung and muscle functions

In the vastus lateralis muscle of these patients and control subjects:

2) To determine the muscle phenotype (fiber type composition and size)
3) To analyze the expression of the following epigenetic mechanisms:
    a. microRNAs
    b. Histone acetylation and deacetylation and total acetylated proteins
4) To assess the levels of muscle-specific transcription factors
5) To explore the expression of SUMOylation events
6) To evaluate a potential differential pattern of expression of the different epigenetic markers in the vastus lateralis of patients with different degrees of airway obstruction (moderate, severe, and very severe) and body composition
7) In each group of COPD patients: to explore the potential correlations between clinical, analytical, functional and structural parameters, epigenetic markers, muscle-specific transcription factors, and SUMOylation events

4- Specific objectives of study #4:

In control subjects and patients with mild COPD:

1) To evaluate the patients characteristics: clinical, analytical, and both lung and muscle functions

In the vastus lateralis muscle of both patients and controls:

2) To assess muscle phenotype (fiber type composition and size)
3) To determine the levels of expression of the following epigenetic mechanisms:
    a. microRNAs
    b. Histone acetylation and deacetylation and total acetylated proteins
4) To assess the levels of muscle-specific transcription factors
5) To explore the expression of SUMOylation events
6) In the COPD patients: to explore the potential correlations between clinical, analytical, functional and structural parameters, epigenetic markers, muscle-specific transcription factors, and SUMOylation events

METHODS

The different methodologies used in the four studies are summarized below (Table 3). Moreover, more details on the specific methodologies used in each study are also being described right after.

Study Subjects

	Control subjects	Patients	
		Non-wasted patients	Muscle-wasted patients
Study #1	N= 10		COPD, N= 16 LC, N=10
Study #2	N= 10	Mild COPD, N= 9 Moderate COPD, N= 6 Severe COPD, N= 3	
Study #3	N=19	Moderate COPD, N= 11 Severe COPD, N= 18	Severe COPD, N= 12
Study #4	N=13	Mild COPD, N=13	

Patient Assessment (for the four studies)

Anthropometrical and blood analytical parameters

Body mass index (BMI), fat free mass index (FFMI), albumin content, total protein content, C reactive protein (CRP), fibrinogen, and globular sedimentation velocity (GSV)

Functional capacity parameters

Lung function testing	*Dynamic lung volumes*: Forced expiratory volume in one second (FEV1), forced vital capacity (FVC) *Static lung volumes*: residual volume (RV), total lung capacity (TLC) *Diffusion capacity*: carbon monoxide transfer (DLco), *Krough* transfer factor (K_{CO}) *Gas exchange:* arterial pressure of oxygen (PaO_2) and carbon dioxide ($PaCO_2$)
Exercise capacity	Peak exercise oxygen uptake (VO_2 peak), peak work rate (W*R* peak) and six minute walking test
Muscle strength	Respiratory muscles: maximal inspiratory pressure at the mouth (MIP) Limb muscles: isometric maximum voluntary contraction of the quadriceps (QMVC)

Samples

	Muscle biopsy	Blood sample
Study #1	Vastus lateralis	Yes
Study #2	Diaphragm	Yes
Study #3	Vastus lateralis	Yes
Study #4	Vastus lateralis	Yes

Molecular biology techniques

	Molecular and cellular events	
Study #1	Enzyme-linked immunosorbent assay (ELISA)	Levels of total oxidized proteins, TNF-α, IL-1β, IFN-γ, VEGF and TGF-β
	Lucigenin-derived chemiluminescence	Superoxide anion production
	Enzyme activity assay (by absorbance)	Superoxide dismutase (SOD) and catalase antioxidants levels
	Histochemistry / Histology & Optical / Electron microscopy	Muscle size and composition of muscle fiber types I and II Muscle damage Ultrastructural damage of sarcomere
	1-D gel electrophoresis and immunoblotting *(see table 1 for specific antibodies)*	Oxidants and antioxidants Signaling pathways Proteolysis Muscle growth factors Structural proteins
	Epigenetic events, muscle-specific transcription factors, and SUMO expression	
Studies #2, #3 & #4	Histochemistry & Optical microscopy	Muscle size and composition of muscle fiber types I and II
	Taqman based qPCR reactions (real-time PCR)	MicroRNA expression: miR-1, -133, -206, -486, -27a, -29b, -181a Gene expression: p300, SUMO2, SUMO3
	1-D gel electrophoresis and immunoblotting *(see table 4 page 38 for specific antibodies)*	Total protein acetylation levels Histone deacetylases Muscle-specific transcription factors

Statistical Analyses		
	Clinical, biological and functional variables	**Correlations**
Study #1	ANOVA+Tukey's post hoc test Mann-Whitney test	Spearman's correlation coefficient
Study #2	T-test	Pearson's correlation coefficient
Study #3	ANOVA+Tukey's post hoc test T-test	Pearson's correlation coefficient
Study #4	T-test	Pearson's correlation coefficient

Table 3. Summary of the methodologies used in the four studies.

	Biomarker	Company	Study used
Oxidants	MDA-protein adducts	Academy Bio-Medical [1]	Study #1
Antioxidants	Mn-SOD	Santa Cruz [2]	Study #1
	Cu/Zn-SOD	Santa Cruz [2]	Study #1
	Catalase	Calbiochem [3]	Study #1
MAPK signaling pathway	ERK 1/2	Santa Cruz [2]	Study #1
	p-ERK 1/2	Santa Cruz [2]	Study #1
	p38	Santa Cruz [2]	Study #1
	p-p38	Santa Cruz [2]	Study #1
NF-kB signaling pathway	NF-kB p50	Santa Cruz [2]	Study #1
	p-NF-kB p50	Santa Cruz [2]	Study #1
	NF-kB p65	Santa Cruz [2]	Study #1
	p-NF-kB p65	Santa Cruz [2]	Study #1
	IkB-α	Santa Cruz [2]	Study #1
	p-IkB-α	Santa Cruz [2]	Study #1
FoXO signaling pathway	FoXO-1	Millipore [4]	Study #1
	p-FoXO-1	Santa Cruz [2]	Study #1
	FoXO-3	Acris [5]	Study #1
	p-FoXO-3	Bioworld [6]	Study #1
AMPK signaling pathway	AMPK	Cell Signaling [7]	Study #1
	p-AMPK	Cell Signaling [7]	Study #1
Proteolysis	C8-20S	Biomol [8]	Study #1
	Atrogin-1	Santa Cruz [2]	Study #1
	MURF-1	Everest Biotech [9]	Study #1
	Ubiquitin	Boston Biochem [10]	Study #1
Muscle growth & differentiation	Myostatin	Bethyl [11]	Study #1
	Myogenin	Santa Cruz [2]	Study #1
Structural proteins	Myosin (clone A4.1025)	Upstate-Millipore [12]	Study #1
	Creatine Kinase	Santa Cruz [2]	Study #1
Acetylation	Lysine acetylation	Santa Cruz [2]	Studies #2, #3 & #4
Deacetylation	HDAC3	Santa Cruz [2]	Studies #2, #3 & #4
	HDAC4	Santa Cruz [2]	Studies #2, #3 & #4
	HDAC6	Epigentek [13]	Studies #2, #3 & #4
	SIRT-1	ProteinTech (Acris) [5]	Studies #2, #3 & #4
Muscle-specific transcription factors	MEF2C	Santa Cruz [2]	Studies #2, #3 & #4
	MEF2D	Santa Cruz [2]	Studies #2, #3 & #4
	YY1	Santa Cruz [2]	Studies #2, #3 & #4
Loading controls	Sarcomeric actin (clone 5C5)	Sigma-Aldrich [14]	Study #1
	Vinculin	Santa Cruz [2]	Studies #2, #3 & #4

Table 4: Specific antibodies used in the four studies.

[1] *Academy Bio-Medical Company, Inc., Houston, TX, USA*

[2] *Santa Cruz Biotechnology, Santa Cruz, CA, USA*

[3] *Calbiochem, Darmstadt, Germany*

[4] *Millipore, Billerica, MA, USA*

[5] *Acris, Aachen, Germany*

[6] *Bioworld Technology, Brussels, Belgium*

[7] *Cell Signaling Technology, Inc., Danvers, MA, USA*

[8] *Biomol, Plymouth Meeting, PA, USA*

[9] *Everest Biotech, Oxfordshire, UK*

[10] *Boston Biochem, Cambridge, MA, USA*

[11] *Bethyl, Montgomery, TX, USA*

[12] *Upstate-Millipore, Temecula, CA, USA*

[13] *Epigentek Group Inc., Farmingdale, NY, USA*

[14] *Sigma-Aldrich, St. Louis, MO, USA*

1- Methods Study #1

1.1- Study subjects

This is a hospital-based study in which a group of 26 stable male patients with cachexia of different etiologies were recruited from the COPD (110-112) and Lung Cancer Clinics at Hospital del Mar and Hospital Clinic (Barcelona). Cachectic patients were further subdivided into those with severe COPD and low fat-free mass index (FFMI) $\leq$ 18 kg/m^2 (cachectic-COPD patients, n=16) and patients with lung cancer (stages I-IV) and cachexia (cachectic-cancer patients, n=10) in accordance with current international consensus on the definition of cachexia (25) and previously published criteria (110, 113-116). Lung cancer patients had not previously received any specific treatment for the lung neoplasm: chemotherapy, radiotherapy or systemic corticosteroids at the time of entry into this specific investigation. Clinical staging was assessed in all cachectic patients with lung cancer following currently available international guidelines (117, 118). Additionally, 10 healthy non-smoker (60% ex-smokers and 40% never-smokers) male sedentary control subjects were also recruited from the general population (patients' relatives or friends). The healthy controls were ex-smokers or never smokers, while patients in both groups were active or ex-smokers. All 3 groups of individuals were Caucasian.

Exclusion criteria for COPD patients and control subjects included other chronic respiratory or cardiovascular disorders, acute exacerbations in the last 3 months, limiting osteoarticular condition, chronic metabolic diseases, suspected para-neoplastic or myopathic syndromes, and/or treatment with drugs known to alter muscle structure and/or function including oral corticosteroids, chemotherapy or radiotherapy. COPD patients and healthy controls were qualified as sedentary after being specifically inquired about whether they were conducting any regular outdoor physical activity, going regularly to the gymnasium, or participating in any specific training program.

The current investigation was designed in accordance with both the ethical standards on human experimentation in our institutions and the World Medical Association guidelines (Helsinki Declaration of 2008) for research on human beings. Approval was obtained from the institutional Ethics Committees on Human Investigation (*Hospital del Mar and Hospital Clinic,* Barcelona). Informed written consent was obtained from all individuals.

1.2- Anthropometrical and functional assessment

Anthropometrical evaluation included BMI and determination of the FFMI by bioelectrical impedance (119, 120). Nutritional parameters were also evaluated through conventional blood tests.

Lung function was evaluated through determination of spirometric values, static lung volumes, diffusion capacity, and blood gases using standard procedures and reference values by Roca et al (121-123).

Quadriceps muscle strength was evaluated in both patients and controls by isometric maximum voluntary contraction (QMVC) of the dominant lower limb as formerly described (124, 125). Patients were seated with both trunk and thigh fixed on a rigid support of an exercise platform (Domyos HGH 050, Decathlon, Lille, France). The highest value from three brief reproducible maneuvers (<5% variability among them) was accepted as the MVC.

1.3- Muscle biopsies and blood samples

Muscle samples were obtained from the quadriceps muscle (vastus lateralis) of both groups of patients and control subjects using the open muscle biopsy technique, as described previously (32, 43, 113, 115). Muscle sample biopsies were always performed before chemotherapy in the corresponding cancer patients. Samples were 60-80 mg size in average. Muscle sample specimens were always cleaned out of any blood contamination with saline. They were immediately frozen in liquid nitrogen and stored in the –80ºC freezer (under permanent alarm control) for further analysis or immersed in an alcohol-formol bath for 2h to be thereafter embedded in paraffin. All subjects were prevented from doing any potentially exhausting physical exercise 10 to 14 days before coming to the hospital to undergo the surgical procedures.

Blood samples were drawn at 8:00h am after an overnight fasting period in both patients and healthy controls.

1.4- Molecular biology analyses

1.4.1- Immunoblotting of 1D electrophoresis. Protein levels of the different molecular markers analyzed in the study were explored by means of immunoblotting procedures as previously described (38, 43, 115, 126). Briefly, frozen muscle samples from the vastus lateralis of both groups of patients and healthy control subjects were homogenized in a buffer containing HEPES 50 mM, NaCl 150 mM, NaF 100 mM, Na pyrophosphate 10 mM, EDTA 5 mM, Triton-X 0.5%, leupeptin 2 μg/ml, PMSF 100

μg/ml, aprotinin 2 μg/ml and pepstatin A 10 μg/ml. Myofibrillar proteins were also isolated in order to identify levels of myosin heavy chain (MyHC) (38, 115, 126, 127). All procedures were always conducted at 5ºC (on ice). Protein levels in crude homogenates were spectrophotometrically determined with the Bradford technique using triplicates in each case and bovine serum albumin (BSA) as the standard (Bio-Rad protein reagent, Bio-Rad Inc., Hercules, CA, USA). The final protein concentration in each sample was calculated from at least two Bradford measurements that were almost identical. Equal amounts of total protein (ranging from 5 to 20 micrograms, depending on the antigen and antibody) from crude muscle homogenates were always loaded onto the gels, as well as identical sample volumes/lanes.

For the purpose of comparisons among the two groups of patients and healthy controls, muscle sample specimens were always run together and kept in the same order. Two fresh 10-well mini-gels were always loaded for each of the antigens. Antigens were not identified from stripped membranes in any case.

Proteins were then separated by electrophoresis, transferred to polyvinylidene difluoride (PVDF) membranes, blocked with non-fat milk and incubated overnight with selective primary antibodies. Protein content of markers of proteolysis, signaling pathways of muscle atrophy, redox balance, and different muscle proteins were identified using specific primary antibodies: anti-malondialdehyde (MDA)-protein adducts (Academy Bio-Medical Company, Inc., Houston, TX, USA), Mn-superoxide dismutase (SOD) and CuZn-SOD (anti-Mn-SOD and CuZn-SOD antibodies, Santa Cruz Biotechnology Inc., CA, USA), catalase (anti-catalase antibody, Calbiochem, Darmstadt, Germany), MyHC (anti-MyHC antibody, clone A4.1025, Upstate-Millipore, Temecula, CA, USA), actin (anti-alpha-sarcomeric actin antibody, clone 5C5, Sigma Sigma-Aldrich, St. Louis, MO, USA), creatine kinase (anti-creatine kinase antibody, Santa Cruz), total ubiquitinated proteins (anti-ubiquitin proteins, Boston Biochem, Cambridge, MA, USA), 20S proteasome subunit C8 (anti-C8 antibody, Biomol, Plymouth Meeting, PA, USA), ubiquitin-ligase atrogin-1 (anti-atrogin-1 antibody, Santa Cruz), ubiquitin-ligase muscle ring finger (MURF)-1 (anti-MURF-1 antibody, Everest Biotech, Oxfordshire, UK), transcription factor fork-head box O (FoxO-1, anti-FoxO-1, Millipore, Billerica, MA, USA), p-FoxO-1 (anti-p-FoxO-1, Santa Cruz), FoxO-3 (anti-FoxO-3 antibody, Acris, Aachen, Germany), p-FoxO-3 (anti-p-FoxO-3, Bioworld Technology, Brussels, Belgium), 5’ adenosine monophosphate-activated protein kinase (AMPK) and p-AMPK (anti-AMPK and anti-p-AMPK antibodies, Cell Signaling Technology, Inc., Danvers, MA, USA), mitogen activated kinase (MAPK) extracellular

kinase (ERK1/2, anti-ERK1/2 antibody, Santa Cruz), MAPK p38 (anti-p38 antibody, Santa Cruz), nuclear factor (NF)-κB p50 (anti-p50 antibody, Santa Cruz), phospho-NF-κB p50 (anti-p-p50 antibody, Santa Cruz), NF-κB p65 (anti-p65 antibody, Santa Cruz), phospho-NF-κB p65 (anti-p-p65 antibody, Santa Cruz), inhibitor of κB-alpha (IκB-alpha (anti-IκB-alpha antibody, Santa Cruz), phospho-IκB-alpha (anti-p-IκB-alpha antibody, Santa Cruz), myostatin (anti-myostatin antibody, Bethyl, Montgomery, TX, USA), and myogenin (anti-myogenin antibody, Santa Cruz).

Specific proteins from all samples were detected with horseradish peroxidase (HRP)-conjugated secondary antibodies and a chemiluminescence kit. For each of the antigens, samples from the different groups were always detected in the same picture under identical exposure times. The specificity of the different antibodies was confirmed by omission of the primary antibody, and incubation of the membranes only with secondary antibodies.

PVDF membranes were scanned with the Molecular Imager Chemidoc XRS System (Bio–Rad Laboratories, Hercules, CA, USA) using the software Quantity One version 4.6.5 (Bio–Rad Laboratories). Optical densities of specific proteins were quantified using the software Image Lab version 2.0.1 (Bio-Rad Laboratories). Values of total MDA-protein adduct formation and total protein ubiquitination in a given sample were calculated by addition of optical densities (arbitrary units) of individual protein bands in each case. Final optical densities obtained in each specific group of subjects corresponded to the mean values of the different samples (lanes) of each of the antigens studied. In order to validate equal protein loading among various lanes, SDS-PAGE gels were stained with Coomassie Blue and sarcomeric actin was used as the protein loading control (Figure 5, left and right panels respectively).

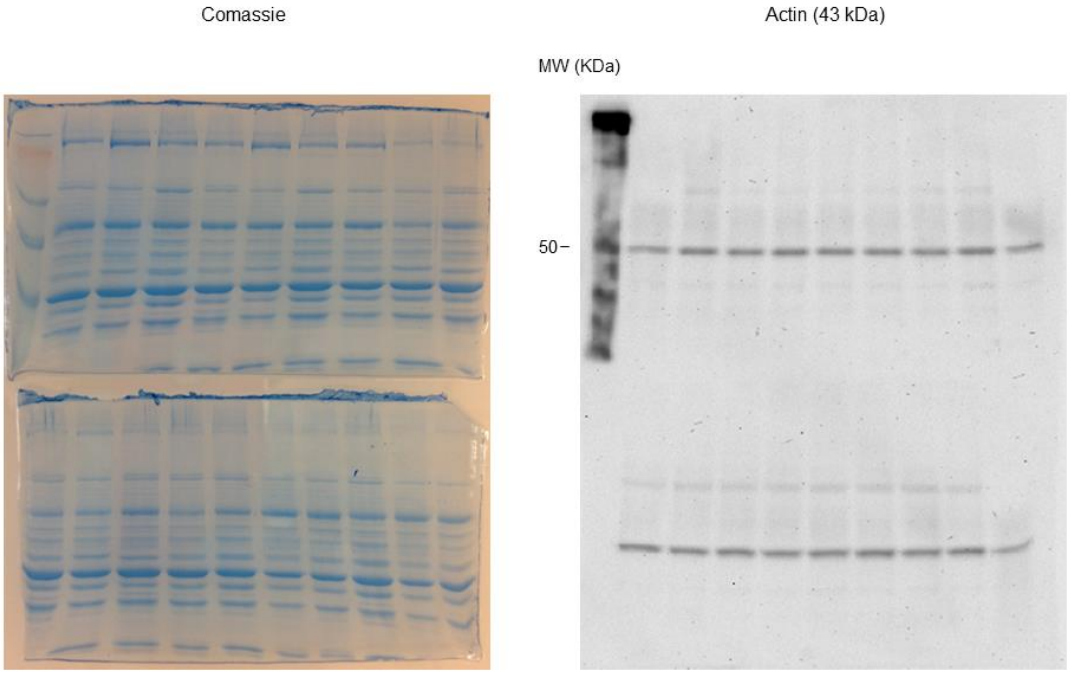

Figure 5. Protein loading controls. Coomassie Blue staining of the SDS-PAGE gels (left panel) and sarcomeric actin immunoblotting (right panel) of the vastus lateralis of all study groups.

1.4.2- Superoxide dismutase (SOD) and catalase activity assays. Commercially available SOD and catalase assay kits (Cayman Chemical Co., Ann Arbor, MI, USA) were used according to the corresponding manufacturer's instructions and previous studies (113, 128) to determine the activity of these two enzymes in all muscle and blood specimens from both groups of patients and controls. A plate reader with 450 nm and 540 nm filters was used for both SOD and catalase activities, respectively. Total SOD activity was expressed as U/mg, while the activity of catalase was expressed as nmol/min/ml/mg. Samples were always run in triplicates and their corresponding activity was expressed as the mean value of the 3 measurements. For SOD and catalase activity measurements the intra-assay coefficient of variation was 3.2% and 3.8%, respectively. Likewise, the inter-assay coefficient of variation was 3.7% and 9.9%, respectively.

1.4.3- Protein carbonylation using enzyme-linked immunosorbent assay (ELISA). EDTA plasma samples and muscle homogenates from both groups of cachectic patients and healthy controls were used in this assay (Zenith Technologies Corp. Ltd., Dunedin, New Zealand) following the precise manufacturer's instructions and previous studies (32, 128). Briefly, 200 micro liters of diluted DNP solution were poured into

each reaction tube. Subsequently, 5 microL of each sample were added, mixed, and incubated for 45 minutes. Moreover, 1mL EIA buffer was also added into each tube together with 5 microL of each DNP-treated sample and adequately mixed. For the ELISA procedure, 200 micro liters of each sample were added to the assigned ELISA-plate wells, which were covered with sealing tape. Plates were then incubated overnight at 4ºC, washed with EIA buffer for several times, and again incubated with 200 microL of diluted anti-DNP-biotin-antibody for 1 hour at 37ºC. Finally, the samples were also incubated with 200 microL of diluted streptavidin-HRP for 1 hour at room temperature. A standard curve was always generated with each assay run. Absorbances were read at 450 nm using as a reference filter that of 655 nm. Intra-assay and inter-assay coefficients of variation for blood protein carbonyl formation ranged from 4.5% to 5.0% in both types of tissue measurements. The minimum detectable concentration of protein carbonyls in the samples was set to be 0.1 nmol/mg (Biocell Corporation Ltd.).

1.4.4- Cytokine ELISA. The protein expression of the cytokines tumor necrosis factor (TNF)-alpha, interleukin (IL)-1beta, interferon-gamma, transforming growth factor (TGF)-beta, and vascular endothelial growth factor (VEGF) was quantified in the vastus lateralis and blood of both groups of patients and healthy controls using specific sandwich ELISA kits (RayBiotech, Norcross, GA, USA) following similar previously published methodologies (32, 43, 115, 128). In the case of muscle samples, frozen muscle specimens were homogenized and protein concentration calculated as described above. For all the sample specimens equal amounts of total protein from muscle homogenates were always loaded in triplicates (15 μg in 200μL total volume each singlet for all the triplicates of all the study samples) onto the ELISA plates. All samples were incubated with the specific primary antibodies and were always run together in each assay. Before commencing the assay, samples and reagents were equilibrated to room temperature. A standard curve was always run with each assay run. Standards (200 μL) were performed as indicated by the manufacturer's instructions. Protocol was also followed according to the corresponding manufacturer's instructions for each cytokine. Absorbances were read at 450 nm using as a reference filter that of 655 nm. Intra-assay coefficients of variation for the different cytokines and studies ranged from 4.5% to 10%. Inter-assay coefficients of variation for the same cytokines ranged from 8% to 12%.

1.4.5- Measurement of superoxide anion radicals by lucigenin-derived chemiluminescence. The reagents employed in these methodologies were all purchased from Sigma (Sigma, Saint Louis, MO, USA). In order to quantify superoxide anion production, lucigenin-derived chemiluminescence (LDCL) signals were determined in all blood (serum) samples from both groups of patients and control subjects using a luminometer (Lumat LB 9507, Berthold Technologies GmbH, Bad Wildbad, Germany) as formerly described (38, 115). Briefly, 50 µL of each serum sample was poured in a tube containing 950 µL Krebs-HEPES buffer. The mixture was incubated for 10 minutes at 37ºC in a water bath. Lucigenin (0.1 mM) was immediately added after the 10-minute incubation period and the tubes were subsequently placed in the luminometer. The luminometer output was read during 10 minutes in all the samples. LDCL signals were measured in the presence of lucigenin alone (baseline levels) and in the presence of 0.5 U/mL SOD.

1.4.6- Muscle fiber counts and morphometry. On 3-micrometer muscle paraffin-embedded sections from both patients and controls (N=10/group), MyHC-I and –II isoforms were identified using anti-MyHC-I (clone MHC, Biogenesis Inc., Poole, England, UK) and anti-MyHC-II antibodies (clone MY-32, Sigma, Saint Louis, MO), respectively, as published elsewhere (38, 43, 115). The cross-sectional area, mean least diameter, and proportions of type I and type II fibers were assessed using a light microscope (Olympus, Series BX50F3, Olympus Optical Co., Hamburg, Germany) coupled with an image-digitizing camera (Pixera Studio, version 1.0.4, Pixera Corporation, Los Gatos, CA, USA) and a morphometry program (NIH Image, version 1.60, Scion Corporation, Frederick, MD, USA). At least 100 fibers were measured and counted in each muscle specimen from cachectic and noncachectic severe patients and healthy controls.

1.4.7- Muscle structure abnormalities. The area fraction of normal and abnormal muscle was evaluated on 3-micrometer paraffin-embedded sections of the vastus lateralis of all patients and healthy controls (N=10/group) following previously published methodologies (115, 129). Briefly, normal and abnormal tissue was quantified using computer-assisted point counting in all the limb muscle sections, previously stained with hematoxylin-eosin. A grid of 63 point-intercepts (7 x 9 rectangular pattern), built by means of the software Imaging Cell-B (Olympus Corporation), was superimposed onto the image of the muscle cross section at a magnification of x400 under the light

microscope (Olympus BX 61, Olympus Corporation) using an image digitizing camera (Olympus DP 71, Olympus Corporation). Each point-intercept was assigned to a specific category and entered into the software. Categories for point counting were defined as follows: 1) normal muscle, 2) internal nucleus, 3) inflammatory cell, 4) lipofuscin, 5) abnormal viable, 6) inflamed/necrotic, 7) vessel, and 0) no count. The area fraction for each category was defined as the percentage of points that fell on each of these traits relative to the total number of points superimposed on all viable fields (all features except for categories 0 and 7) of each cross section. It follows that the area fraction of normal muscle was equivalent to the proportion of points falling in category 1, while the area fraction of abnormal muscle was determined by calculating the proportion of points in categories 2, 3, 4, 5, and 6 (Figure 6).

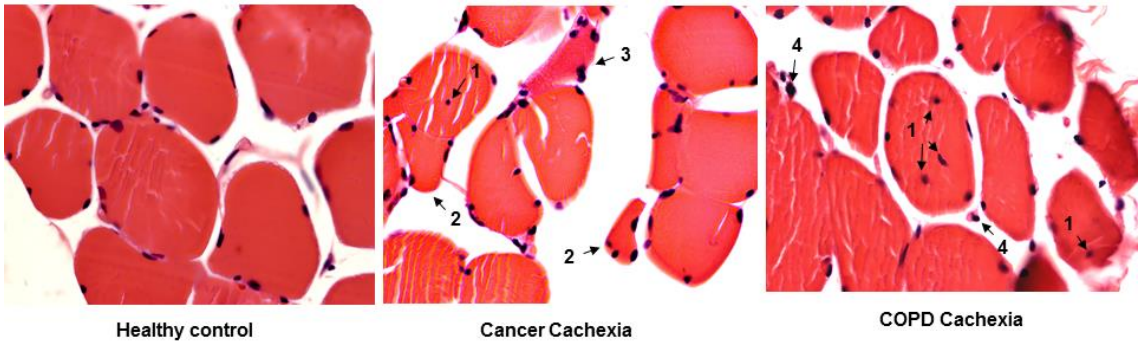

Figure 6. Muscle structure abnormalities. Representative examples of hematoxylin-eosin staining (x 400) of the vastus lateralis of the study subjects, in which the different categories used for point were identified. Those categories were defined using a specific number as defined in the above: internal nuclei (1), abnormal fibers (2), inflamed fibers (3), and the presence of inflammatory cells (4).

1.4.8- Ultrastructural evaluation. Electron microscopic assessment was conducted in vastus lateralis of both groups of patients and healthy controls (N=6/group) following similar methodologies and criteria previously published (50, 130, 131). A fragment of the muscle samples was fixed with 2.5% glutaraldehyde in cacodylate buffer solution, postfixed in 1% osmium tetroxide, dehydrated through a passage in a series of graded ethanols, and embedded in Epon following standard procedures. Ultrathin sections were cut with a diamond knife and collected on bare 200-mesh nickel grids. Sections were stained with uranyl acetate and lead citrate and examined in a transmission electron microscope (Philips CM100, Eindhoven, The Netherlands) with an acceleration voltage of 60 kV. Three different aspects of muscle ultrastructure were

evaluated in the study: sarcomere length, mitochondrial diameters, and sarcomere disruptions.

1.4.8.1- Sarcomere length. Micrographs of the muscle samples were taken from 10 randomly selected fields at constant calibrated magnification (X 3,400). Initial sarcomere length was the average of at least 100 sarcomere measurements in each field (1,000 total sarcomeres/sample), taking Z bands as the reference. In order to normalize sarcomere length, retraction (to control for potential artifacts during muscle sample processing) and contraction (to control for potential artifacts during sample obtaining) coefficients were calculated. In each of the 10 micrograph, an average of 30 both I bands and A bands was measured. Contraction and retraction coefficients were calculated as the ratios between the lengths of both I and A bands to the initial length of sarcomere, respectively. Final sarcomere length values, expressed in nm were normalized according to both contraction and retraction coefficients in each sample. The reported results are the actual normalized sarcomere length values in both groups of patients and control subjects.

1.4.8.2- Mitochondrial diameter. Micrographs of the muscle samples were taken from 10 selected fields at constant calibrated magnification= X 19,000. A first field, in which abundant mitochondria were clearly observed, was chosen. Thereafter, pictures from 9 consecutive fields were captured in which groups of mitochondria were also localized, either in subsarcolemmal or intermyofibrilar regions. Mitochondrial diameter was defined as the smallest cross-sectional length of every mitochondria in each field. The mean or average diameter, expressed in nm, was calculated from the total number of measured mitochondria. Results were expressed as the average mitochondrial diameter, which was normalized according to the retraction coefficient (calculations explained above). Additionally, both total area and number of mitochondria counted in the 10 selected fields were measured in order to determine mitochondrial density in each muscle sample.

1.4.8.3- Sarcomere disruptions. Micrographs of the muscle samples were taken from 10 randomly selected fields at constant calibrated magnification = X 3,400. Disrupted sarcomeres were assessed as a sign of muscle injury and were defined as a zone with distinct distortion of the usual sarcomeric architecture according to the following criteria: discontinuity of a group of myofibrils, A- and I-band disruption, Z-band streaming, embedded subcellular components (mitochondria or collagen), preserved adjacent sarcomere, and absence of regional sectioning artifacts (mainly scratches and holes). In all muscle specimens, injury was quantified using two different types of

parameters: i) density of disruptions, which was expressed as the number of abnormal areas contained in the measured area (n/μm^2) and ii) proportion of abnormal area regarding total measured area, expressed as a percentage. Values for sarcomeric disruption were normalized taking into account the coefficient of retraction as mentioned above.

1.5- Statistical analyses

Statistical analyses were performed using the *Statistical Package for the Social Sciences* (Portable SPSS, PASW Statistics 18.0 version for windows, SPSS Inc., Chicago, IL, USA). For the purpose of the study the following sets of comparisons were made: i) cancer cachectic patients and healthy controls, ii) COPD cachectic patients and control subjects, and iii) cancer cachectic versus COPD cachectic patients. Comparisons of physiological, clinical, and structural variables among healthy controls, lung cancer and COPD cachectic patients were analyzed using parametric one-way analysis of variance (ANOVA) and results are expressed as mean (standard deviation). Tukey's *post hoc* analysis was used to adjust for multiple comparisons.

Biological results are presented as box and whisker plots in the figures. Non-parametric Kruskal-Wallis test was used to examine significant differences among the 3 study groups of subjects for each variable and tissue (blood and muscle). Furthermore, nonparametric Mann-Whitney test was also employed in order to specifically explore significant differences in the study biological variables between groups in each pair of comparisons. Correlations between physiological and biological variables were explored using the Spearman's correlation coefficient among both groups of patients. The sample size chosen was based on previous studies, where very similar approaches were employed (32, 43, 50, 113, 115, 128, 130-140) and on assumptions of 80% power to detect an improvement of more than 20% in measured outcomes at a level of significance of $P \leq 0.05$. In all the biological variables involving the study of redox balance, inflammation, and proteolysis, mean differences between groups was initially estimated at a minimum of 20-25% and standard deviation was approximately 25-30% of the mean value for each of the variables.

2- Methods Study #2

2.1- Study subjects:

Eighteen patients with stable COPD [mild (n=9), moderate (n=6) and severe (n=3)] with normal body composition and 10 age-matched sedentary controls were recruited on an out-patient basis. Diaphragm muscle specimens were obtained from all subjects who underwent thoracotomy for a localized lung neoplasm.

COPD patients were recruited from the COPD Clinic at Hospital del Mar (Barcelona) (110, 111, 116, 141) and the control subjects were recruited from the general population (patients' relatives or friends) at Hospital del Mar. Smoking history was similar between patients and healthy controls. All patients were on bronchodilators. They were clinically stable at the time of the study, without episodes of exacerbation or oral steroid treatment in the previous four months. None of them presented significant comorbidities. The two groups of individuals were Caucasian.

Exclusion criteria for COPD patients and control subjects included other chronic respiratory or cardiovascular disorders, acute exacerbation in the last 3 months, limiting osteoarticular condition, chronic metabolic diseases, suspected para-neoplastic or myopathic syndromes, and/or treatment with drugs known to alter muscle structure and/or function including oral corticosteroids. COPD patients and healthy controls were qualified as sedentary after being specifically inquired about whether they were conducting any regular outdoor physical activity, going regularly to the gymnasium, or participating in any specific training program.

The current cross-sectional investigation was designed in accordance with both the ethical standards on human experimentation in our institutions and the World Medical Association guidelines (Helsinki Declaration of 2008) for research on human beings. Approval was obtained from the institutional Ethics Committees on Human Investigation (*Hospital del Mar,* Barcelona). Informed written consent was obtained from all individuals.

2.2- Anthropometrical and functional assessment

Anthropometrical evaluation included BMI and determination of the FFMI by bioelectrical impedance (119, 120). Nutritional parameters were also evaluated through conventional blood tests.

Lung function was evaluated through determination of spirometric values, static lung volumes, diffusion capacity, and blood gases using standard procedures and reference values by Roca *et al* (121-123).

Inspiratory muscle strength was assessed through determination of maximal inspiratory pressure at the mouth (Sibelmed-163; Sibel, Barcelona, Spain) during an occluded maneuver from residual volume. Both COPD patients and control subjects underwent maximal transdiaphragmatic pressure (Pdi_{max}) measurements, which were calculated from the difference between both maximal gastric and esophageal pressures obtained during a sniff maneuver from forced residual capacity (40). Two balloon catheters were positioned in the mid-esophagus and gastric cavity, and then coupled to pressure transducers (Transpac II, Abbot, Chicago, IL, USA) connected to a digital recorder (BIOPAC Systems Inc, Santa Barbara, CA, USA).

Quadriceps muscle strength was evaluated in both patients and controls by isometric maximum voluntary contraction (QMVC) of the dominant lower limb as formerly described (115). Patients were seated with both trunk and thigh fixed on a rigid support of an exercise platform (Domyos HGH 050, Decathlon, Lille, France). The highest value from three brief reproducible maneuvers (<5% variability among them) was accepted as the MVC.

2.3- Muscle biopsies and blood samples

During thoracotomy for localized lung lesions, diaphragm biopsy specimens were obtained from the anterior costal diaphragm lateral to the insertion of the phrenic nerve (31, 40). The localized lesions were always either peripheral solitary nodes or small lung neoplasms not showing major airway obstruction in any case, as assessed by fiberoptic bronchoscopy. Muscle samples were 30-50 mg size in average.

Muscle sample specimens were always cleaned out of any blood contamination with saline. They were immediately frozen in liquid nitrogen and stored in the –80ºC freezer (under permanent alarm control) for further analysis or immersed in an alcohol-formol bath for 2h to be thereafter embedded in paraffin. Frozen tissues were used for immunoblotting techniques and real time-PCR amplification (qRT-PCR), while paraffin-embedded tissues were used for the assessment of muscle morphometry (immunohistochemical analysis).

Blood samples were drawn at 8:00h am after an overnight fasting period in both patients and healthy controls.

2.4- Molecular biology analyses

2.4.1- RNA isolation. Total RNA was first isolated from snap-frozen skeletal muscles using Trizol reagent following the manufacturer's protocol (Life technologies, Carlsbad, CA, USA). Total RNA concentrations were determined photometrically using the NanoDrop 1000 (Thermo Scientific, Waltham, MA, USA).

2.4.2- MicroRNA and mRNA reverse transcription (RT). MicroRNA RT was performed using TaqMan® microRNA assays (Life Technologies) following the manufacturer's instructions. First-strand cDNA was generated from mRNA using oligo$(dT)_{12\text{-}18}$ primers and the Super-Script^{TM} III reverse transcriptase following the manufacturer's instructions (Life technologies).

2.4.3- Real time-PCR amplification (qRT-PCR). TaqMan based qPCR reactions were performed using the ABI PRISM 7900HT Sequence Detector System (Applied BioSystems, Foster City, CA, USA) together with a commercially available predesigned microRNA assay, primers, and probes as shown in Table 5. Taqman microRNA assay for small nuclear RNA U6 (snU6) was used to normalize the miRNAs amplifications, whereas the housekeeping gene glyceraldehyde-3-phosphate dehydrogenase (GAPDH) served as the endogenous control for mRNA gene expression. MicroRNA and mRNA data were collected and subsequently analyzed using the SDS Relative Quantification Software version 2.1 (Applied BioSystems), in which the comparative C_T method ($2^{-\Delta\Delta CT}$) for relative quantification was employed (142). Results in the figures are expressed as the expression of fold change relative to mean value of the control group, which was equal to 1.

MicroRNA assays		
Assay Name	**Assay ID**	**miRBase accession #**
Muscle-specific, myomiRs		
hsa-miR-1	002222	MIMAT0000416
hsa-miR-133a	002246	MIMAT0000427
hsa-miR-206	000510	MIMAT0000462
Other miRNAs (highly expressed in muscles)		
hsa-miR-486	001278	MIMAT0002177
hsa-miR-27a	000408	MIMAT0000084
hsa-miR-29b	000413	MIMAT0000100
hsa-miR-181a	000480	MIMAT0000256
		NCBI accession #
U6 snRNA, housekeeping gene	001973	NR_004394

Primers and Probes		
Gene Symbol	**Assay ID**	**Genbank accession #**
EP300	Hs00914223_m1	NM_001429.3
SUMO2	Hs02743873_g1	NM_006937.3
SUMO3	Hs00739248_m1	NM_006936.2
GAPDH	Hs99999905_m1	NM_002046.4

Table 5. Predesigned microRNA assays, primers and probes used for the TaqMan based qPCR reactions.

2.4.4- Immunoblotting of 1D electrophoresis. Protein levels of the different molecular markers analyzed in the study were explored by means of immunoblotting procedures as previously described (31, 38-40, 43, 113, 115, 126, 143). Briefly, frozen muscle samples from the diaphragm muscles of both patients and control subjects were homogenized in a buffer containing HEPES 50 mM, NaCl 150 mM, NaF 100 mM, Na pyrophosphate 10 mM, EDTA 5 mM, Triton-X 0.5%, leupeptin 2 μg/ml, PMSF 100 μg/ml, aprotinin 2 μg/ml and pepstatin A 10 μg/ml. The entire procedures were always conducted at 4ºC. Protein levels in crude homogenates were spectrophotometrically determined with the Bradford method using triplicates in each case and bovine serum albumin (BSA) as the standard (Bio-Rad protein reagent, Bio-Rad Inc., Hercules, CA, USA). The final protein concentration in each sample was calculated from at least two Bradford measurements that were almost identical. Equal amounts of total protein (ranging from 20 to 100 micrograms, depending on the antigen and antibody) from crude muscle homogenates were always loaded onto the gels, as well as identical sample volumes/lanes. For the purpose of comparisons between COPD patients and controls, muscle sample specimens were always run together and kept in the same order.

Three fresh 10-well mini-gels were always simultaneously loaded for each of the antigens and run together in the same mini-cell box. Experiments were confirmed at least twice for all the antigens analyzed in the investigation. Fresh gels were specifically loaded for each of the antigens in most of cases. However, in a few cases, antigens were identified from stripped membranes.

Proteins were then separated by electrophoresis, transferred to polyvinylidene difluoride (PVDF) membranes, blocked with bovine serum albumin and incubated overnight with selective primary antibodies. Protein levels of total acetylated proteins, HDACs, HATs, and myogenic transcription factors were identified using specific primary antibodies: Total acetylated proteins (anti-acetyl lysine antibody, Santa Cruz Biotechnology, Santa Cruz, CA, USA), HDAC3 (anti-HDAC3 antibody, Santa Cruz), HDAC6 (anti-HDAC6 antibody, Epigentek, Farmingdale, NY, USA), HDAC4 (anti-HDAC4 antibody, Santa Cruz), NAD-dependent protein deacetylase sirtuin-1 (SIRT1) (anti-SIRT1 antibody, ProteinTech Group Inc., Chicago, IL, USA), MEF2C (anti-MEF2C antibody, Santa Cruz), MEF2D (anti-MEF2D antibody, Santa Cruz), YY1 (anti-YY1 antibody, Santa Cruz), and vinculin (anti-vinculin antibody, Santa Cruz). Antigens from all samples were detected with horseradish peroxidase (HRP)-conjugated secondary antibodies and a chemiluminescence kit. For each of the antigens, samples from the different groups were always detected in the same picture under identical exposure times. The specificity of the different antibodies was confirmed by omission of the primary antibody, and incubation of the membranes only with secondary antibodies.

PVDF membranes were scanned with the Molecular Imager Chemidoc XRS System (Bio–Rad Laboratories, Hercules, CA, USA) using the software Quantity One version 4.6.5 (Bio–Rad Laboratories). Optical densities of specific proteins were quantified using the software Image Lab version 2.0.1 (Bio-Rad Laboratories). Final optical densities obtained in each specific group of subjects corresponded to the mean values of the different samples (lanes) of each of the antigens studied. In order to validate equal protein loading among various lanes, SDS-PAGE gels were stained with Coomassie Blue, and the cytoskeletal protein vinculin (117 kDa, Figure 7) was used as the protein loading controls in all the immunoblots.

Standard stripping methodologies were employed when detection of the antigens required the loading of a large amount of protein. Very briefly, membranes were stripped of primary and secondary antibodies through one 30-minute washes with a stripping solution (25 mM glycine, pH 2.0 and 1% SDS) followed by two consecutive 10-minute washes containing phosphate buffered saline with tween (PBST) at room

temperature. Membranes were blocked with bovine serum albumin and reincubated with primary and secondary antibodies following the procedures described above.

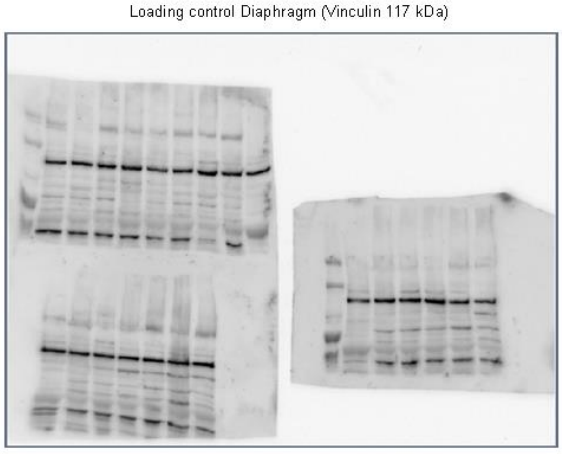

Figure 7. Protein loading control. Representative immunoblot of the cytoskeletal protein vinculin (117 kDa) used as the protein loading control in the diaphragms of COPD patients and healthy controls.

2.4.5- Muscle fiber counts and morphometry. On 3-micrometer muscle paraffin-embedded sections from diaphragm of all study subjects, MyHC-I and –II isoforms were identified using anti-MyHC-I (clone MHC, Biogenesis Inc., Poole, England, UK) and anti-MyHC-II antibodies (clone MY-32, Sigma, Saint Louis, MO), respectively, as published elsewhere (31, 38, 40, 115, 128). The cross-sectional area, mean least diameter, and proportions of type I and type II fibers were assessed using a light microscope (Olympus, Series BX50F3, Olympus Optical Co., Hamburg, Germany) coupled with an image-digitizing camera (Pixera Studio, version 1.0.4, Pixera Corporation, Los Gatos, CA, USA) and a morphometry program (NIH Image, version 1.60, Scion Corporation, Frederick, MD, USA). At least 100 fibers were measured and counted in diaphragm COPD patients and healthy controls.

2.5- Statistical analyses

Statistical analyses were performed using the Statistical Package for the Social Sciences (Portable SPSS, PASW Statistics 18.0 version for windows, SPSS Inc., Chicago IL, USA). For the purpose of the study, results were analyzed with the group of COPD patients as a whole and compared to healthy controls. Data are expressed as mean (standard deviation). Comparisons of physiological, clinical, molecular and structural variables between the two study groups were analyzed using the Student's T-test. Correlations between clinical, physiological and biological variables were explored using the Pearson's correlation coefficient among patients. A level of significance of $P \leq 0.05$ was established. The sample size chosen was based on previous studies (31, 40, 50, 144), where very similar approaches were employed and on assumptions of 80% power to detect an improvement of more than 20% in measured outcomes at a level of significance of $P \leq 0.05$.

3- Methods Study #3

3.1- Study subjects

Forty-one patients with stable COPD and 19 age-matched sedentary controls were recruited. Specimens from the vastus lateralis were obtained from all subjects on an out-patient basis. COPD patients were further subdivided into those with moderate (n=11) and severe COPD (n=30). Additionally, the latter group was also divided into muscle-wasted (n=12) and non-wasted (n=18) COPD patients. Muscle wasting associated with chronic conditions was defined in accordance with current international consensus (25) and previously published criteria (113, 115, 145).

COPD patients were recruited from the COPD Clinic at Hospital del Mar and Hospital Clinic (Barcelona) (110, 111, 116, 141) and the control subjects were recruited from the general population (patients' relatives or friends) at Hospital del Mar. Smoking history was similar between patients and healthy controls. All patients were on bronchodilators. They were clinically stable at the time of the study, without episodes of exacerbation or oral steroid treatment in the previous four months. None of them presented significant comorbidities. All groups of individuals were Caucasian.

Exclusion criteria for COPD patients and control subjects included other chronic respiratory or cardiovascular disorders, acute exacerbation in the last 3 months, limiting osteoarticular condition, chronic metabolic diseases, suspected para-neoplastic or myopathic syndromes, and/or treatment with drugs known to alter muscle structure and/or function including oral corticosteroids. COPD patients and healthy controls were qualified as sedentary after being specifically inquired about whether they were conducting any regular outdoor physical activity, going regularly to the gymnasium, or participating in any specific training program.

The current cross-sectional investigation was designed in accordance with both the ethical standards on human experimentation in our institutions and the World Medical Association guidelines (Helsinki Declaration of 2008) for research on human beings. Approval was obtained from the institutional Ethics Committees on Human Investigation (Hospital del Mar and Hospital Clinic, Barcelona). Informed written consent was obtained from all individuals.

3.2- Anthropometrical and functional assessment

Anthropometrical evaluation included BMI and determination of the FFMI by bioelectrical impedance (119, 120). Nutritional parameters were also evaluated through conventional blood tests.

Lung function was evaluated through determination of spirometric values, static lung volumes, diffusion capacity, and blood gases using standard procedures and reference values by Roca *et al* (121-123).

Quadriceps muscle strength was evaluated in both patients and controls by isometric maximum voluntary contraction (QMVC) of the dominant lower limb as formerly described (124, 125). Patients were seated with both trunk and thigh fixed on a rigid support of an exercise platform (Domyos HGH 050, Decathlon, Lille, France). The highest value from three brief reproducible maneuvers (<5% variability among them) was accepted as the MVC.

3.3- Muscle biopsies and blood samples

Muscle samples were obtained from the quadriceps muscle (vastus lateralis) of all study subjects using the open muscle biopsy technique, as described previously (32, 43, 115, 128). Samples were 60-80 mg size in average.

Muscle sample specimens were always cleaned out of any blood contamination with saline. They were immediately frozen in liquid nitrogen and stored in the –80ºC freezer (under permanent alarm control) for further analysis or immersed in an alcohol-formol bath for 2h to be thereafter embedded in paraffin. Frozen tissues were used for immunoblotting techniques and real time-PCR amplification (qRT-PCR), while paraffin-embedded tissues were used for the assessment of muscle morphometry (immunohistochemical analysis).

Blood samples were drawn at 8:00h am after an overnight fasting period in both patients and healthy controls.

3.4- Molecular biology analyses

3.4.1- RNA isolation. Total RNA was first isolated from snap-frozen skeletal muscles using Trizol reagent following the manufacturer's protocol (Life technologies, Carlsbad, CA, USA). Total RNA concentrations were determined photometrically using the NanoDrop 1000 (Thermo Scientific, Waltham, MA, USA).

3.4.2- MicroRNA and mRNA reverse transcription (RT). MicroRNA RT was performed using TaqMan® microRNA assays (Life Technologies) following the manufacturer's instructions. First-strand cDNA was generated from mRNA using oligo(dT)$_{12-18}$ primers and the Super-Script^{TM} III reverse transcriptase following the manufacturer's instructions (Life technologies).

3.4.3- Real time-PCR amplification (qRT-PCR). TaqMan based qPCR reactions were performed using the ABI PRISM 7900HT Sequence Detector System (Applied BioSystems, Foster City, CA, USA) together with a commercially available predesigned microRNA assay, primers, and probes as previously shown in Table 5 of methods study #2 (page 54). Taqman microRNA assay for small nuclear RNA U6 (snU6) was used to normalize the miRNAs amplifications, whereas the housekeeping gene glyceraldehyde-3-phosphate dehydrogenase (GAPDH) served as the endogenous control for mRNA gene expression. MicroRNA and mRNA data were collected and subsequently analyzed using the SDS Relative Quantification Software version 2.1 (Applied BioSystems), in which the comparative C_T method ($2^{-\Delta\Delta CT}$) for relative quantification was employed (142). Results in the figures are expressed as the expression of fold change relative to mean value of the control group, which was equal to 1.

3.4.4- Immunoblotting of 1D electrophoresis. Protein levels of the different molecular markers analyzed in the study were explored by means of immunoblotting procedures as previously described (31, 38-40, 43, 113, 115, 126, 143). Briefly, frozen muscle samples from the vastus lateralis muscles of all study groups were homogenized in a buffer containing HEPES 50 mM, NaCl 150 mM, NaF 100 mM, Na pyrophosphate 10 mM, EDTA 5 mM, Triton-X 0.5%, leupeptin 2 μg/ml, PMSF 100 μg/ml, aprotinin 2 μg/ml and pepstatin A 10 μg/ml. The entire procedures were always conducted at 4ºC. Protein levels in crude homogenates were spectrophotometrically determined with the Bradford method using triplicates in each case and bovine serum albumin (BSA) as the standard (Bio-Rad protein reagent, Bio-Rad Inc., Hercules, CA, USA). The final protein concentration in each sample was calculated from at least two Bradford measurements that were almost identical. Equal amounts of total protein (ranging from 20 to 100 micrograms, depending on the antigen and antibody) from crude muscle homogenates were always loaded onto the gels, as well as identical sample volumes/lanes. For the purpose of comparisons among the different groups of

COPD patients and controls, muscle sample specimens were always run together and kept in the same order.

Four fresh 10-well mini-gels were always simultaneously loaded for each of the antigens and run together in the same mini-cell box. Experiments were confirmed at least twice for all the antigens analyzed in the investigation. Fresh gels were specifically loaded for each of the antigens in most of cases. However, in a few cases, antigens were identified from stripped membranes.

Proteins were then separated by electrophoresis, transferred to polyvinylidene difluoride (PVDF) membranes, blocked with bovine serum albumin and incubated overnight with selective primary antibodies. Protein levels of total acetylated proteins, HDACs, HATs, and myogenic transcription factors were identified using specific primary antibodies: Total acetylated proteins (anti-acetyl lysine antibody, Santa Cruz Biotechnology, Santa Cruz, CA, USA), HDAC3 (anti-HDAC3 antibody, Santa Cruz), HDAC6 (anti-HDAC6 antibody, Epigentek, Farmingdale, NY, USA), HDAC4 (anti-HDAC4 antibody, Santa Cruz), NAD-dependent protein deacetylase sirtuin-1 (SIRT1) (anti-SIRT1 antibody, ProteinTech Group Inc., Chicago, IL, USA), MEF2C (anti-MEF2C antibody, Santa Cruz), MEF2D (anti-MEF2D antibody, Santa Cruz), YY1 (anti-YY1 antibody, Santa Cruz), and vinculin (anti-vinculin antibody, Santa Cruz). Antigens from all samples were detected with horseradish peroxidase (HRP)-conjugated secondary antibodies and a chemiluminescence kit. For each of the antigens, samples from the different groups were always detected in the same picture under identical exposure times. The specificity of the different antibodies was confirmed by omission of the primary antibody, and incubation of the membranes only with secondary antibodies.

PVDF membranes were scanned with the Molecular Imager Chemidoc XRS System (Bio–Rad Laboratories, Hercules, CA, USA) using the software Quantity One version 4.6.5 (Bio–Rad Laboratories). Optical densities of specific proteins were quantified using the software Image Lab version 2.0.1 (Bio-Rad Laboratories). Final optical densities obtained in each specific group of subjects corresponded to the mean values of the different samples (lanes) of each of the antigens studied. In order to validate equal protein loading among various lanes, SDS-PAGE gels were stained with Coomassie Blue, and the cytoskeletal protein vinculin (117 kDa, Figure 8) was used as the protein loading controls in all the immunoblots.

Standard stripping methodologies were employed when detection of the antigens required the loading of a large amount of protein. Very briefly, membranes were stripped of primary and secondary antibodies through one 30-minute washes with a

stripping solution (25 mM glycine, pH 2.0 and 1% SDS) followed by two consecutive 10-minute washes containing phosphate buffered saline with tween (PBST) at room temperature. Membranes were blocked with bovine serum albumin and reincubated with primary and secondary antibodies following the procedures described above.

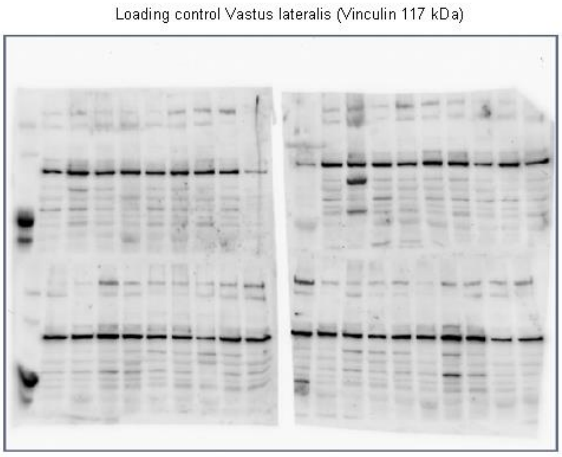

Figure 8. Protein loading control. Representative immunoblot of the cytoskeletal protein vinculin (117 kDa) used as the protein loading control in the vastus lateralis of all study groups.

3.4.5- Muscle fiber counts and morphometry. On 3-micrometer muscle paraffin-embedded sections from vastus lateralis of all study subjects, MyHC-I and –II isoforms were identified using anti-MyHC-I (clone MHC, Biogenesis Inc., Poole, England, UK) and anti-MyHC-II antibodies (clone MY-32, Sigma, Saint Louis, MO), respectively, as published elsewhere (31, 38, 40, 115, 128). The cross-sectional area, mean least diameter, and proportions of type I and type II fibers were assessed using a light microscope (Olympus, Series BX50F3, Olympus Optical Co., Hamburg, Germany) coupled with an image-digitizing camera (Pixera Studio, version 1.0.4, Pixera Corporation, Los Gatos, CA, USA) and a morphometry program (NIH Image, version 1.60, Scion Corporation, Frederick, MD, USA). At least 100 fibers were measured and counted in vastus lateralis from all study groups.

3.5- Statistical analyses

Statistical analyses were performed using the Statistical Package for the Social Sciences (Portable SPSS, PASW Statistics 18.0 version for windows, SPSS Inc., Chicago IL, USA). For the purpose of the study, results obtained were analyzed following these two sets of comparisons and statistical tests: i) comparisons among the different patients groups (moderate, severe non-wasted, and severe muscle-wasted) and control subjects were analyzed using one-way and Tukey's post hoc analysis of variance (ANOVA), and ii) comparisons between severe non-wasted versus severe muscle-wasted COPD patients were assessed using the Student's T-test. Correlations between clinical, physiological and biological variables were explored using the Pearson's correlation coefficient among the different groups of patients.

Data are expressed as mean (standard deviation). A level of significance of $P \leq 0.05$ was established. The sample size chosen was based on previous studies (32, 43, 50, 113, 115), where very similar approaches were employed and on assumptions of 80% power to detect an improvement of more than 20% in measured outcomes at a level of significance of $P \leq 0.05$.

4- Methods Study #4

4.1- Study subjects

Thirteen patients with stable COPD and 13 age-matched sedentary controls were recruited. Specimens from the vastus lateralis were obtained from all subjects on an out-patient basis. COPD patients were recruited from the COPD (110, 111, 116, 141) Clinic at Hospital del Mar (Barcelona) and the control subjects were recruited from the general population (patients' relatives or friends) at Hospital del Mar. Smoking history was similar between patients and healthy controls. All patients were on bronchodilators. They were clinically stable at the time of the study, without episodes of exacerbation or oral steroid treatment in the previous four months. None of them presented significant comorbidities. All groups of individuals were Caucasian.

Exclusion criteria for COPD patients and control subjects included other chronic respiratory (asthma) or cardiovascular disorders, acute exacerbations in the last 3 months, limiting osteoarticular condition, chronic metabolic diseases including diabetes, suspected para-neoplastic or myopathic syndromes, and/or treatment with drugs known to alter muscle structure and/or function including systemic corticosteroids. COPD patients and healthy controls were qualified as sedentary after being specifically inquired about whether they were conducting any regular outdoor physical activity, going regularly to the gymnasium, or participating in any specific training program.

The current investigation was designed in accordance with both the ethical standards on human experimentation in our institutions and the World Medical Association guidelines (Helsinki Declaration of 2008) for research on human beings. Approval was obtained from the institutional Ethics Committees on Human Investigation (*Hospital del Mar,* Barcelona). Informed written consent was obtained from all individuals.

4.2- Anthropometrical and functional assessment

Anthropometrical evaluation included BMI and determination of the FFMI by bioelectrical impedance (119, 120). Nutritional parameters were also evaluated through conventional blood tests.

Lung function was evaluated through determination of spirometric values, static lung volumes, diffusion capacity, and blood gases using standard procedures and reference values by Roca *et al* (121-123).

Quadriceps muscle strength was evaluated in both patients and controls by isometric maximum voluntary contraction (QMVC) of the dominant lower limb as formerly described (124, 125). Patients were seated with both trunk and thigh fixed on a rigid support of an exercise platform (Domyos HGH 050, Decathlon, Lille, France). The highest value from three brief reproducible maneuvers (<5% variability among them) was accepted as the MVC.

4.3- Muscle biopsies and blood samples

Muscle samples were obtained from the quadriceps muscle (vastus lateralis) of both groups of patients and control subjects using the open muscle biopsy technique, as described previously (43, 115). Samples were 60-80 mg size in average.

Muscle sample specimens were always cleaned out of any blood contamination with saline. They were immediately frozen in liquid nitrogen and stored in the –80ºC freezer (under permanent alarm control) for further analysis or immersed in an alcohol-formol bath for 2h to be thereafter embedded in paraffin. Frozen tissues were used for immunoblotting techniques and real time-PCR amplification (qRT-PCR), while paraffin-embedded tissues were used for the assessment of muscle morphometry (immunohistochemical analysis).

Blood samples were drawn at 8:00 am after an overnight fasting period in both patients and healthy controls.

4.4- Molecular biology analyses

4.4.1- RNA isolation. Total RNA was first isolated from snap-frozen skeletal muscles using Trizol reagent following the manufacturer's protocol (Life technologies, Carlsbad, CA, USA). Total RNA concentrations were determined photometrically using the NanoDrop 1000 (Thermo Scientific, Waltham, MA, USA).

4.4.2- MicroRNA and mRNA reverse transcription (RT). MicroRNA RT was performed using TaqMan® microRNA assays (Life Technologies) following the manufacturer's instructions. First-strand cDNA was generated from mRNA using oligo$(dT)_{12\text{-}18}$ primers and the Super-Script^{TM} III reverse transcriptase following the manufacturer's instructions (Life technologies).

4.4.3- Real time-PCR amplification (qRT-PCR). TaqMan based qPCR reactions were performed using the ABI PRISM 7900HT Sequence Detector System (Applied BioSystems, Foster City, CA, USA) together with a commercially available predesigned microRNA assay, primers, and probes as previously shown in Table 5 of methods study #2 (page 54). Taqman microRNA assay for small nuclear RNA U6 (snU6) was used to normalize the miRNAs amplifications, whereas the housekeeping gene glyceraldehyde-3-phosphate dehydrogenase (GAPDH) served as the endogenous control for mRNA gene expression. MicroRNA and mRNA data were collected and subsequently analyzed using the SDS Relative Quantification Software version 2.1 (Applied BioSystems), in which the comparative C_T method ($2^{-\Delta\Delta CT}$) for relative quantification was employed (142). Results in the figures are expressed as the expression of fold change relative to mean value of the control group, which was equal to 1.

4.4.4- Immunoblotting of 1D electrophoresis. Protein levels of the different molecular markers analyzed in the study were explored by means of immunoblotting procedures as previously described (31, 40, 43, 113, 115). Briefly, frozen muscle samples from the vastus lateralis muscles of both patients and control subjects were homogenized in a buffer containing HEPES 50 mM, NaCl 150 mM, NaF 100 mM, Na pyrophosphate 10 mM, EDTA 5 mM, Triton-X 0.5%, leupeptin 2 μg/ml, PMSF 100 μg/ml, aprotinin 2 μg/ml and pepstatin A 10 μg/ml. The entire procedures were always conducted at 4ºC. Protein levels in crude homogenates were spectrophotometrically determined with the Bradford method using triplicates in each case and bovine serum albumin (BSA) as the standard (Bio-Rad protein reagent, Bio-Rad Inc., Hercules, CA, USA). The final protein concentration in each sample was calculated from at least two Bradford measurements that were almost identical. Equal amounts of total protein (ranging from 20 to 100 micrograms, depending on the antigen and antibody) from crude muscle homogenates were always loaded onto the gels, as well as identical sample volumes/lanes. For the purpose of comparisons between COPD patients and control subjects, muscle sample specimens were always run together and kept in the same order.

Two fresh 10-well mini-gels were always simultaneously loaded for each of the antigens and run together in the same mini-cell box. Experiments were confirmed at least twice for all the antigens analyzed in the investigation. Fresh gels were specifically loaded for each of the antigens in most of cases. However, in a few cases,

antigens were identified from stripped membranes.

Proteins were then separated by electrophoresis, transferred to polyvinylidene difluoride (PVDF) membranes, blocked with bovine serum albumin and incubated overnight with selective primary antibodies. Protein levels of total acetylated proteins, HDACs, HATs, and myogenic transcription factors were identified using specific primary antibodies: Total acetylated proteins (anti-acetyl lysine antibody, Santa Cruz Biotechnology, Santa Cruz, CA, USA), HDAC3 (anti-HDAC3 antibody, Santa Cruz), HDAC6 (anti-HDAC6 antibody, Epigentek, Farmingdale, NY, USA), HDAC4 (anti-HDAC4 antibody, Santa Cruz), NAD-dependent protein deacetylase sirtuin-1 (SIRT1) (anti-SIRT1 antibody, ProteinTech Group Inc., Chicago, IL, USA), MEF2C (anti-MEF2C antibody, Santa Cruz), MEF2D (anti-MEF2D antibody, Santa Cruz), YY1 (anti-YY1 antibody, Santa Cruz), and vinculin (anti-vinculin antibody, Santa Cruz). Antigens from all samples were detected with a horseradish peroxidase (HRP)-conjugated secondary antibodies and a chemiluminescence kit. For each of the antigens, samples from the different groups were always detected in the same picture under identical exposure times. The specificity of the different antibodies was confirmed by omission of the primary antibody, and incubation of the membranes only with secondary antibodies.

PVDF membranes were scanned with the Molecular Imager Chemidoc XRS System (Bio-Rad Laboratories, Hercules, CA, USA) using the software Quantity One version 4.6.5 (Bio-Rad Laboratories). Optical densities of specific proteins were quantified using the software Image Lab version 2.0.1 (Bio-Rad Laboratories). Final optical densities obtained in each specific group of subjects corresponded to the mean values of the different sample (lanes) of each of the antigens studied. In order to validate equal protein loading among various lanes, SDS-PAGE gels were stained with Coomassie Blue, and the cytoskeletal protein vinculin (117 kDa, Figure 9) was used as the protein loading controls in all the immmunoblots.

Standard stripping methodologies were employed when detection of the antigens required the loading of a relatively greater amount of total muscle protein. Very briefly, membranes were stripped of primary and secondary antibodies through one 30-minute wash with a stripping solution (25 mM glycine, pH 2.0 and 1% SDS) followed by two consecutive 10-minute washes containing phosphate buffered saline with tween (PBS-T) at room temperature. Membranes were blocked with bovine serum albumin and reincubated with primary and secondary antibodies following the procedures described above.

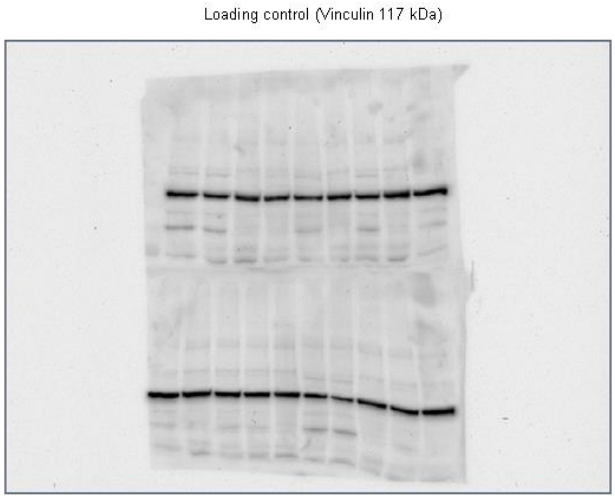

Figure 9. Protein loading control. Representative immunoblot of the cytoskeletal protein vinculin (117 kDa) used as the protein loading control in the vastus lateralis of both COPD patients and healthy controls.

4.4.5- Muscle fiber counts and morphometry. On 3-micrometer muscle paraffin-embedded sections from vastus lateralis of all study subjects, MyHC-I and –II isoforms were identified using anti-MyHC-I (clone MHC, Biogenesis, Inc., Poole, England, UK) and anti-MyHC-II antibodies (clone MY-32, Sigma, Saint Louis, MO), respectively, as published elsewhere (40, 43, 115). The cross-sectional area, mean least diameter, and proportions of type I and type II fibers were assessed using a light microscope (Olympus, Series BX50F3, Olympus Optical Co., Hamburg, Germany) coupled with an image-digitizing camera (Pixera Studio, version 1.0.4, Pixera Corporation, Los Gatos, CA, USA) and a morphometry program (NIH Image, version 1.60, Scion Corporation, Frederick, MD, USA). At least 100 fibers were measured and counted in vastus lateralis from both study groups.

4.5- Statistical analyses

Statistical analyses were performed using the Statistical Package for the Social Sciences (Portable SPSS, PASW Statistics 18.0 version for windows, SPSS Inc., Chicago IL, USA). Data are expressed as mean (standard deviation). Comparisons of physiological, clinical, molecular and structural variables between the two study groups were analyzed using the Student's T-test. Correlations between clinical, physiological and biological variables were explored using the Pearson's correlation coefficient among patients. A level of significance of $P <= 0.05$ was established. The sample size chosen was based on previous studies (31, 32, 40, 43, 50, 102, 108, 109, 113, 115, 134), where very similar approaches were employed and on assumptions of 80% power to detect an improvement of more than 20% in measured outcomes at a level of significance of $P<= 0.05$.

RESULTS

1- Results Study #1

1.1- Clinical characteristics

Table 6 illustrates all clinical and functional variables of the study groups. Age did not significantly differ among the study subjects. Compared to healthy controls, BMI and FFMI were significantly reduced in both groups of cachectic patients, and BMI, but not FFMI, was lower in COPD than in cancer cachectic patients. COPD patients had very severe airflow obstruction, while cancer patients exhibited mild-to-moderate airflow limitation. COPD patients exhibited functional signs of severe emphysema compared to both healthy subjects and cancer cachectic patients. The diagnosis of lung cancer was pathologically confirmed in all patients: 6 squamous cell carcinoma, 1 adenocarcinoma, 2 large cell carcinoma, and 1 small cell carcinoma. Half of lung cancer patients had a localized disease and were active smokers or ex-smokers in similar proportions to COPD patients. Body weight loss was confirmed in all patients, and most of them had lost between 1 and 8 kg in the year prior to study entry. Exercise capacity and quadriceps muscle strength were decreased in both groups of patients compared to the controls, and they were also more reduced in COPD than in cancer cachectic patients. From a nutritional standpoint, systemic albumin levels, but not total protein concentration, were diminished in both groups of patients compared to controls, whereas levels of fibrinogen and C-reactive protein were higher in the patients, especially in the lung cancer group, than in control subjects. Globular sedimentation velocity was only significantly increased in cancer cachectic patients compared to controls.

	Control	Cancer cachexia	COPD cachexia
	N = 10	N = 10	N = 16
Anthropometry			
Age (years)	65 (11)	65 (9)	64 (9)
BMI (kg/m^2)	27 (3)	23 (4) *	19 (3) ***, ††
FFMI (kg/m^2)	20 (2)	17 (2) *	16 (2) ***
Body weight loss, kg			
0, N	10	1 ***	3 ***
1-4, N	0	3 ***	8 ***
5-8, N	0	5 ***	4 ***
>9, N	0	1 ***	1 ***
Lung cancer classification			
NSCLC, N	NA	9	NA
SCLC, N	NA	1	NA
Lung cancer staging, N	NA	Ia/Ib/IIIa/IIIb/IV 1 / 1 / 2 / 1 / 5	NA
Smoking History			
Active: N, %	0, 0	7, 70 **	10, 63 **
Ex-smoker: N, %	6, 60	3, 30 **	6, 37 **
Never Smoker: N, %	4, 40	0, 0 **	0, 0 **
Pack-years	48 (22)	60 (15)	60 (39)
Lung function			
FEV_1 (% pred)	101 (15)	64 (15) ***	33 (15) ***, †††
FVC (% pred)	98 (13)	70 (14) ***	62 (16) ***
FEV_1/FVC (%)	77 (5)	65 (7) ***	40 (11) ***, †††
RV (% pred)	98 (34)	108 (34)	176 (97) ***, †
TLC (% pred)	98 (11)	86 (19)	101 (44)
RV/TLC (%)	38 (6)	47 (11) *	65 (9) ***, †††
DLco (% pred)	96 (16)	70 (16) ***	37 (16) ***, †††
K_{CO} (% pred)	91 (15)	85 (18)	54 (19) ***, †††
PaO_2 (kPa)	12.7 (1)	10.5 (1.1) ***	10.1 (1.4) ***
$PaCO_2$ (kPa)	5.1 (0.5)	5.2 (0.4)	5.7 (1.1)
Exercise capacity & muscle force			
VO_2 peak (% pred)	88 (22)	56 (6) **	47 (17) ***
W*R* peak (% pred)	75 (21)	53 (6) **	33 (13) ***, †††
QMVC (kg)	40 (2.6)	34 (2.6) ***	29 (2.5) ***, †††
Six-minute walking distance (m)	548 (87)	415 (50) **	410 (122) ***
Blood parameters			
Albumin (g/dL)	4.6 (0.4)	3.3 (0.4) ***	3.8 (0.7) **
Total proteins (g/dL)	7.3 (0.4)	6.7 (0.5)	6.7 (0.8)
CRP (mg/dL)	0.7 (0.3)	7.7 (5.1) **	4.1 (2.5) *, †
Fibrinogen (mg/dL)	360 (105)	719 (186) ***	515 (194) *,†
GSV (mm/h)	18 (15)	53 (16) *	26 (37)

Table 6. Anthropometric characteristics and functional status of all the study subjects undergoing vastus laterales biopsy. Values are expressed as mean (standard deviation).

Statistical significance: *, p≤0.05, **, p≤0.01, ***, p≤0.001 between any group of patients and the control subjects; †, p≤0.05, ††, p≤0.01, †††, p≤0.001 between COPD and cancer cachexia patients.

1.2- Muscle and systemic redox balance

1.2.1- Protein oxidation. Levels of total reactive carbonyls and MDA-protein adducts were significantly increased in muscles of cancer and COPD cachectic patients compared to controls (Figures 10A-10B). Additionally, systemic levels of protein carbonylation and superoxide anion were also significantly greater in both groups of patients than in control subjects (Figures 10C-10D). Importantly, among cachectic COPD patients and when considering all patients together as a group, significant negative correlations were found between BMI and FFMI and total muscle protein carbonylation levels (Table 7, pages 88-89).

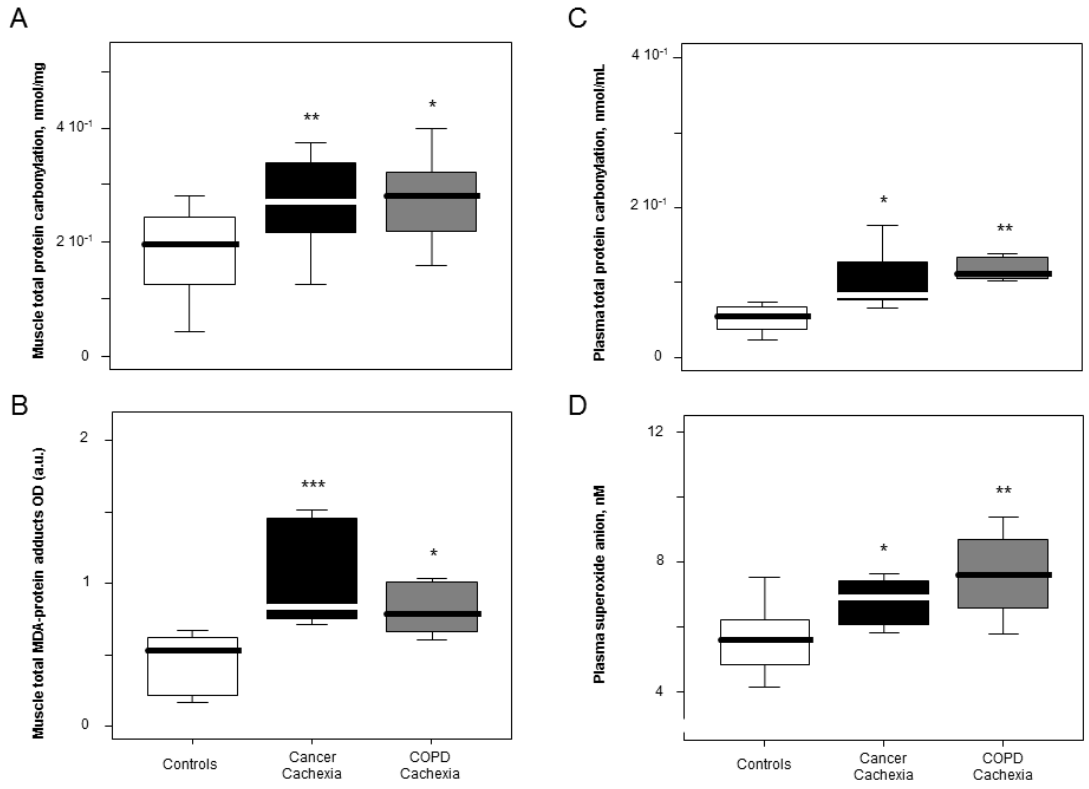

Figure 10. Protein oxidation markers. Standard box plots with median (25th and 7th percentiles) and whiskers (at minimum and maximum values. **A**. Total protein carbonylation levels in vastus lateralis of all study subjects**. B.** MDA-protein adducts levels in vastus lateralis of all study subjects**. C**. Total reactive carbonyls levels in blood of all study subjects. **D.** Superoxide anion levels in blood of all study subjects.

Statistical significance: *, p≤0.05; **, p≤0.01; and ***, p≤0.001 between any group of patients and healthy controls.

1.2.2- Antioxidants. Protein content of both mitochondrial and cytosolic SOD isoforms and SOD enzyme activity were increased in vastus lateralis of both cancer and COPD cachectic patients compared to controls (Figures 11A-11C), while systemic levels of SOD did not differ between the study groups (Figure 11D). Catalase protein content and enzyme activity levels were not significantly different between patients and controls in either muscle or blood compartments (Figures 12A-12C). No significant correlations were found between antioxidant levels and other variables in any of the study groups.

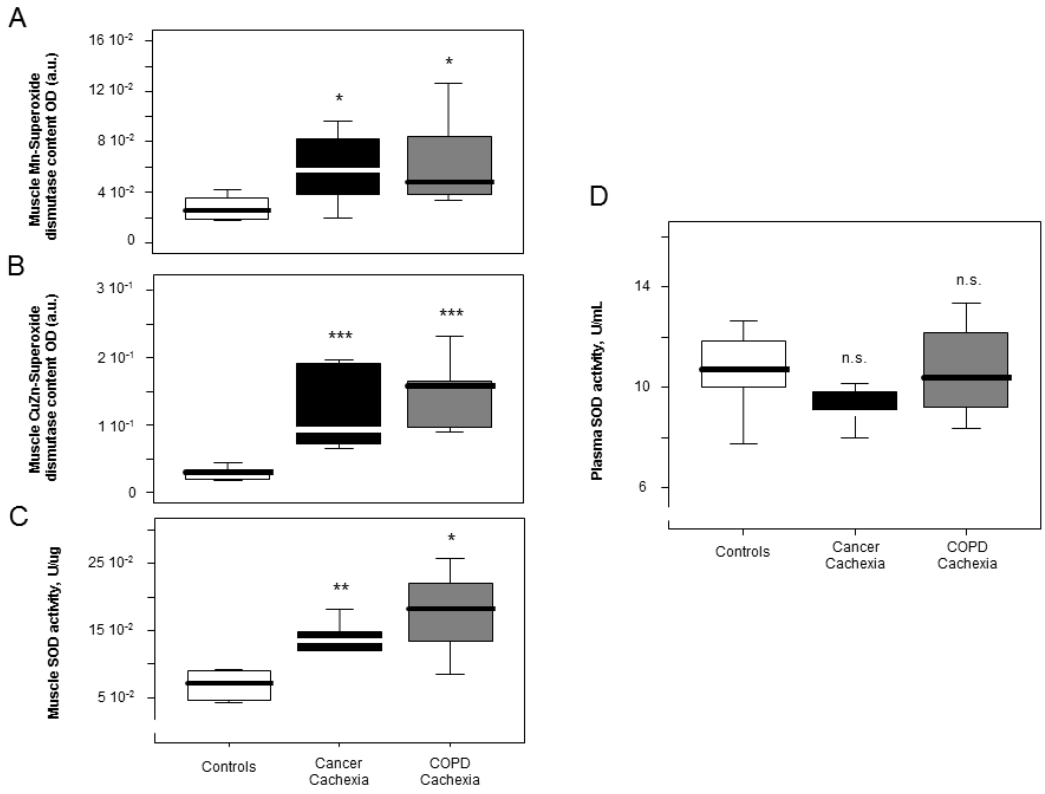

Figure 11. Antioxidants markers. Standard box plots with median (25th and 7th percentiles) and whiskers (at minimum and maximum values. **A**. Levels of the mitochondrial antioxidant Mn-SOD in vastus lateralis of all study subjects. **B**. Levels of the cytosolic antioxidant CuZn-SOD in vastus lateralis of all study subjects. **C.** Total SOD enzyme activity levels in vastus lateralis of all study subjects. **D.** Total SOD enzyme activity levels in blood of all study subjects.
Statistical significance: n.s., non-significant; *, p≤0.05; **, p≤0.01; and ***, p≤0.001 between any group of patients and healthy controls.

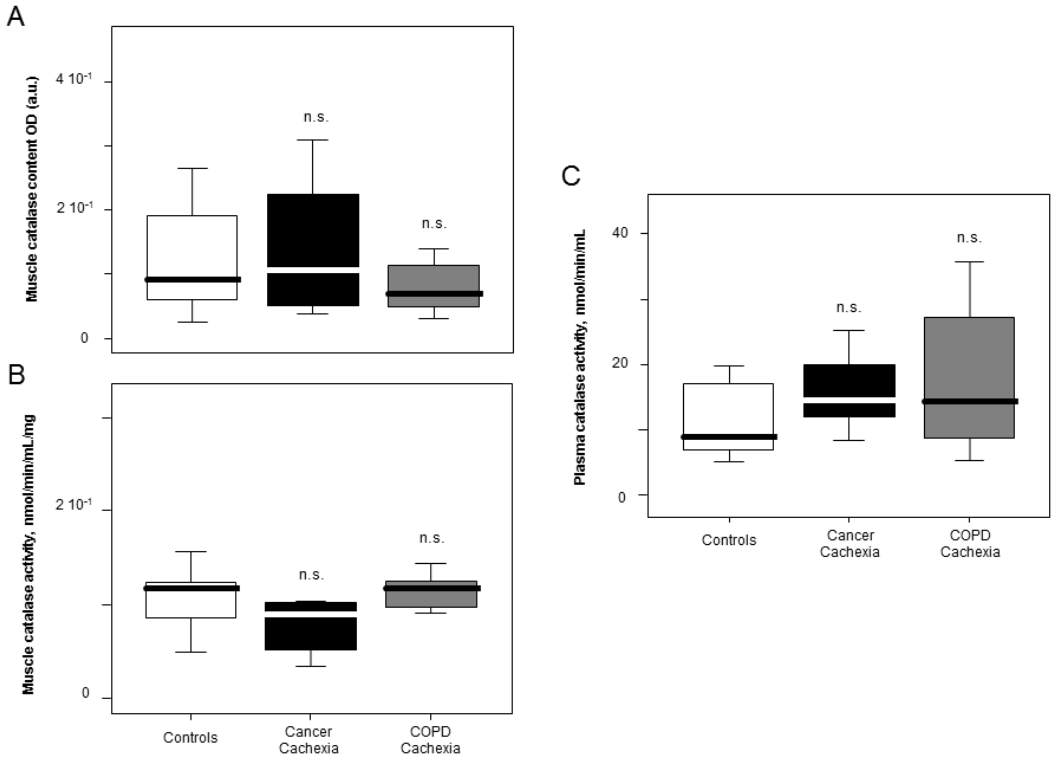

Figure 12. Antioxidants markers. Standard box plots with median (25th and 7th percentiles) and whiskers (at minimum and maximum values. **A.** Levels of the antioxidant catalase protein in vastus lateralis of all study subjects. **B.** Levels of the antioxidant catalase enzyme activity in vastus lateralis of all study subjects. **C**. Levels of catalase enzyme activity in blood of all study subjects.

Statistical significance: n.s., non-significant between any group of patients and healthy controls.

1.3- Muscle and systemic inflammation

Inflammatory cytokines. Muscle and systemic TNF-alpha levels did not differ between the study groups (Table 8). Compared to controls, muscle IL-1beta levels were higher in both groups of patients, while systemic levels were only increased in the COPD cachectic patients (Table 8). Interferon-gamma levels were significantly increased in muscles and blood of all patients compared to control subjects (Table 8). Systemic levels of VEGF and TGF-beta were greater in both groups of patients than in controls, while only VEGF levels were increased in muscles of both groups of cachectic patients (Table 8). Among lung cancer cachexia patients, significant correlations were found between plasma TNF-alpha levels and BMI, six-minute walking distance, and total muscle ubiquitinated protein levels (Table 7, page 88).

	Control	Cancer Cachexia	COPD Cachexia
Muscle Inflammation			
TNF-α (pg/mL)	19.8 (4.3)	19.9 (3.2)	18.9 (3.5)
IL-1β (pg/mL)	0.9 (0.2)	1.3 (0.4) *	1.8 (0.9) *
Interferon-γ (pg/mL)	19.8 (6.8)	28.4 (4.4) *	40.3 (13) **
VEGF (pg/mL)	34.1 (11.1)	56.5 (17.9) **	54.5 (11.4) *
TGF-β (pg/mL)	1344 (540.1)	1286.7 (847.5)	1487.1 (317.6)
Plasma inflammation			
TNF-α (pg/mL)	30.1 (4.3)	30.8 (5.5)	29.4 (3)
IL-1β (pg/mL)	2.9 (2.6)	4.36 (2.4)	12.2 (7.8) *
Interferon-γ (pg/mL)	468.7 (189.5)	861.9 (261.3) **	810.7 (235.6) *
VEGF (pg/mL)	55.6 (32.4)	192.5 (182.2) ***	390.5 (197.6) ***
TGF-β (pg/mL)	244 (165.3)	596.2 (415.7) *	833.9 (585)*

Table 8. Muscle and systemic inflammatory cytokines in vastus lateralis and blood of all study subjects.

Values are expressed as median (interquartile ranges).

Statistical significance: *, p≤0.05, **, p≤0.01, ***, p≤0.001 between any group of patients and the control subjects.

1.4- Redox-signaling markers in muscles

1.4.1- MAPK signaling pathway. Muscle levels of ERK1/2 and p-ERK1/2 did not differ among the study groups (Figures 13A-13B). A significant rise in p-p38 levels, but not total p38, was observed in muscles of both groups of patients compared to control subjects (Figures 13C-13D).

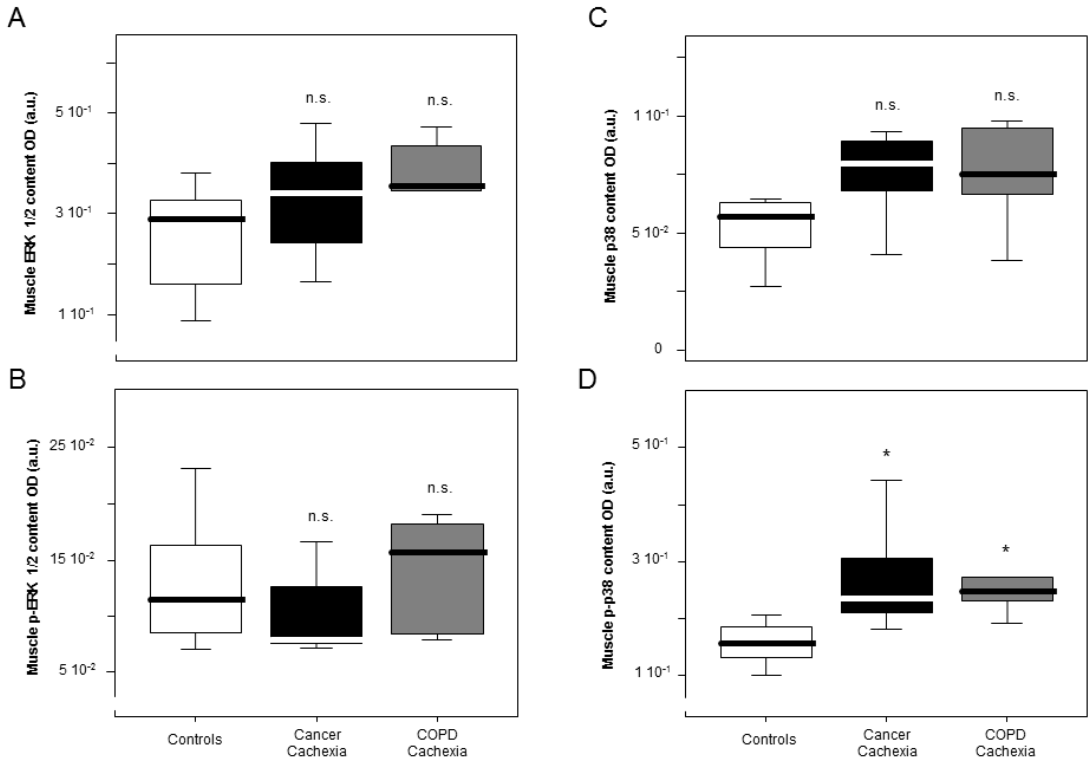

Figure 13. MAPK signaling pathway markers. Standard box plots with median (25th and 7th percentiles) and whiskers (at minimum and maximum values. **A.** Protein levels of ERK1/2 in vastus lateralis of all study subjects. **B**. Protein levels of p-ERK1/2 in vastus lateralis of all study subjects. **C**. Protein levels of p38 in vastus lateralis of all study subjects. **D**. Protein levels of p-p38 in vastus lateralis of all study subjects.

Statistical significance: n.s., non-significant; and *, p≤0.05 between any group of patients and healthy controls.

1.4.2- NF-κB signaling pathway. Muscle levels of NF-κB p50 and p-NF-κB p50 did not differ among the study groups (Figures 14A-14B). Nevertheless, levels of total NF-κB p65 and p-NF-κB p65 were significantly greater in limb muscles of both groups of patients compared to controls (Figures 14C-14D). Muscle levels of both IκB-alpha and p-IκB-alpha were significantly lower in both cancer and COPD cachectic patients than in control subjects (Figures 14E-14F). Among cachectic COPD patients, a negative correlation was found between muscle NF-κB p65 and BMI, while among all patients, significant inverse correlations were observed between p-NF-κB p65 and either FEV_1 or QMVC (Table 7, pages 88-89).

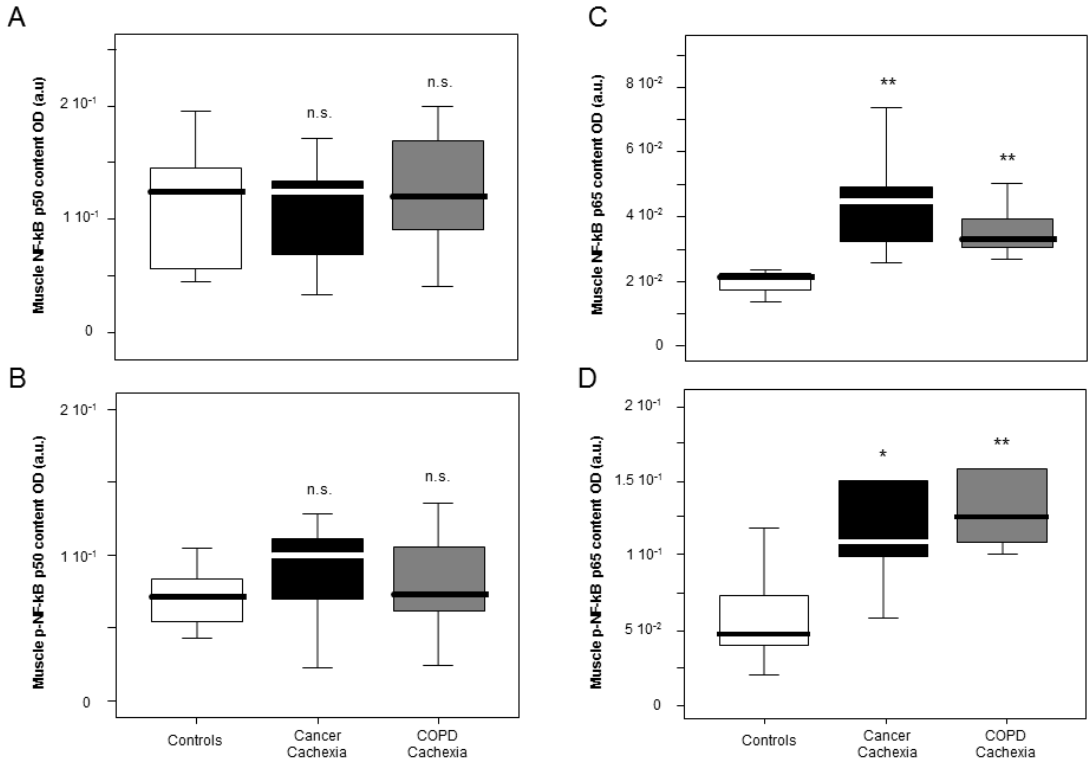

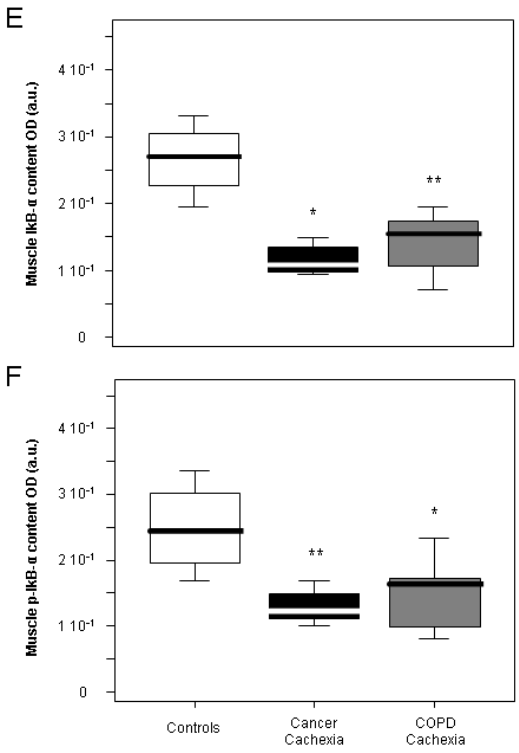

Figure 14. NF-kB signaling pathway markers. Standard box plots with median (25th and 7th percentiles) and whiskers (at minimum and maximum values. **A**. Protein levels of NF-kB p50 in vastus lateralis of all study subjects. **B**. Protein levels of NF-kB p-p50 in vastus lateralis of all study subjects. **C**. Protein levels of NF-kB p65 in vastus lateralis of all study subjects. **D**. Protein levels of NF-kB p-p65 in vastus lateralis of all study subjects. **E**. Protein levels of IkB-alpha in vastus lateralis of all study subjects. **F**. Protein levels of p-IkB-alpha in vastus lateralis of all study subjects.

Statistical significance: n.s., non-significant; *, p≤0.05; and **, p≤0.01 between any group of patients and healthy controls.

1.4.3- FoxO signaling pathway. Compared to controls, muscle protein levels of total FoxO-1 and FoxO-3 were increased in both groups of patients (Figures 15A and 15C), while only p-FoxO-3 levels were higher in muscles of all patients (Figure 15D). In cancer cachexia patients, total FoxO-1 levels inversely correlated with FFMI, while in cachectic COPD patients, muscle p-FoxO-3 levels were associated with either DL_{CO} or K_{CO} (Table 7, page 88).

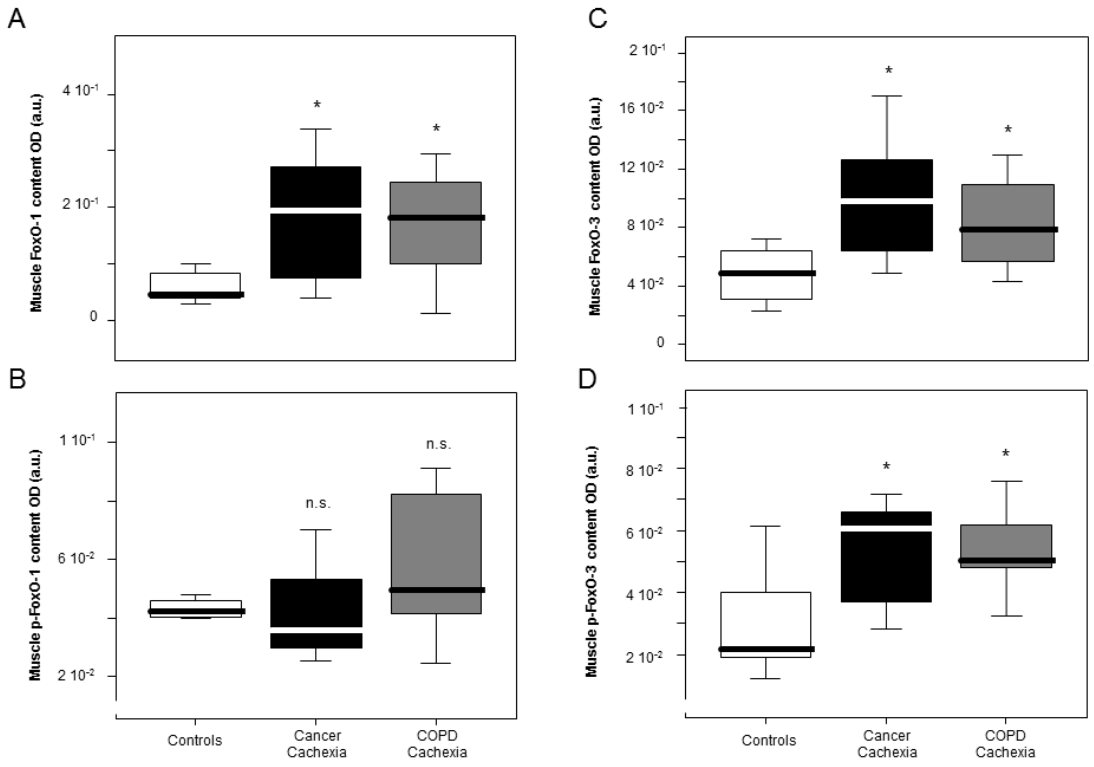

Figure 15. FoxO signaling pathway markers. Standard box plots with median (25th and 7th percentiles) and whiskers (at minimum and maximum values. **A.** Protein levels of FoxO-1 in vastus lateralis of all study subjects. **B**. Protein levels of p-FoxO-1 in vastus lateralis of all study subjects. **C**. Protein levels of FoxO-3 in vastus lateralis of all study subjects. **D.** Protein levels of p-FoxO-3 in vastus lateralis of all study subjects.

Statistical significance: n.s., non-significant; and *, p≤0.05 between any group of patients and healthy controls.

1.4.4- AMPK signaling pathway. Muscle levels of AMPK and p-AMPK did not differ among the study groups (Figure 16).

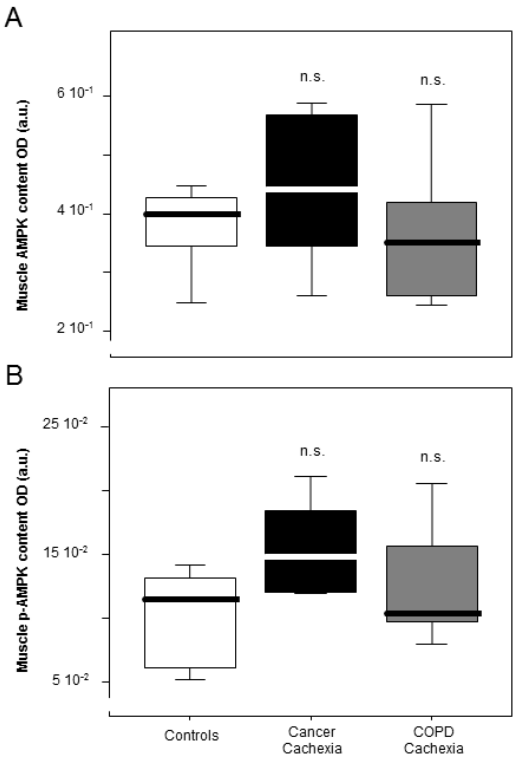

Figure 16. AMPK signaling pathway markers. Standard box plots with median (25th and 7th percentiles) and whiskers (at minimum and maximum values. **A**. Protein levels of AMPK in vastus lateralis of all study subjects. **B.** Protein levels of p-AMPK in vastus lateralis of all study subjects.

Statistical significance: n.s., non-significant between any group of patients and healthy controls.

1.5- Muscle proteolysis markers

Ubiquitin-proteasome system. Compared to controls, muscle levels of both E3 ligases atrogin-1 and MURF-1 and total ubiquitinated proteins were significantly increased in both groups of patients (Figures 17B-17D), while levels of 20S proteasome subunit C8 did not differ among groups (Figure 17A). In COPD patients, PaO_2 inversely correlated with total protein ubiquitination levels (Table 7, page 88). Among all patients together, total muscle protein ubiquitination levels positively correlated with those of MDA-protein adducts and inversely with IκB-alpha levels (Table 7, page 89). Moreover, total muscle protein ubiquitination levels also correlated with those of MDA-protein adducts when each group of patients was considered separately (Table 7, page 88).

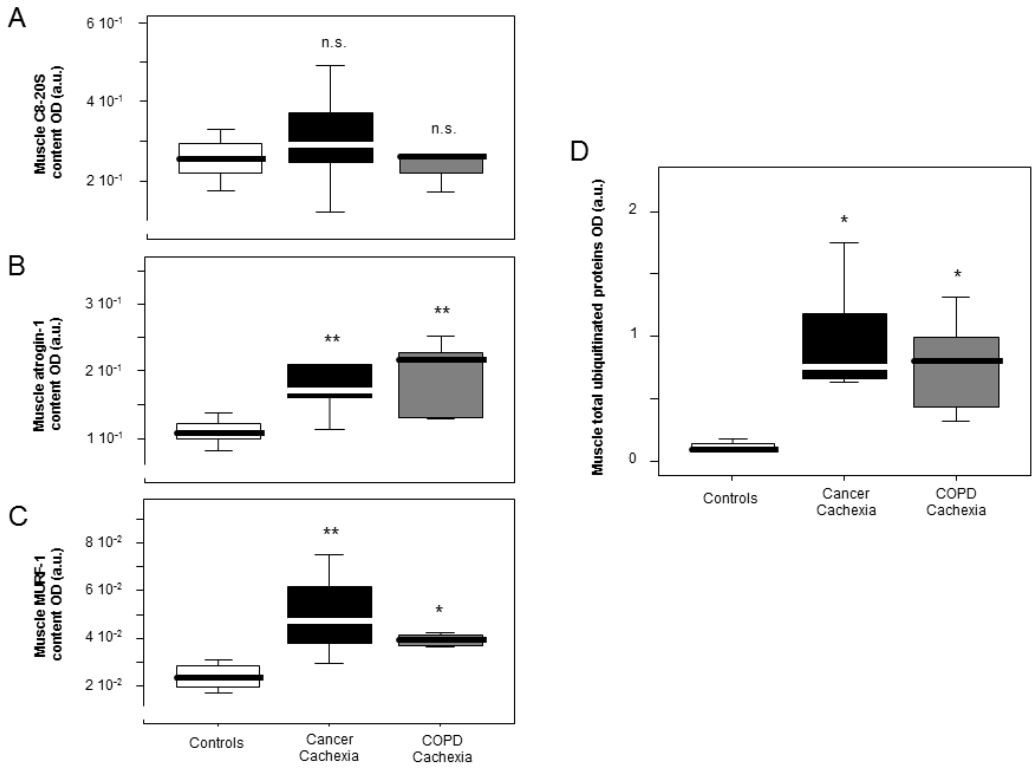

Figure 17. Ubiquitin-proteasome system markers. Standard box plots with median (25th and 7th percentiles) and whiskers (at minimum and maximum values. **A.** Protein levels of the C8-20S proteasome subunit in vastus lateralis of all study subjects**. B**. Protein levels of the E3-ligase atrogin-1 in vastus lateralis of all study subjects. **C.** Protein levels of the E3-ligase MURF-1 in vastus lateralis of all study subjects. **D.** Levels of total protein ubiquitination in vastus lateralis of all study subjects.

Statistical significance: n.s., non-significant; *, p≤0.05; and **, p≤0.01 between any group of patients and healthy controls.

1.6- Muscle growth and differentiation

Muscle levels of myostatin protein did not differ between patients and healthy controls (Figure 18A). Nonetheless, protein content of myogenin was significantly reduced within limb muscles of both cancer and COPD cachectic patients compared to controls (Figure 18B).

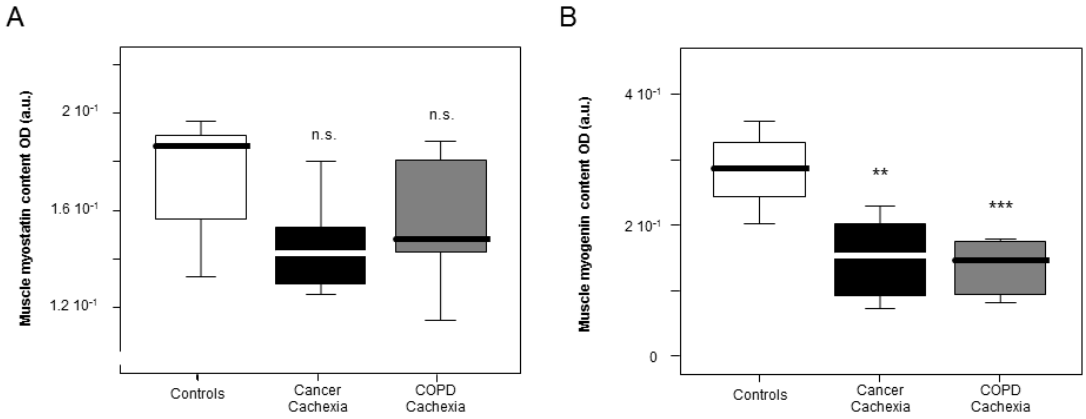

Figure 18. Muscle growth and differentiation markers. Standard box plots with median (25th and 7th percentiles) and whiskers (at minimum and maximum values. **A.** Levels of myostatin protein in vastus lateralis of all study subjects. **B.** Levels of myogenin protein in vastus lateralis of all study subjects.

Statistical significance: n.s., non-significant; **, p≤0.01; and ***, p≤0.001 between any group of patients and healthy controls.

1.7- Contractile and functional muscle proteins

Protein levels of MyHC and creatine kinase were significantly reduced in limb muscles of both groups of patients compared to control subjects (Figure 19).

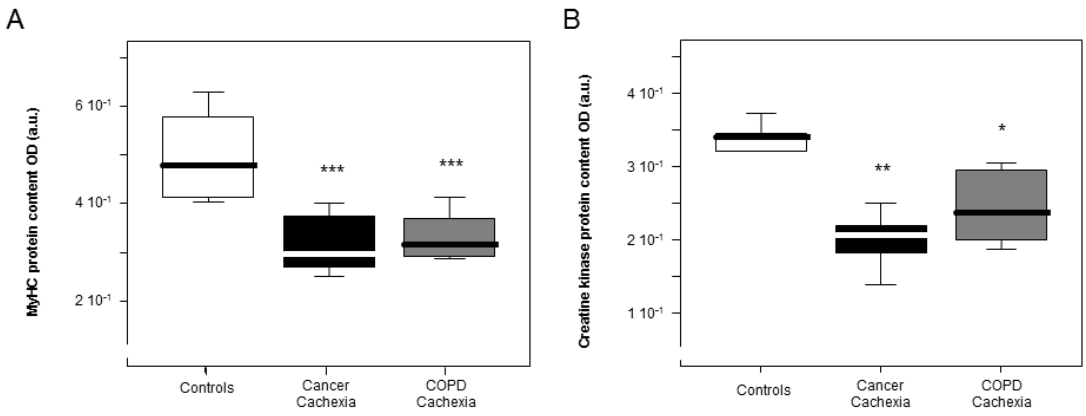

Figure 19. Contractile and funcional muscle protein markers. Standard box plots with median (25th and 7th percentiles) and whiskers (at minimum and maximum values. **A.** Protein levels of

contractile MyHC in vastus lateralis of all study subjects. **B.** Protein levels of the enzyme creatine kinase in vastus lateralis of all study subjects.

Statistical significance: *, p≤0.05; **, p≤0.01; and ***, p≤0.001 between any group of patients and healthy controls.

1.8- Muscle structure

1.8.1- Fiber type composition. Compared to controls, proportions of type I fibers were significantly decreased only in limb muscles of COPD cachectic patients (Table 9). Interestingly, the size of type II fibers was significantly decreased in vastus lateralis of both cancer and COPD cachectic patients (24% and 36%, respectively) compared to control subjects (Table 9 and Figure 20). Significant correlations were found between proportions of type I and II fibers and BMI, FFMI, K_{CO}, and muscle FoxO-3 levels, in all patients together and in COPD patients separately (Table 7, pages 88-89).

	Controls N= 10	Cancer Cachexia N= 10	COPD Cachexia N= 10
Muscle fiber type composition			
Type I fibers, %	31 (4)	28 (4)	23 (6) **
Type II fibers, %	69 (4)	72 (4)	77 (6) **
Type I fibers, CSA (μm^2)	2920 (458)	2639 (172)	2582 (214)
Type II fibers, CSA (μm^2)	3279 (452)	2499 (594) *	2109 (416) **

Table 9. Fiber type composition of the study subjects.

Values are expressed as mean (standard deviation).

Statistical significance: *, p≤0.05, **, p≤0.01 between any group of patients and the control subjects.

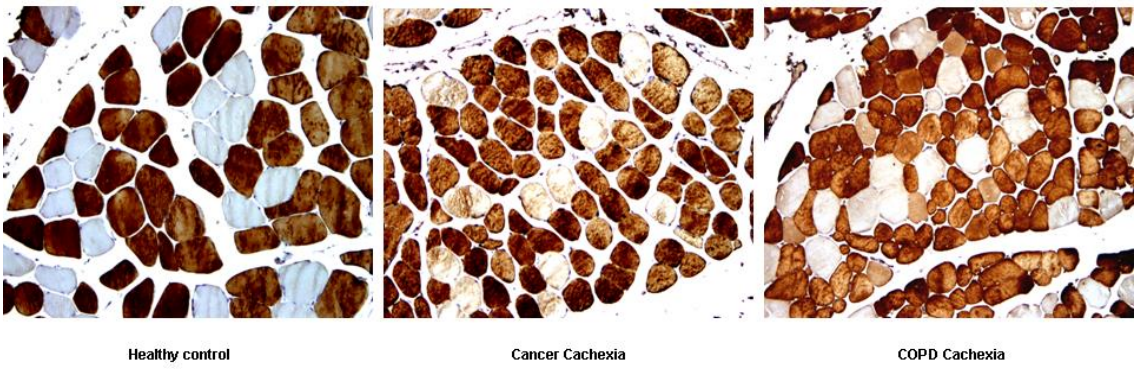

Figure 20. Muscle fiber type composition. Representative examples of stained muscle fibers (x100) within the vastus lateralis of a healthy control subject (left panel) and both cancer cachectic (medium panel) and COPD cachectic (right panel) patients. Type II fibers were

positively stained (brown color) with the corresponding antibody. Note that type II fibers were of smaller size in the limb muscles of the patients that in the healthy controls (Table 9).

1.8.2- Muscle abnormalities. Proportions of total muscle structural abnormalities were greater in the muscles of both groups of patients compared to controls (Table 10).

	Controls N= 10	Cancer Cachexia N= 10	COPD Cachexia N= 10
Muscle structure			
Total abnormal fraction area, %	1.49 (0.4)	2.39 (0.4) **	2.5 (0.9) **
Internal nuclei, %	0.59 (0.4)	0.67 (0.3)	0.47 (0.3)
Inflammatory cells, %	0.79 (0.3)	1.25 (0.5)	1.34 (0.5) *
Other items (§), %	0.11 (0.1)	0.46 (0.2)	0.68 (0.8) *

Table 10. Muscle structure of the study subjects.

Values are expressed as mean (standard deviation).

(§) Other items: Percentage of the sum of abnormal and inflammed fibers and lipofucsin.

Statistical significance: *, p≤0.05, **, p≤0.01 between any group of patients and the control subjects.

1.9- Electron microscopy features

Electron microscopy revealed that sarcomere length, mitochondrial diameter, and mitochondrial density values did not differ among the study groups (Figures 21A-21C). The number of disrupted sarcomeres, however, was significantly greater in muscles of both cancer and COPD cachectic patients than in control subjects, expressed as either density or proportions of disrupted muscle areas (Figures 21D-21E). Importantly, among all patients, a significant inverse correlation was observed between MyHC protein levels and the proportions of sarcomere disruptions (Table 7, page 89).

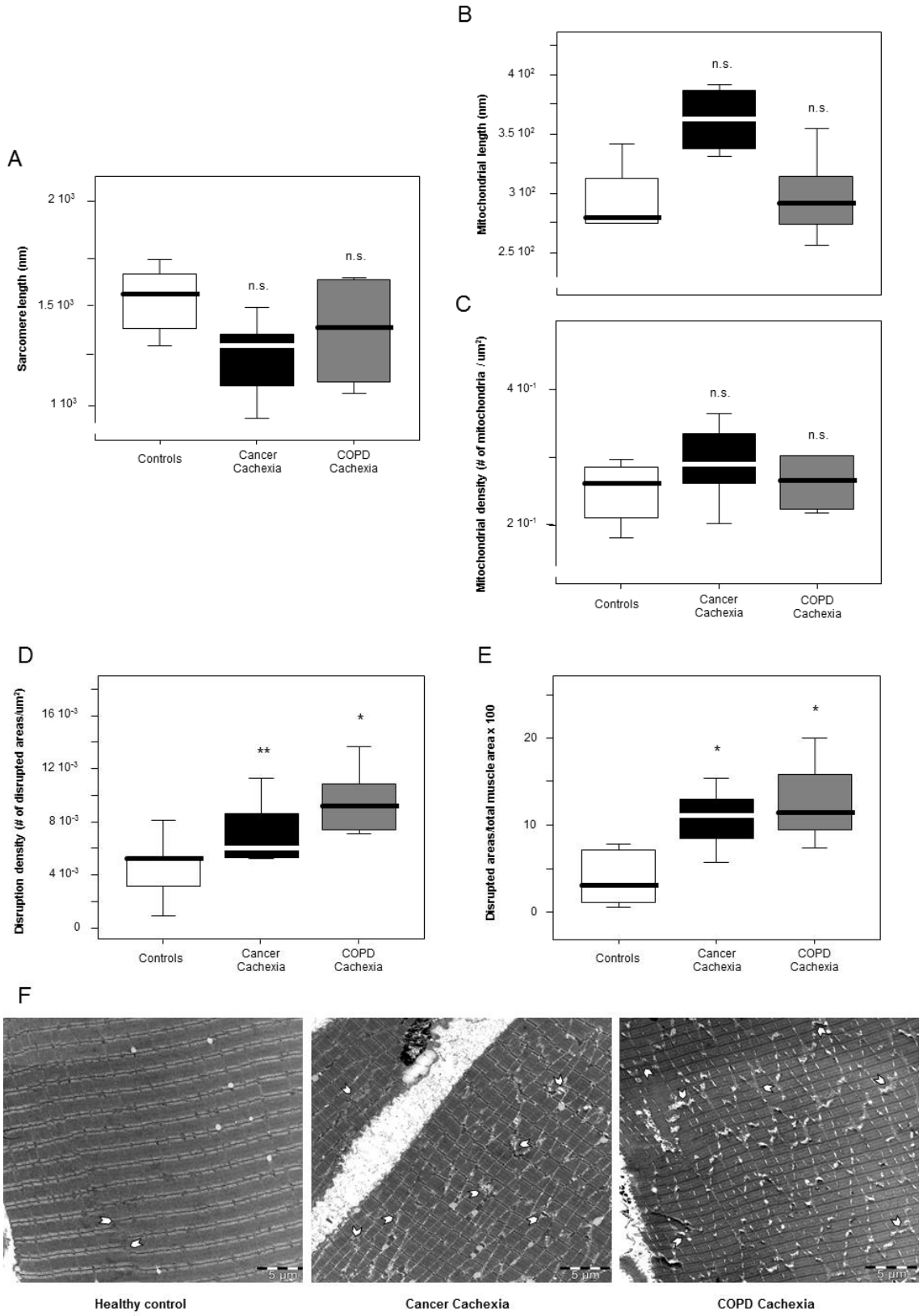

Figure 21. Electron microscopy features. Standard box plots with median (25th and 7th percentiles) and whiskers (at minimum and maximum values. **A.** Sarcomere length, as

measured using electron microscopy, in vastus lateralis of all study subjects. **B.** Mitochondrial length, as measured using electron microscopy, in vastus lateralis of all study subjects. **C.** Mitochondrial density, as measured using electron microscopy, in vastus lateralis of all study subjects. **D.** Sarcomere damage, as measured using the parameter of disruption density, in vastus lateralis of all study subjects. **E.** Sarcomere damage, as measured using the parameter of proportions of disrupted areas, in vastus lateralis of all study subjects. **F.** Representative examples of ultrastructural images of the vastus lateralis in both controls and patients. White arrows point towards disrupted areas of sarcomeres in limb muscles of a control individual (left panel micrograph, x3400), a cancer cachectic patient (medium panel micrograph, x3400), and a cachectic COPD patient (right panel micrograph, x3400).

Statistical significance: n.s., non-significant; *, $p \leq 0.05$; and **, $p \leq 0.01$ between any group of patients and healthy controls.

A. Cancer cachexia patients

	BMI	FFMI	Six-minute walking distance	Muscle total MDA-protein adducts	Plasma TNF-alpha
Plasma, TNF-alpha	r=0.695 p=0.038		r=-0.866 p=0.003		
Muscle, FoxO-1		r=-0.955 p=0.001			
Muscle, total ubiquitinated proteins				r=0.829 p=0.042	r=0.943 p=0.005

B. COPD cachexia patients

	BMI	FFMI	DLco	Kco	PaO_2	Muscle total MDA-protein adducts	Muscle FoxO-3
Muscle, total protein carbonylation	r=-0.652 p=0.016	r=-0.797 p=0.001					
Muscle, NF-kB p65	r=-0.714 p=0.047						
Muscle, p-FoxO-3			r=-0.762 p=0.028	r=-0.738 p=0.037			
Muscle, total ubiquitinated proteins					r=-0.812 p=0.050	r=0.886 p=0.019	
Type I fibers, percentages	r=0.917 p=0.000	r=0.668 p=0.007					r=-0.714 p=0.047
Type II fibers, percentages	r=-0.917 p=0.000	r=-0.668 p=0.007					r=0.714 p=0.047

C. All patients

	BMI	FFMI	FEV_1	Kco	QMVC	Muscle total MDA-protein adducts	Muscle IkB-alpha	MyHC
Muscle, total protein carbonylation	r=-0.464 p=0.034	r=-0.633 p=0.004						
Muscle, p-NF-kB p65			r=-0.676 p=0.016		r=-0.676 p=0.016			
Muscle, total ubiquitinated proteins						r=0.888 p=0.000	r=-0.697 p=0.025	
Type I fibers, percentages	r=0.640 p=0.001	r=0.565 p=0.006		r=0.471 p=0.023				
Type II fibers, percentages	r=-0.640 p=0.001	r=-0.565 p=0.006		r=-0.471 p=0.023				
Proportions of sarcomere disruptions								r=-0.648 p=0.043

Table 7. Significant correlations among variables in the different study patient groups. **A.** Cancer cachexia patients. **B.** COPD cachexia patients.

C All patients. For the sake of clarity in the table, units have been omitted as they are already being shown in the corresponding figures and tables.

2- Results Study #2

2.1- Clinical characteristics

Table 11 illustrates all clinical and functional variables of controls and COPD patients recruited for the diaphragm study. Age did not significantly differ among the study subjects. Body composition as measured by BMI and FFMI was also similar between patients and control subjects. COPD patients exhibited a wide range of airflow limitation from mild-to-moderate to severe disease compared to control subjects. Exercise capacity as measured by six-minute walking distance and cycloergometry and muscle strength as measured by Pdi_{max} and QMVC were decreased in COPD patients compared to healthy controls. Levels of C-reactive protein, of fibrinogen and globular sedimentation velocity were higher in the patients compared to controls.

	Controls	Mild, moderate, and severe COPD
	N = 10	N = 18
Anthropometry		
Age (years)	67 (5)	69 (7)
BMI (kg/m^2)	25 (3)	26 (3)
FFMI (kg/m^2)	18 (1)	18 (1)
Smoking History		
Active, N, %	4, 40	10, 56
Ex-smoker, N, %	5, 50	8, 44
Never smoker, N, %	1, 10	0, 0
Pack/year	46 (13)	59 (30)
Lung function		
FEV_1 (% pred)	81 (8)	62 (15) ***
FVC (% pred)	80 (5)	80 (14)
FEV_1/FVC (%)	70 (5)	57 (8) ***
RV (% pred)	92 (17)	143 (40) ***
TLC (% pred)	98 (18)	101 (15)
RV/TLC	46 (6)	51 (10)
DLco (% pred)	90 (16)	69 (12) **
K_{CO} (% pred)	93 (11)	69 (17) ***
PaO_2 (kPa)	11 (2)	10 (1)
$PaCO_2$ (kPa)	5.5 (0.6)	5.3 (0.8)
Exercise capacity		
VO_2 peak (% pred)	84 (10)	64 (19)***
W*R* peak (% pred)	63 (5)	46 (13) ***
Six-min walking test (m)	511 (69)	425 (101) *
Muscle function		
MIP (cm H_2O)	87 (4)	82 (17)
Pdi_{max} (cm H_2O)	134 (21)	102 (14) ***
QMVC (kg)	37 (1)	34 (3) ***
Blood parameters		
Albumin (g/dL)	4.1 (0.4)	4.0 (0.4)
Total proteins (g/dL)	7.1 (0.9)	6.7 (0.6)
CRP (mg/dL)	0.3 (0.2)	0.6 (0.4) *
Fibrinogen (mg/dL)	316 (23)	470 (178) **
GSV (mm/h)	6.8 (3.5)	15 (9.5) *

Table 11. Anthropometric characteristics and functional status of all the study subjects undergoing thoracotomy.

Values are expressed as mean (standard deviation).

Statistical significance: *, p≤0.05, **, p≤0.01, ***, p≤0.001 between COPD patients and control subjects.

2.2- Muscle biological markers

2.2.1- MicroRNAs expression. In the diaphragm muscle of COPD patients, expression levels of the myomiRs-1, -133, and -206 were significantly reduced compared to controls (Figures 22A-22C), while expression levels of the miRs-486, -27a, -29b, and 181a did not differ between patients and controls (Figures 22D-22G).

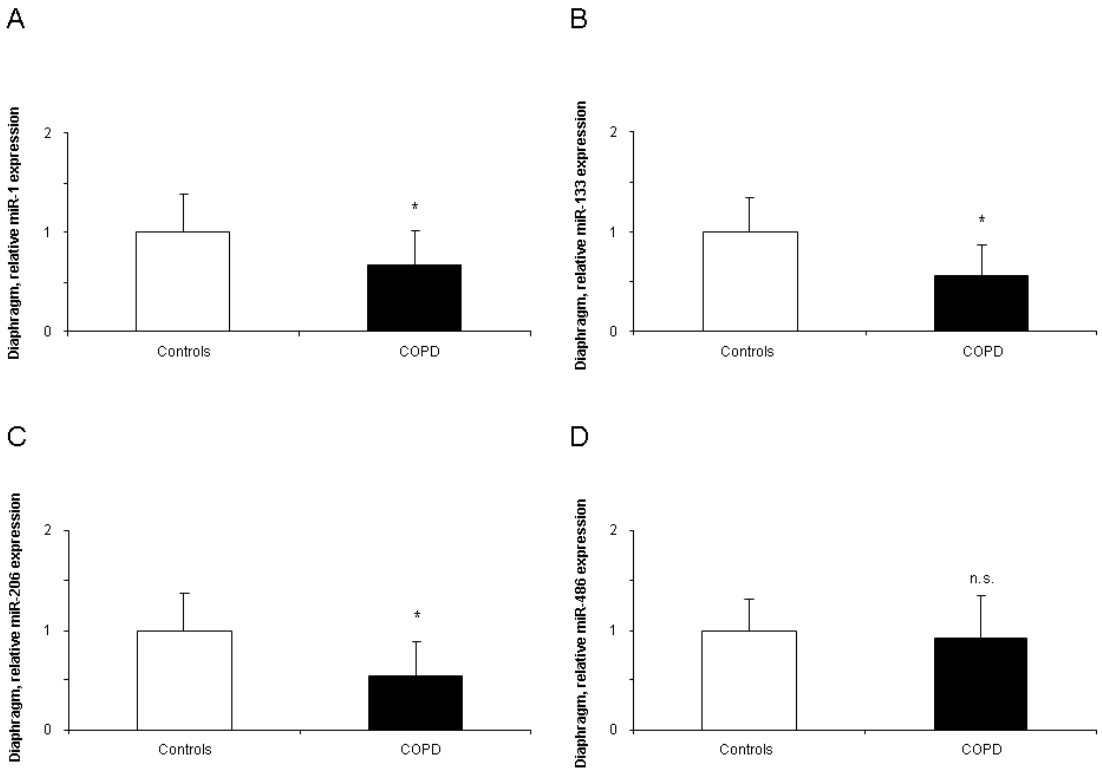

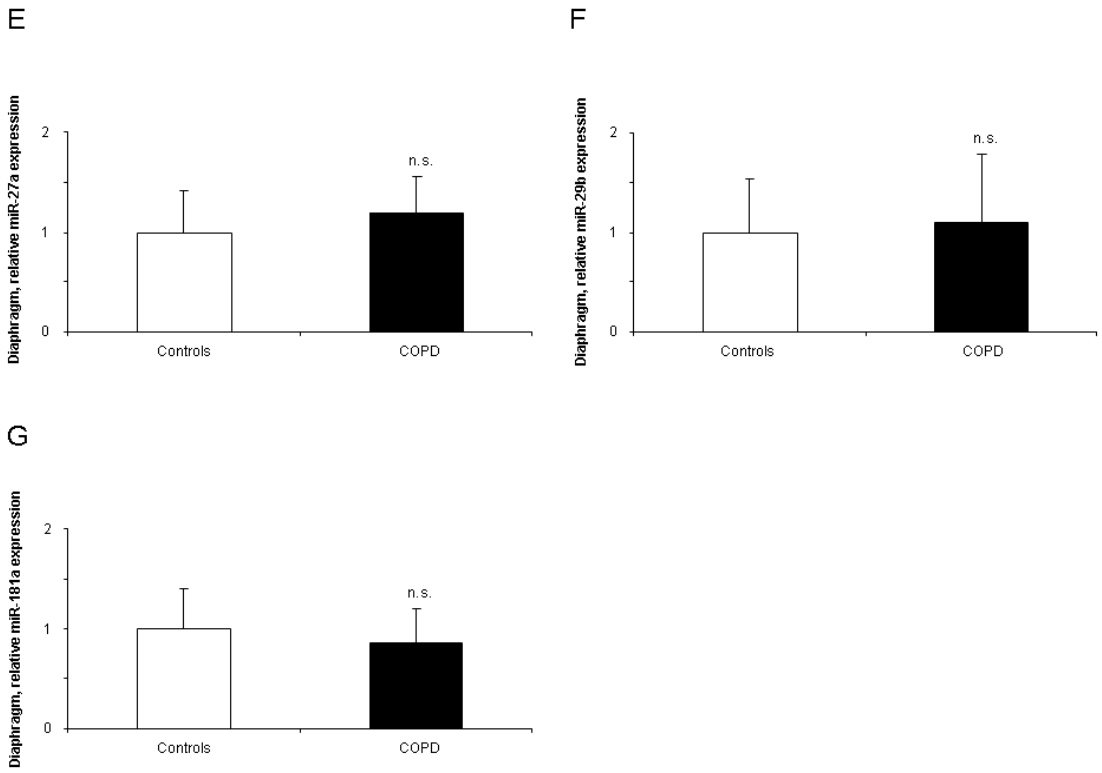

Figure 22. MicroRNAs expression. Mean values and standard deviation (relative expression). **A**. miR-1 expression in diaphragms of COPD and control subjects. **B.** miR-133 expression in diaphragms of COPD and control subjects. **C.** miR-206 expression in diaphragms of COPD and control subjects.**D.** miR-486 expression in diaphragms of COPD and control subjects. **E.** miR-27a expression in diaphragms of COPD and control subjects. **F.** miR-29b expression in diaphragms of COPD and control subjects. **G.** miR-181a expression in diaphragms of COPD and control subjects.

Statistical significance: n.s., non-significant; and *, p≤0.05 between COPD patients and healthy controls.

2.2.2- Histone modifications. Diaphragm levels of total lysine-acetylated proteins and mRNA expression levels of the HTA p300 did not differ between COPD patients and control subjects (Figure 23). Compared to controls, only protein levels of HDAC 4 was found significantly increased in the diaphragm muscle of COPD patients (Figure 24C). Diaphragm protein levels of HDAC3, 6 and SIRT1 did not differ between patients and controls (Figures 24A-24B and 24D).

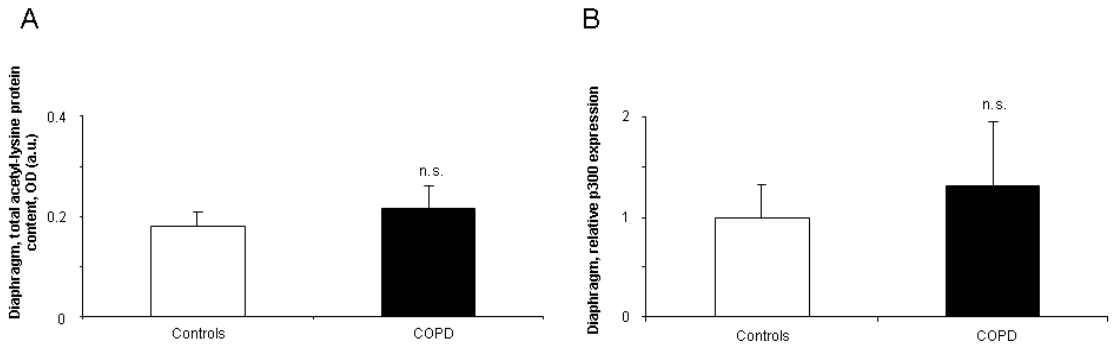

Figure 23. Histone modifications. Mean values and standard deviation. **A**. Levels of total lysine acetylated proteins in diaphragms of COPD and control subjects. **B.** Relative expression of the nuclear cofactor p300 in diaphragms of COPD and control subjects.
Statistical significance: n.s., non-significant between COPD patients and healthy controls.

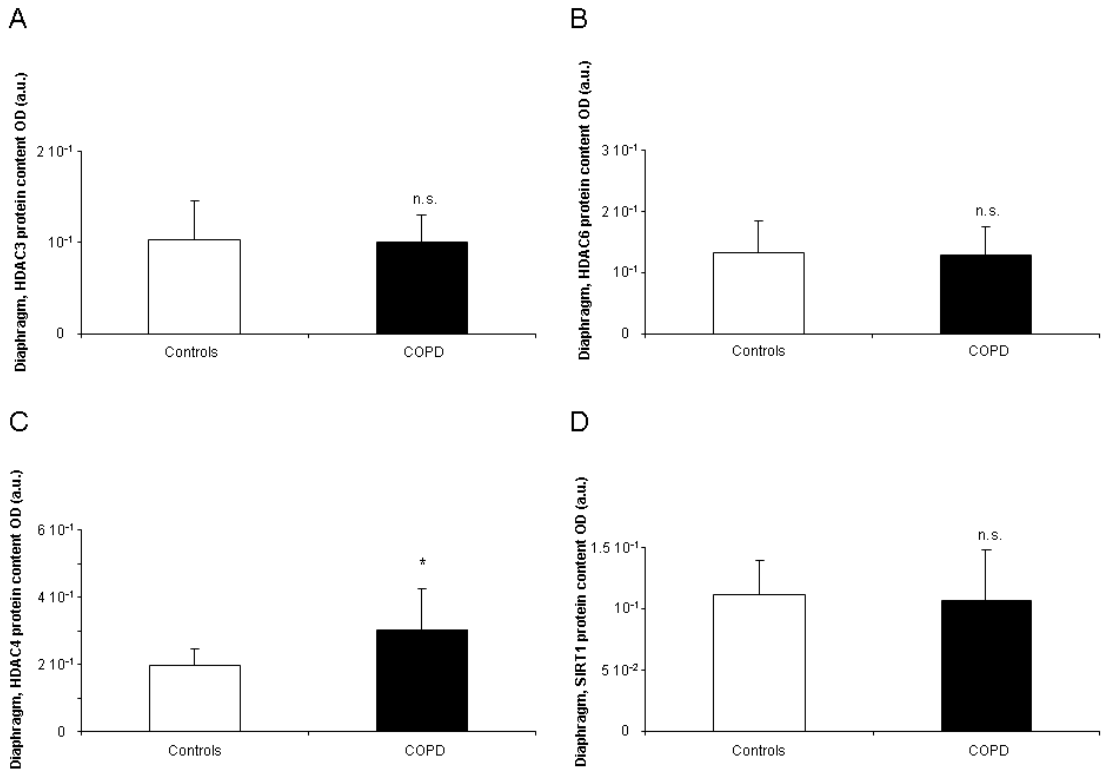

Figure 24. Histone modifications. Mean values and standard deviation. **A.** Protein levels of HDAC3 in diaphragms of COPD and control subjects. **B.** Protein levels of HDAC6 in

diaphragms of COPD and control subjects. **C.** Protein levels of HDAC4 in diaphragms of COPD and control subjects. **D.** Protein levels of SIRT1 in diaphragms of COPD and control subjects.
Statistical significance: n.s., non-significant; and *, p≤0.05 between COPD patients and healthy controls.

2.2.3- Myogenic transcription factors. Protein levels of MEF2C were increased in diaphragm muscle of patients compared to controls (Figure 25A), while protein levels of MEF2D and YY1 did not differ between COPD patients and healthy controls (Figures 25B-25C).

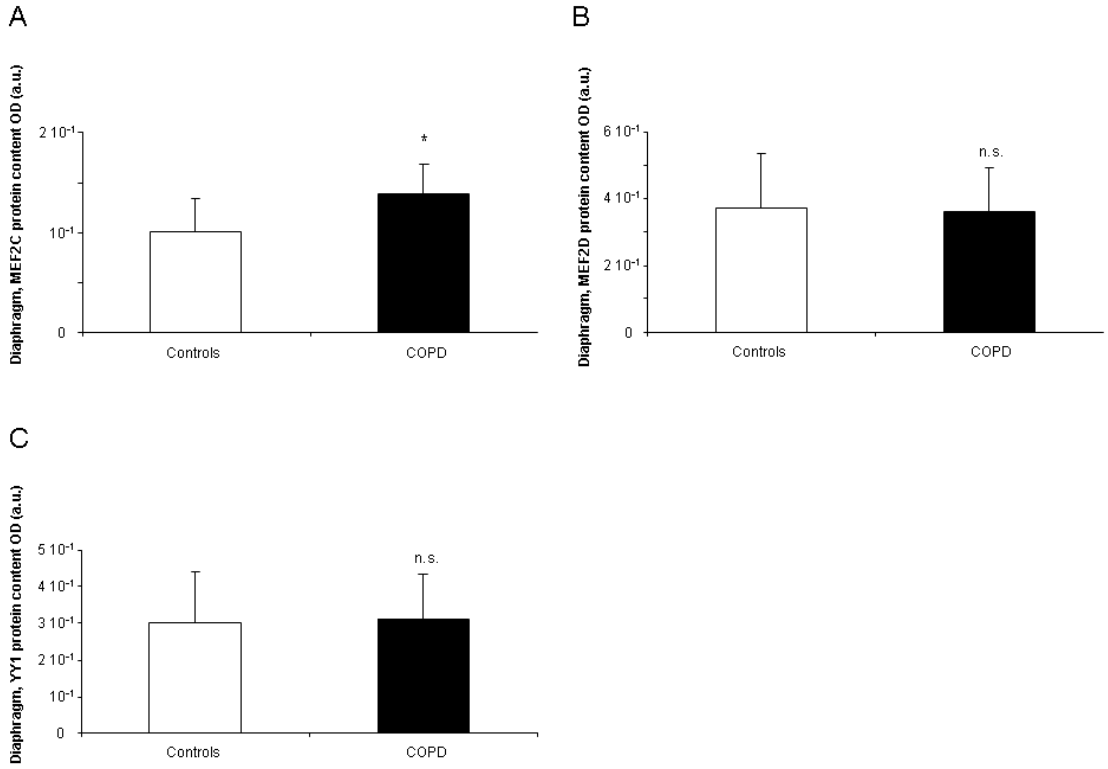

Figure 25. Myogenic transcription factors. Mean values and standard deviation. **A.** Protein levels of MEF2C in diaphragms of COPD and control subjects. **B.** Protein levels of MEF2D in diaphragms of COPD and control subjects. **C.** Protein levels of YY1 in diaphragms of COPD and control subjects
Statistical significance: n.s., non-significant between COPD patients and healthy controls.

2.2.4- Expression of SUMO. In diaphragm, no differences in mRNA expression levels of SUMO2 and SUMO3 were found between patients and controls (Figure 26).

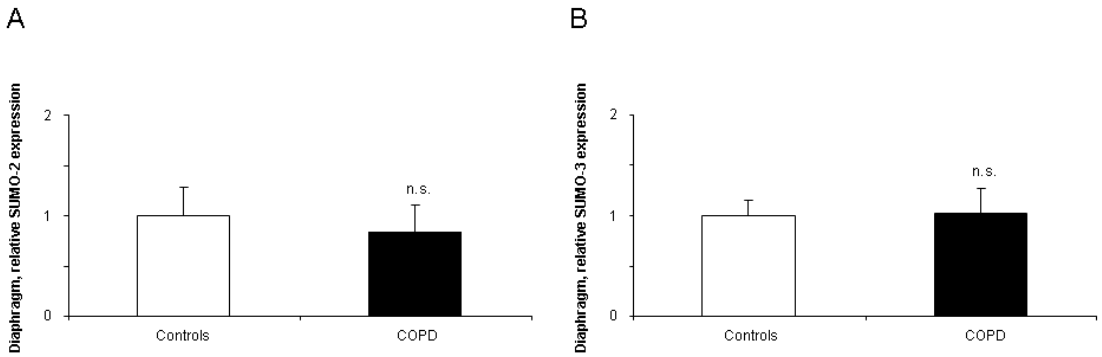

Figure 26. SUMO expression. Mean values and standard deviation (relative expression) of: **A.** SUMO-2 expression in diaphragms of COPD and control subjects. **B.** SUMO-3 expression in diaphragms of COPD and control subjects.

Statistical significance: n.s., non-significant between COPD patients and healthy controls.

2.3- Muscle structure

Fiber type composition. In the respiratory muscle, no significant differences were observed in either fiber type proportions or sizes between patients and controls (Table 12 and Figure 27). In the diaphragm of all COPD patients, an inverse correlation was found between proportions of type I fibers and FEV_1 (r=-0.648, p=0.004).

	Controls N= 10	**Mild, moderate and severe COPD N= 18**
Muscle fiber type composition		
Type I fibers, %	48 (5)	52 (7)
Type II fibers, %	52 (5)	48 (7)
Type I fibers, CSA (μm^2)	2407 (782)	2483 (716)
Type II fibers, CSA (μm^2)	2641 (713)	2410 (983)

Table 12. Fiber type composition in diaphragm muscle of all study subjects.
Values are expressed as mean (standard deviation).

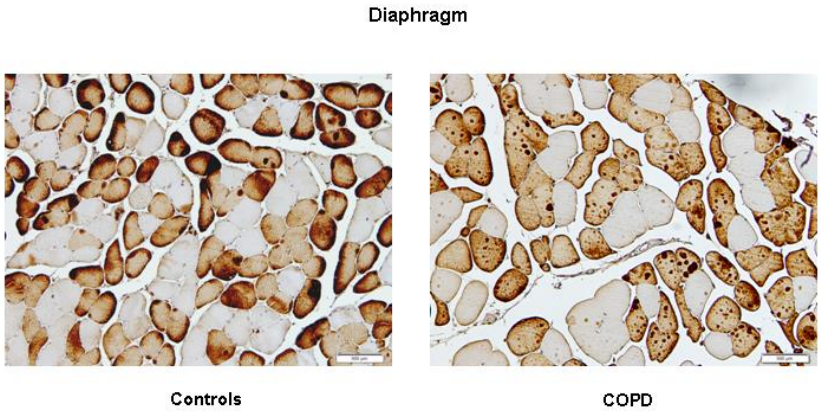

Figure 27. Muscle fiber type compostion. Representative immunohistochemical preparations corresponding to the staining of type II fibers in the diaphragms of a healthy control subject (left panel) and a patient with moderate-to-severe COPD (right panel).

3- Results Study #3

3.1- Clinical characteristics

Table 13 illustrates all clinical and functional variables of controls and COPD patients recruited in the study. Age did not significantly differ among the study subjects. Body composition as measured by BMI and FFMI was significantly reduced in the severe muscle-wasted patients compared to the severe non-wasted patients and the controls, and in the latter group compared to moderate COPD. COPD patients exhibited a range of airflow limitation from moderate to severe disease, both groups of severe patients showed functional signs of severe emphysema compared to control subjects and moderate COPD. Exercise capacity as measured by six-minute walking distance and cycloergometry and muscle strength as measured by QMVC were decreased in all groups of COPD patients compared to healthy controls and in both groups of severe patients compared to moderate COPD. Levels of fibrinogen, C-reactive protein, and globular sedimentation velocity were higher in the patients, especially the muscle-wasted, compared to controls.

	Controls	COPD patients		
		Moderate	Severe non-wasted	Severe muscle-wasted
	N = 19	N = 11	N = 18	N = 12
Anthropometry				
Age (years)	65 (8)	68 (6)	67 (6)	68 (6)
BMI (kg/m^2)	26 (3)	28 (3)	24 (3) ¶¶	18 (2) ***, ¶¶¶, §§§
FFMI (kg/m^2)	19 (2)	20 (2)	18 (2)	14 (2)***, ¶, §§§
Smoking History				
Active, N	6	7	5	4
Ex-smoker, N	8	4	13	8
Never smoker, N	5	0	0	0
Pack/year	54 (20)	58 (32)	60 (20)	64 (22)
Lung function				
FEV_1 (% pred)	93 (12)	55 (2) ***	25 (8) ***, ¶¶¶	29 (10) ***, ¶¶¶
FVC (% pred)	88 (9)	75 (17) **	52 (15) ***, ¶¶	56 (15) ***
FEV_1/FVC (%)	73 (4)	58 (5) ***	37 (6) ***, ¶¶¶	42 (11) ***, ¶¶¶
RV (% pred)	105 (18)	130 (49)	216 (64) ***, ¶	210 (66) ***
TLC (% pred)	101 (12)	102 (17)	113 (17) *	108 (13)
RV/TLC	49 (23)	54 (7)	70 (8) ***	67 (10) **
DLco (% pred)	89 (14)	80 (15)	42 (23) ***, ¶¶¶	40 (21) ***, ¶¶¶
K_{CO} (% pred)	87 (16)	76 (17)	60 (20) ***	56 (21) ***
PaO_2 (kPa)	11.6 (1.1)	9.3 (1.3) ***	9.3 (1.2) ***	8.9 (1) ***
$PaCO_2$ (kPa)	5.2 (0.5)	5.4 (0.9)	5.7 (0.6) **	5.7 (0.6) *
Exercise capacity & muscle function				
VO_2 peak (% pred)	87 (10)	57 (42) ***	43 (21) ***, ¶	37 (11) ***, ¶
W*R* peak (% pred)	81 (21)	77 (33)	39 (12) ***, ¶	36 (18) ***, ¶
Six-min walking test (m)	508 (71)	447 (100) *	430 (31) **	408 (95) ***
QMVC (kg)	39 (2)	32 (3) ***	27 (1) ***, ¶¶¶	27 (1) ***, ¶¶¶
Blood parameters				
Albumin (g/dL)	4.3 (0.4)	4.3 (0.2)	4.5 (0.4)	4.2 (0.6)
Total proteins (g/dL)	7.2 (0.5)	7 (0.6)	7.4 (0.5)	7.2 (0.4)
CRP (mg/dL)	0.3 (0.2)	0.3 (0.1)	1.0 (0.5) *	2.6 (3) ***, §
Fibrinogen (mg/dL)	311 (35)	367 (56) *	415 (60)***	457 (99)***, ¶
GSV (mm/h)	6 (4)	17 (13) **	15 (12) *	42 (25) ***, ¶¶, §§§

Table 13. Anthropometric characteristics and functional status of all the study subjects undergoing vastus laterales biopsy.

Values are expressed as mean (standard deviation).

Statistical significance: *, p≤0.05; **, p≤0.01; ***, p≤0.001 between any of the groups of patients with COPD and the control subjects; ¶, p≤0.05, ¶¶, p≤0.01, ¶¶¶, p≤0.001 between patients with severe and moderate COPD; §, p≤0.05; §§§, p≤0.001 between patients with severe COPD with and without muscle wasting.

3.2- Muscle biological markers

3.2.1- MicroRNAs expression. Compared to healthy controls, expression levels of the microRNAs miR-1, -133, -206, and -486 were significantly upregulated in the limb muscle of the non-wasted severe COPD patients (Figures 28A-28D), and in this group, miR-206 and -486 expression was also significantly increased compared to moderate COPD (Figures 28C-28D). In moderate COPD, levels of miR-1 were also upregulated in the limb muscle compared to control subjects (Figure 28A). However, in the muscle-wasted severe patients, expression levels of the same microRNAs were significantly decreased in the vastus lateralis compared to levels in the non-wasted patients (Figures 28A-28D). The expression of miR-27a, -29b, and -181a was upregulated in the limb muscles of non-wasted severe COPD patients compared to the controls, whereas the expression of the same microRNAs was reduced in muscle-wasted patients compared to non-wasted patients (Figures 28E-28G). When both non-wasted and muscle-wasted severe patients were analyzed together, significant direct correlations were detected between BMI and levels of miR-133, -206, -486, and -29b (Figure 29), between FFMI and miR-206 and -486 (Figures 30B-30C), while almost significant associations were found between FFMI and miR-133 and -29b (Figures 30A and 30D).

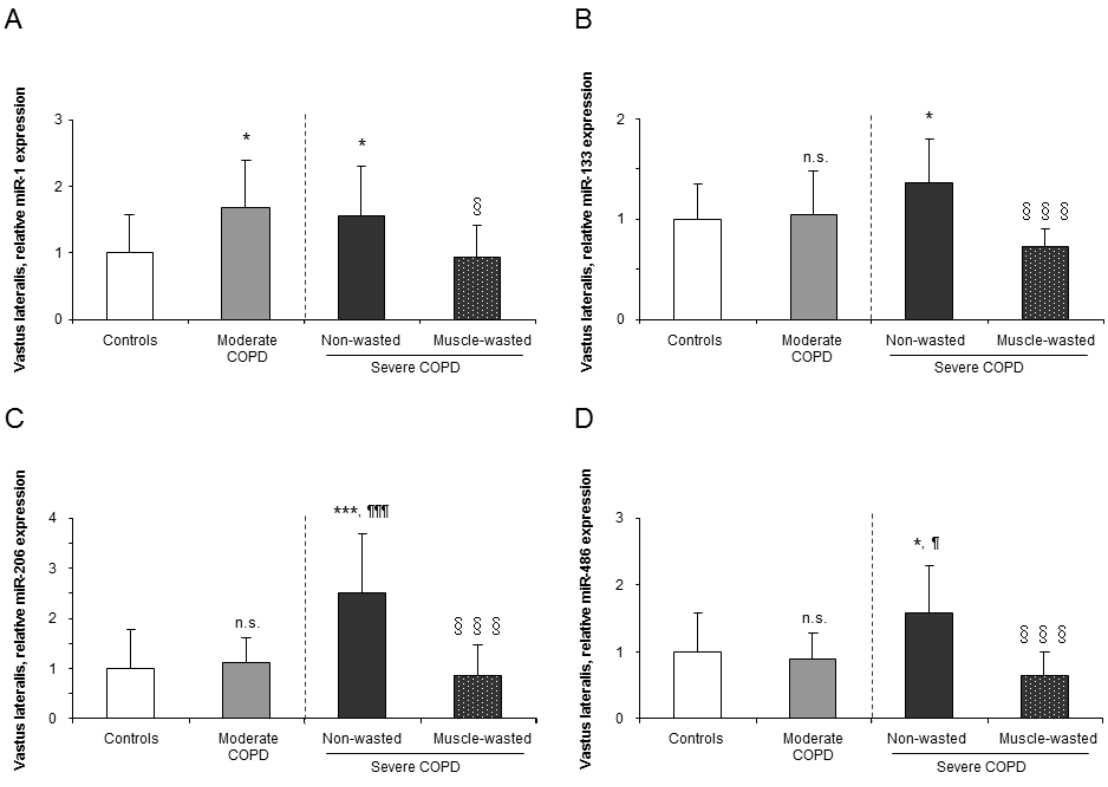

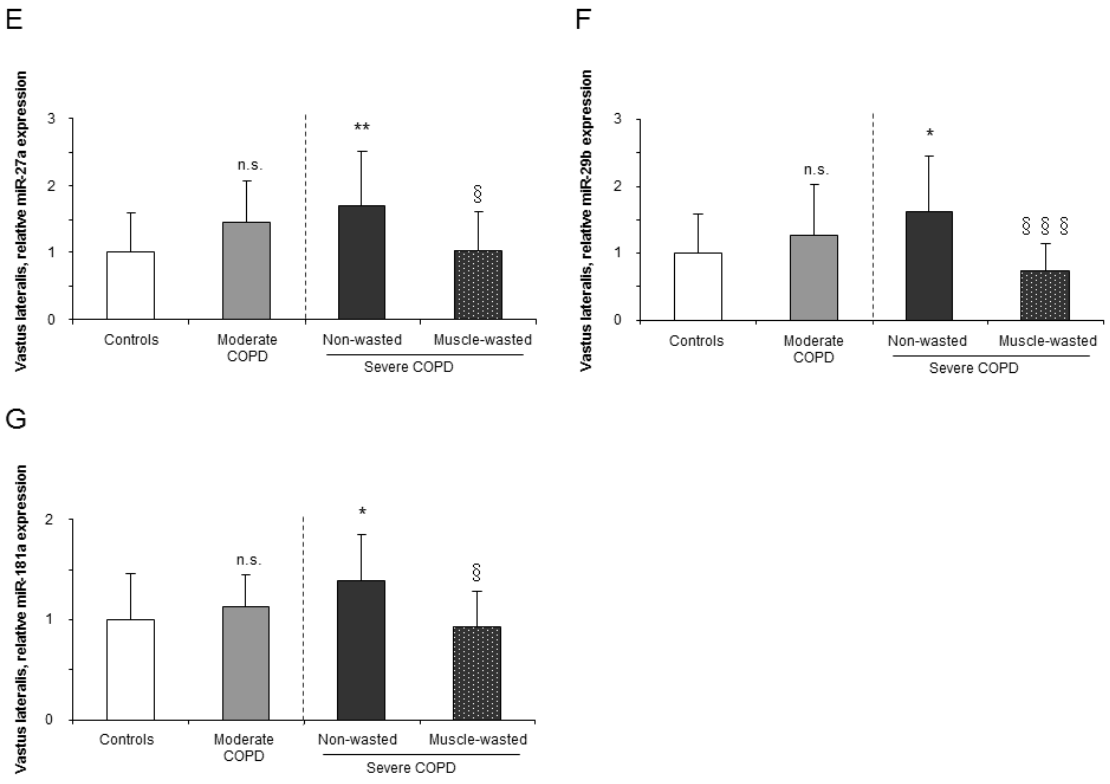

Figure 28. MicroRNAs expression. Mean values and standard deviation (relative expression). **A**. miR-1 expression in vastus lateralis of all study groups. **B.** miR-133 expression in vastus lateralis of all study groups. **C.** miR-206 expression in vastus lateralis of all study groups. **D.** miR-486 expression in vastus lateralis of all study groups. **E.** miR-27a expression in vastus lateralis of all the study subjects. **F.** miR-29b expression in vastus lateralis of all study groups. **G.** miR-181a expression in vastus lateralis of all study groups.

Statistical significance: n.s., non-significant; *, p≤0.05; **, p≤0.01; ***, p≤0.001 between any of the groups of patients with COPD and the control subjects; ¶, p≤0.05; ¶¶¶, p≤0.001 between patients with severe and moderate COPD; §, p≤0.05; §§§, p≤0.001 between patients with severe COPD with and without muscle wasting.

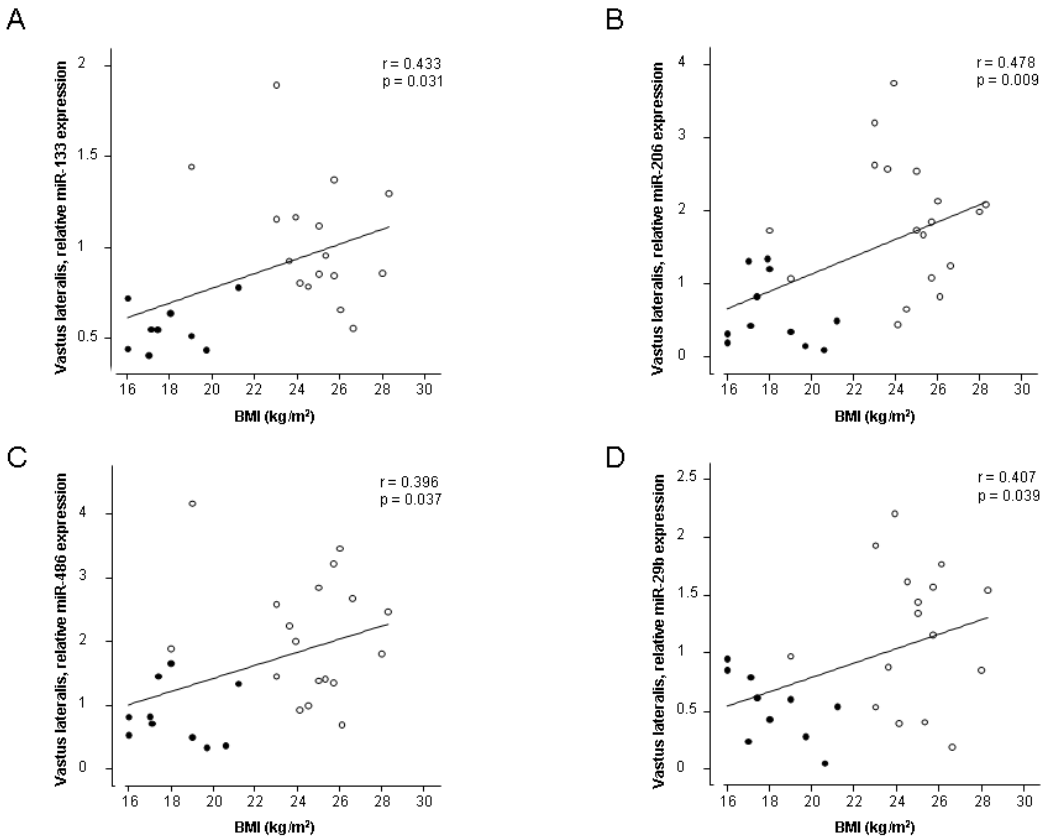

Figure 29. MicroRNAs correlations. Significant positive correlations were observed in vastus lateralis of all severe COPD patients between BMI (kg/m^2) and expression levels of: **A.** miR-133. **B.** miR-206. **C.** miR-486. **D.** miR-29b. In all panels, cachectic severe COPD patients are represented by dark dots, while patients without muscle wasting are represented by open dots.

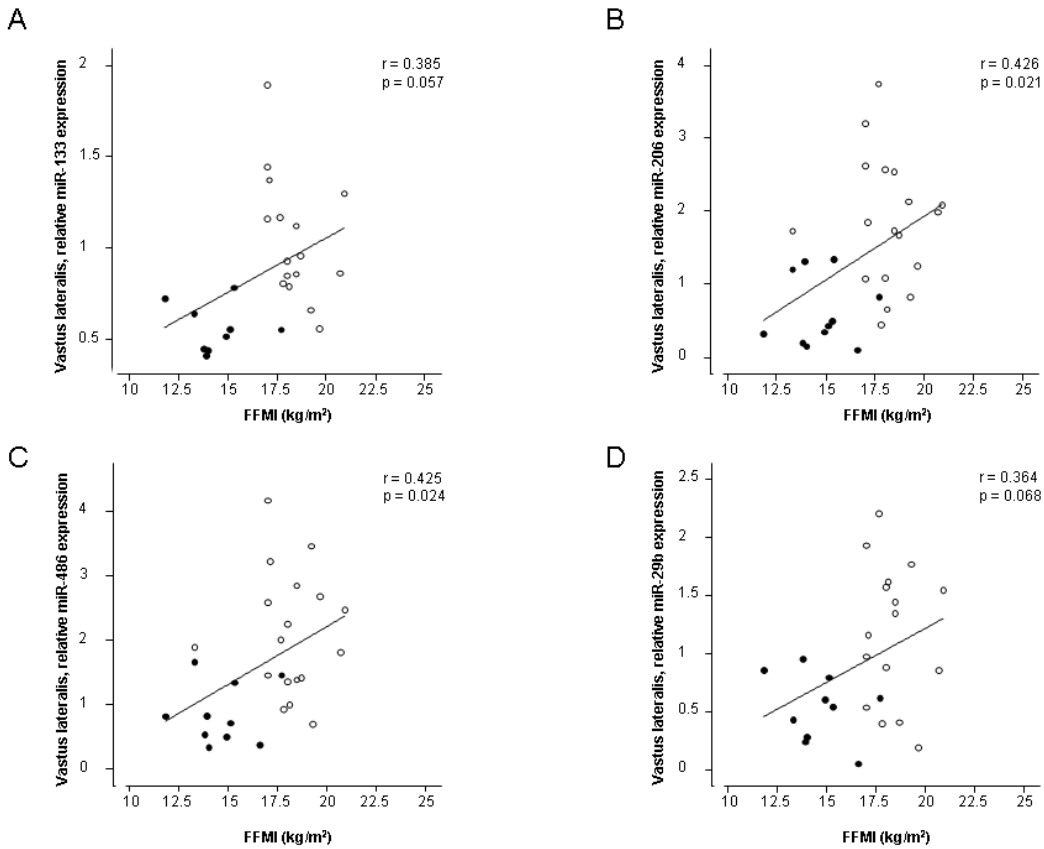

Figure 30. MicroRNAs correlations. Significant and almost significant positive correlations were observed in vastus lateralis of all severe COPD patients between FFMI (kg/m^2) and expression levels of: **A.** miR-133. **B.** miR-206. **C.** miR-486. **D.** miR-29b. In all panels, cachectic severe COPD patients are represented by dark dots, while patients without muscle wasting are represented by open dots.

3.2.2- Histone modifications. Levels of total lysine-acetylated proteins were significantly increased in the vastus lateralis of muscle-wasted severe COPD patients compared to both moderate and non-wasted patients and healthy controls (Figure 31A). Expression levels of HAT p300 did not differ between any of the study groups (Figure 31B). Importantly, in vastus lateralis of muscle-wasted severe patients, protein levels of HDAC3 and SIRT1 were decreased compared to both healthy controls and non-wasted patients, while no differences in these markers were detected in any of the other group of patients and the controls (Figures 32A and 32D). Several positive correlations were observed between SIRT1 protein levels and the expression of miR-133, -206, -486, -181a and HDAC3 in the vastus lateralis of both non-wasted and muscle-wasted severe COPD patients (Figure 33).

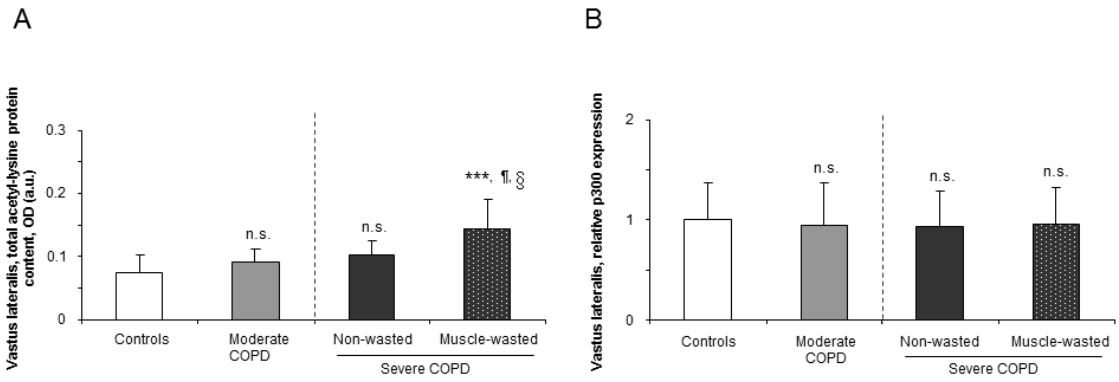

Figure 31. Histone modifications. Mean values and standard deviation. **A.** Levels of total lysine-acetylated proteins in vastus lateralis of all study groups. **B.** Relative expression of the nuclear cofactor p300 in vastus lateralis of all study groups.

Statistical significance: n.s., non-significant; ***, p≤0.001 between any of the groups of patients with COPD and the control subjects; ¶, p≤0.05 between patients with severe and moderate COPD; §, p≤0.05 between patients with severe COPD with and without muscle wasting.

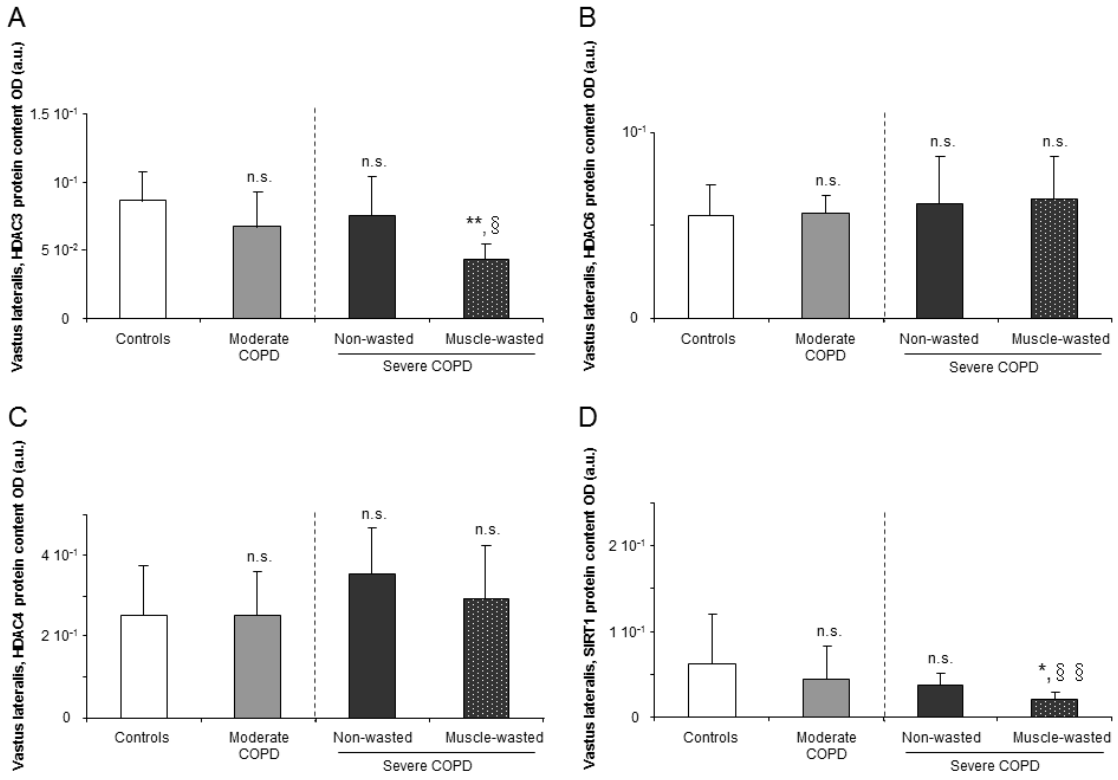

Figure 32. Histone modifications. Mean values and standard deviation. **A.** Protein levels of HDAC3 in vastus lateralis of all study groups. **B.** Protein levels of HDAC6 in vastus lateralis of all study groups. **C.** Protein levels of HDAC4 in vastus lateralis of all study groups. **D.** Protein levels of SIRT1 in vastus lateralis of all study groups.

Statistical significance: n.s., non-significant; *, p≤0.05; **, p≤0.01 between any of the groups of patients with COPD and the control subjects; §, p≤0.05; §§, p≤0.01 between patients with severe COPD with and without muscle wasting.

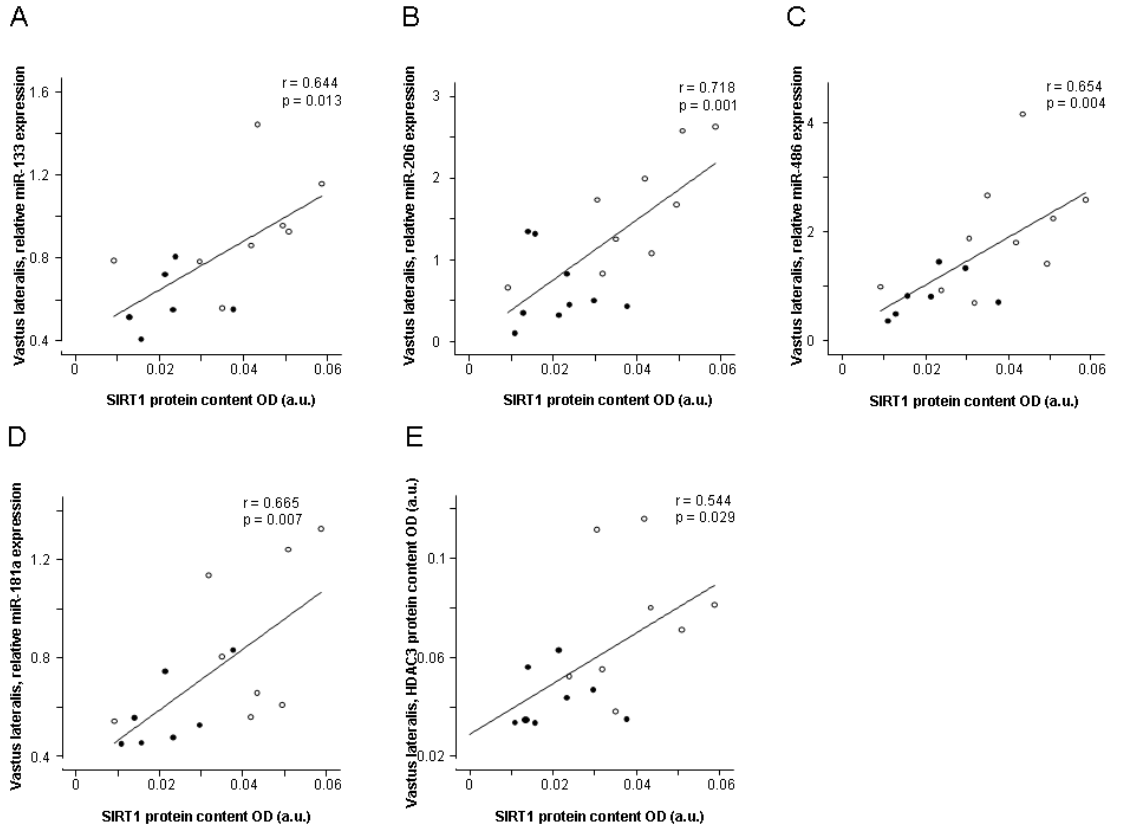

Figure 33. SIRT1 correlations. Significant positive correlations were found in vastus lateralis of all severe COPD patients between protein levels of SIRT1 and: **A.** Expression of miR-133. **B.** Expression of miR-206. **C.** Expression of miR-486. **D.** Expression of miR-181a. **E.** Protein levels of HDAC3. In all panels, cachectic severe COPD patients are represented by dark dots, while patients without muscle wasting are represented by open dots.

3.2.3- Myogenic transcription factors. Protein levels of MEF2C, MEF2D and YY1 did not significantly differ in the vastus lateralis of any study group (Figure 34).

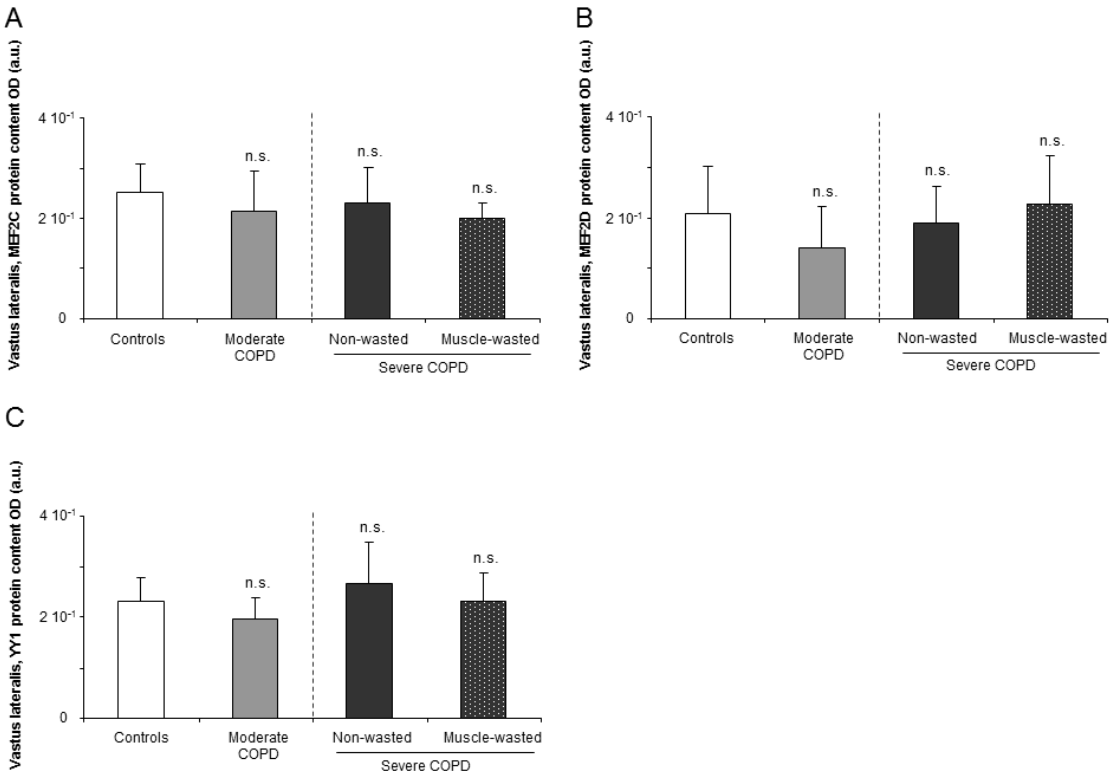

Figure 34. Myogenic transcription factors. Mean values and standard deviation. **A.** Protein levels of MEF2C in vastus lateralis of all study groups. **B.** Protein levels of MEF2D in vastus lateralis of all study groups. **C.** Protein levels of YY1 in vastus lateralis of all study groups.
Statistical significance: n.s., non-significant among study groups.

3.2.4- Expression of SUMO. Vastus lateralis mRNA expression levels of SUMO2 and SUMO3 did not differ between any study group (Figure 35).

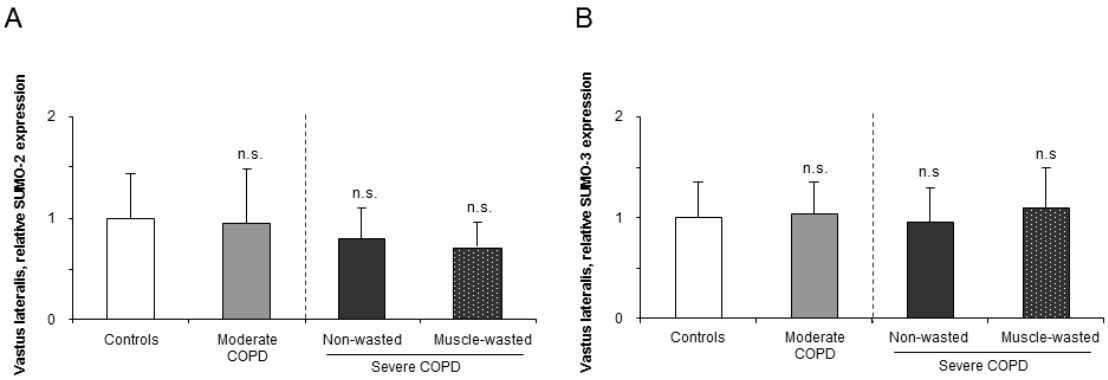

Figure 35. SUMO expression. Mean values and standard deviation. **A.** Relative expression of SUMO-2 in vastus lateralis of all study groups. **B.** Relative expression of SUMO-3 in vastus lateralis of all study groups.

Statistical significance: n.s., non-significant among study groups.

3.3- Muscle structure

Fiber type composition. Compared to controls, proportions of type I fibers were significantly decreased in limb muscles of both groups of severe COPD patients (Table 14). In addition, muscle-wasted severe COPD patients also showed reduced proportions of type I fibers compared to moderate COPD patients (Table 14). Interestingly, the size of type II fibers was decreased in vastus lateralis of muscle-wasted patients compared to healthy controls and non-wasted severe COPD patients (29% and 38% reduction, respectively, Table 14 and Figure 36). Moreover, in the vastus lateralis of both non-wasted and muscle-wasted severe patients, direct correlations were observed between type I fiber proportions and FFMI ($r=0.645$, $p=0.024$) and between the size of type II fibers and BMI ($r=0.555$, $p=0.006$).

	Controls N= 19	COPD		
		Moderate N= 11	Severe non-wasted N= 18	Severe muscle-wasted N= 12
Muscle fiber type composition				
Type I fibers, %	39 (6)	37 (11)	28 (9) ***	23 (10) ***, ¶
Type II fibers, %	61 (6)	63 (11)	72 (9) ***	77 (10) ***, ¶
Type I fibers, CSA (μm^2)	2698 (894)	2482 (966)	2513 (840)	2480 (769)
Type II fibers, CSA (μm^2)	2915 (755)	2785 (1269)	2569 (920)	1819 (456) ***, §

Table 14. Fiber type composition in vastus lateralis muscle of all the study subjects.
Values are expressed as mean (standard deviation)
Statistical significance: ***, p≤0.001 between any of the groups of patients with COPD and the control subjects; ¶, p≤0.05, between patients with severe and moderate COPD; §, p≤0.05 between muscle-wasted and non-wasted patients with severe COPD.

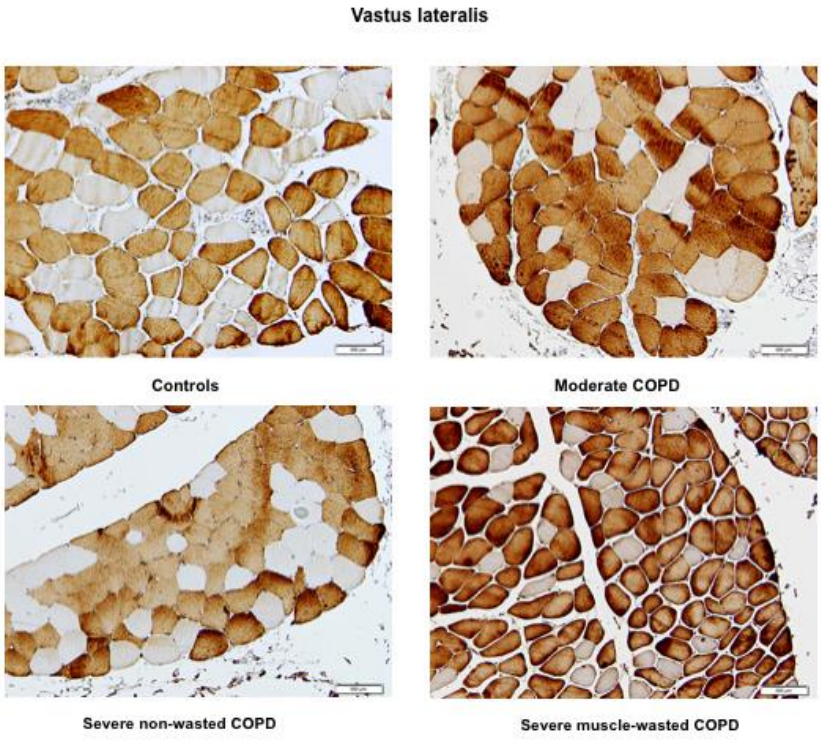

Figure 36. Muscle fiber type composition. Representative immunohistochemical preparations corresponding to the staining of type II fibers in the vastus laterales of a healthy control subject (top left panel), and of patients with moderate (top right panel), severe non-wasted (bottom left panel) and severe muscle-wasted COPD (bottom left panel).

4- Results Study #4

4.1- Clinical characteristics

Table 15 illustrates all clinical and functional variables of controls and COPD patients recruited in the study. No significant differences were observed in age, smoking history, or body composition between patients and control subjects. COPD patients exhibited mild airflow limitation and diffusion capacity impairment. Exercise capacity as measured by six-minute walking distance and cycloergometry, and muscle strength were mildly decreased in the COPD patients compared to healthy controls. Levels of fibrinogen and globular sedimentation velocity were moderately increased in the patients compared to controls.

	Controls	Mild COPD
	N = 13	N = 13
Anthropometry		
Age (years)	67 (5)	70 (6)
BMI (kg/m^2)	25 (3)	25 (3)
FFMI (kg/m^2)	18 (2)	18 (1)
Smoking History		
Active, N, %	6, 46	7, 54
Ex-smoker, N, %	4, 31	6, 46
Never smoker, N, %	3, 23	0, 0
Pack/year	53 (20)	50 (22)
Lung function		
FEV_1 (% pred)	90 (11)	72 (4) ***
FVC (% pred)	92 (11)	80 (7) **
FEV_1/FVC (%)	72 (4)	62 (5) ***
RV (% pred)	105 (11)	121 (28)
TLC (% pred)	104 (11)	101 (9)
RV/TLC (%)	44 (5)	48 (10)
DLco (% pred)	91 (15)	76 (15) *
K_{CO} (% pred)	90 (15)	73 (11) **
PaO_2 (kPa)	11.6 (1.2)	11.1 (1.5)
$PaCO_2$ (kPa)	5.5 (0.4)	5.2 (0.3)
Exercise capacity & muscle force		
VO_2 peak (% pred)	92 (14)	74 (10) *
W*R* peak (% pred)	96 (18)	76 (8) *
Six-min walking test (m)	517 (57)	426 (17) ***
QMVC (kg)	38 (2)	36 (1) ***
Blood parameters		
Albumin (g/dL)	4.2 (0.4)	4.1 (0.5)
Total proteins (g/dL)	7.2 (0.5)	6.9 (0.8)
CRP (mg/dL)	0.3 (0.2)	0.4 (0.2)
Fibrinogen (mg/dL)	309 (36)	350 (50) *
GSV (mm/h)	5 (4)	13 (11) *

Table 15. Anthropometric characteristics and functional status of all the study subjects undergoing vastus laterales biopsy.

Values are expressed as mean (standard deviation).

Statistical significance: *, p≤0.05, **, p≤0.01, ***, p≤0.001 between COPD patients and control subjects.

4.2- Muscle biological markers

4.2.1- MicroRNAs expression. Compared to healthy controls, expression levels of miR-1 were significantly greater in the vastus lateralis of the patients than in the control subjects (Figure 37A). Nevertheless, the expression of miR-133, -206, -486, -27a, -29b, and -181a did not significantly differ between patients and controls (Figures 37B-37G). Among the patients, significant positive correlations were found between muscle miR-1 expression levels and both the degree of airway obstruction (FEV_1) and quadriceps muscle force (Figure 38). Additionally, positive correlations were also observed between miR-1 expression levels and those of miR-133 (r=0.809, p=0.001) and miR-486 (r=0.712, p=0.009) in the vastus lateralis of the patients.

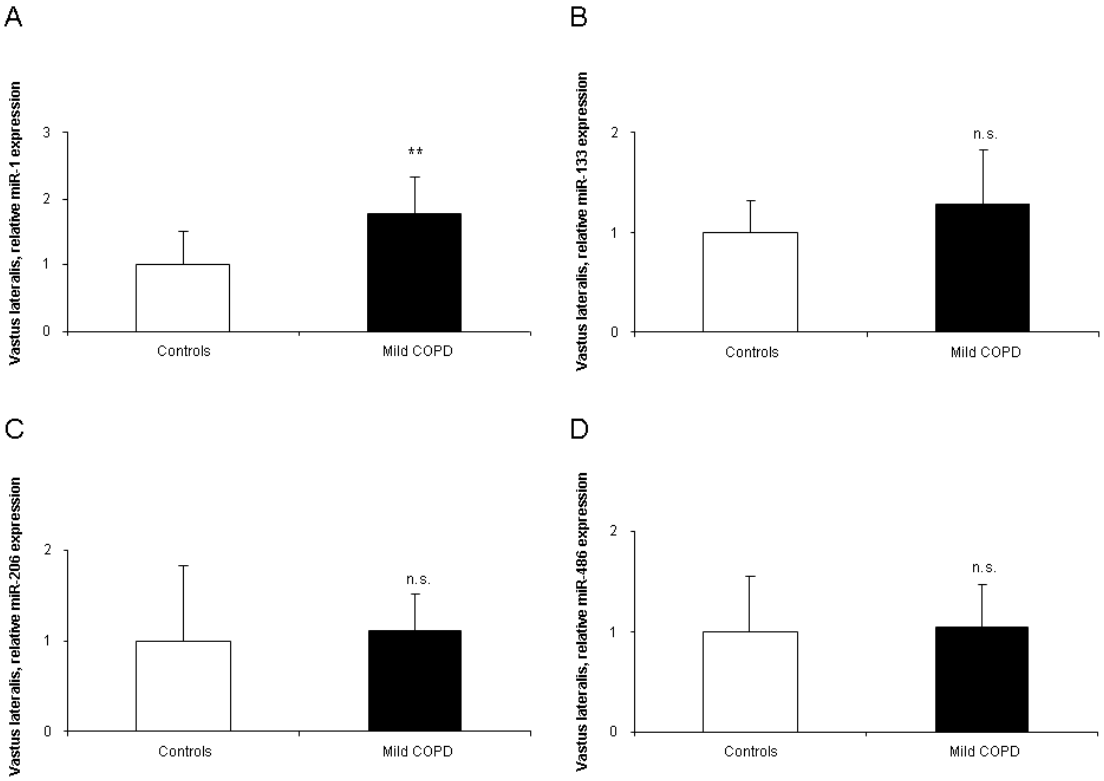

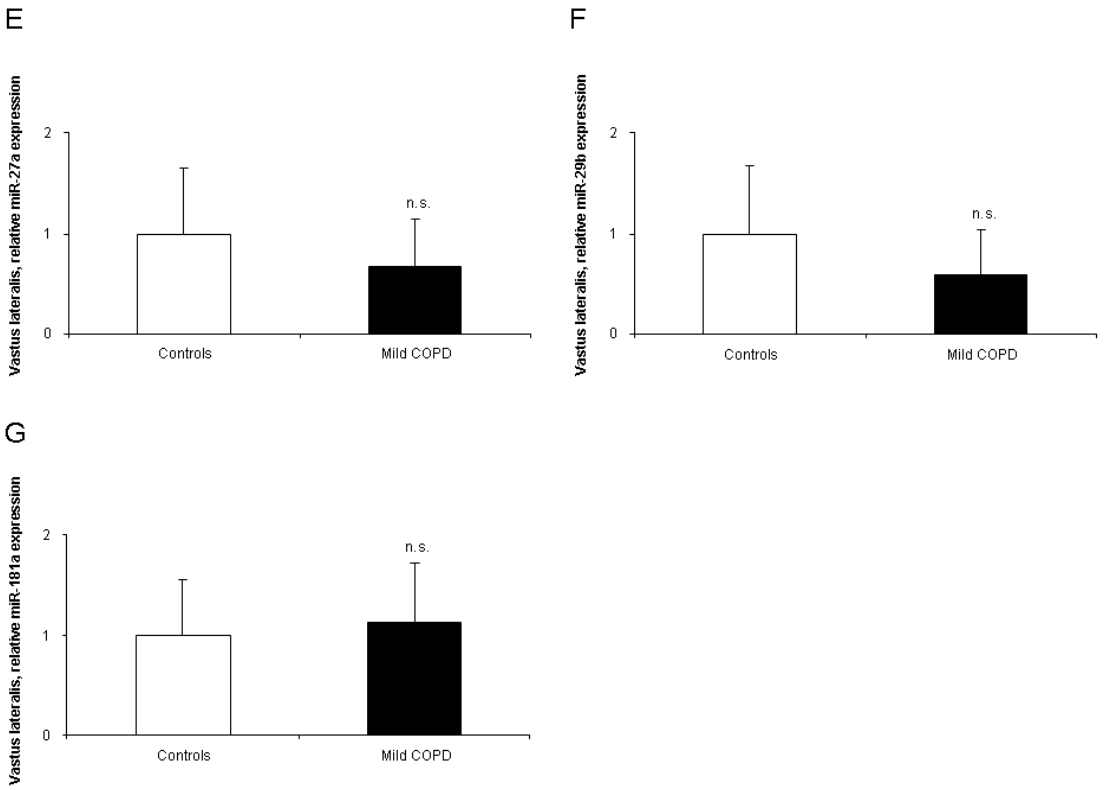

Figure 37. MicroRNAs expression. Mean values and standard deviation (relative expression) **A.** miR-1 expression in vastus lateralis of COPD and control subjects. **B.** miR-133 expression in vastus lateralis of COPD and control subjects. **C.** miR-206 expression in vastus lateralis of COPD and control subjects.**D.** miR-486 expression in vastus lateralis of COPD and control subjects. **E.** miR-27a expression in vastus lateralis of COPD and control subjects. **F.** miR-29b expression in vastus lateralis of COPD and control subjects. **G.** miR-181a expression in vastus lateralis of COPD and control subjects.

Statistical significance: n.s., non-significant; and **, p≤0.01 between COPD patients and healthy controls.

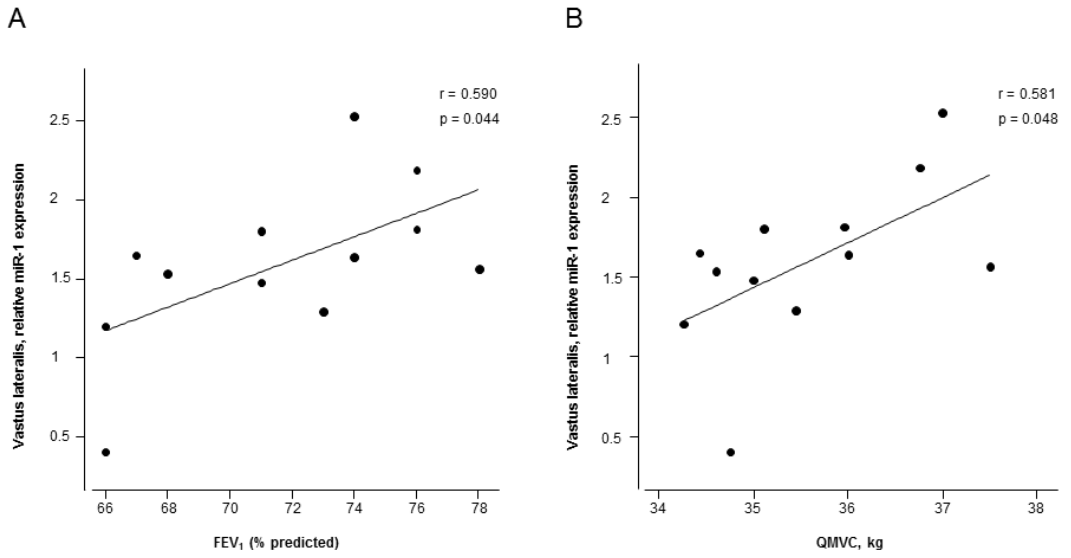

Figure 38. miR-1 correlations. Significant positive correlations found in vastus lateralis of mild COPD patients between expression levels of miR-1 and: **A.** FEV_1 (% predicted). **B.** QMVC (kg).

4.2.2- Histone modifications. Total protein acetylation levels in muscles did not differ between patients and control subjects (Figure 39A). Expression levels of the HTA p300 did not differ between patients and healthy controls (Figure 39B). Muscle protein levels of the HDAC3 and 6 and SIRT1 did not differ between patients and controls (Figures 40A-40C), while levels of HDAC4 were significantly increased in the vastus lateralis of the patients compared to healthy subjects (Figure 40D).

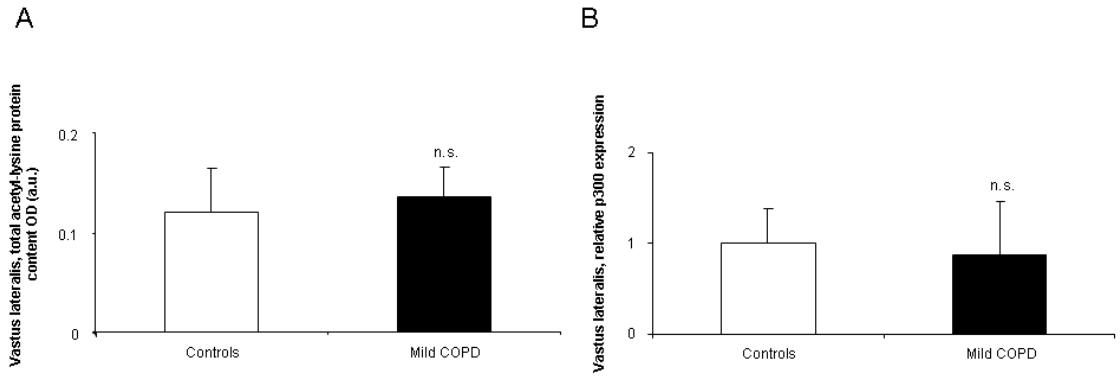

Figure 39. Histone modifications. Mean values and standard deviation. **A.** Levels of total lysine acetylated proteins in vastus lateralis of COPD and control subjects. **B.** Relative expression of the nuclear cofactor p300 in vastus lateralis of COPD and control subjects.
Statistical significance: n.s., non-significant between COPD patients and healthy controls.

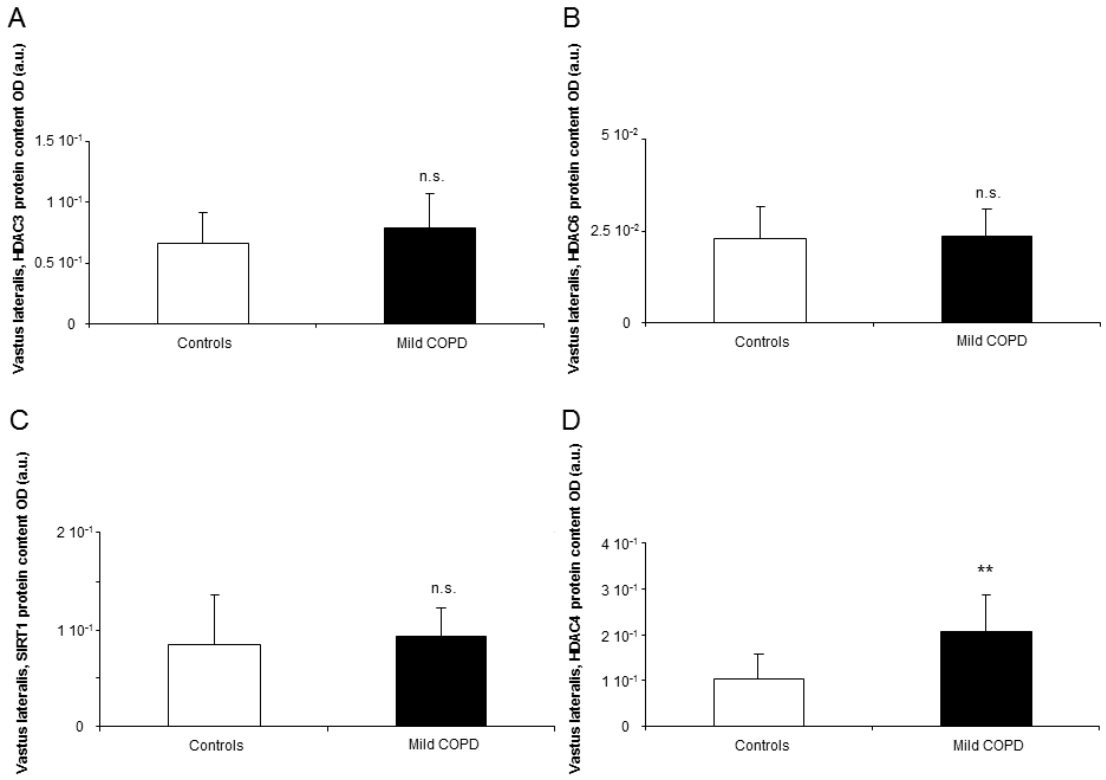

Figure 40. Histone modifications. Mean values and standard deviation. **A**. Protein levels of HDAC3 in vastus lateralis of COPD and control subjects. **B.** Protein levels of HDAC6 in vastus lateralis of COPD and control subjects. **C.** Protein levels of HDAC4 in vastus lateralis of COPD and control subjects. **D.** Protein levels of SIRT1 in vastus lateralis of COPD and control subjects.

Statistical significance: n.s., non-significant; and **, p≤0.01 between COPD patients and healthy controls.

4.2.3- Myogenic transcription factors. Compared to controls, protein levels of MEF2C, MEF2D and YY1 did not differ between patients and healthy controls in the limb muscles (Figure 41). Significant inverse correlations were observed between protein levels of MEF2C and miR-1 (r=-0.734, p=0.024) and miR-486 (r=-0.694, p=0.038) mRNA expression levels.

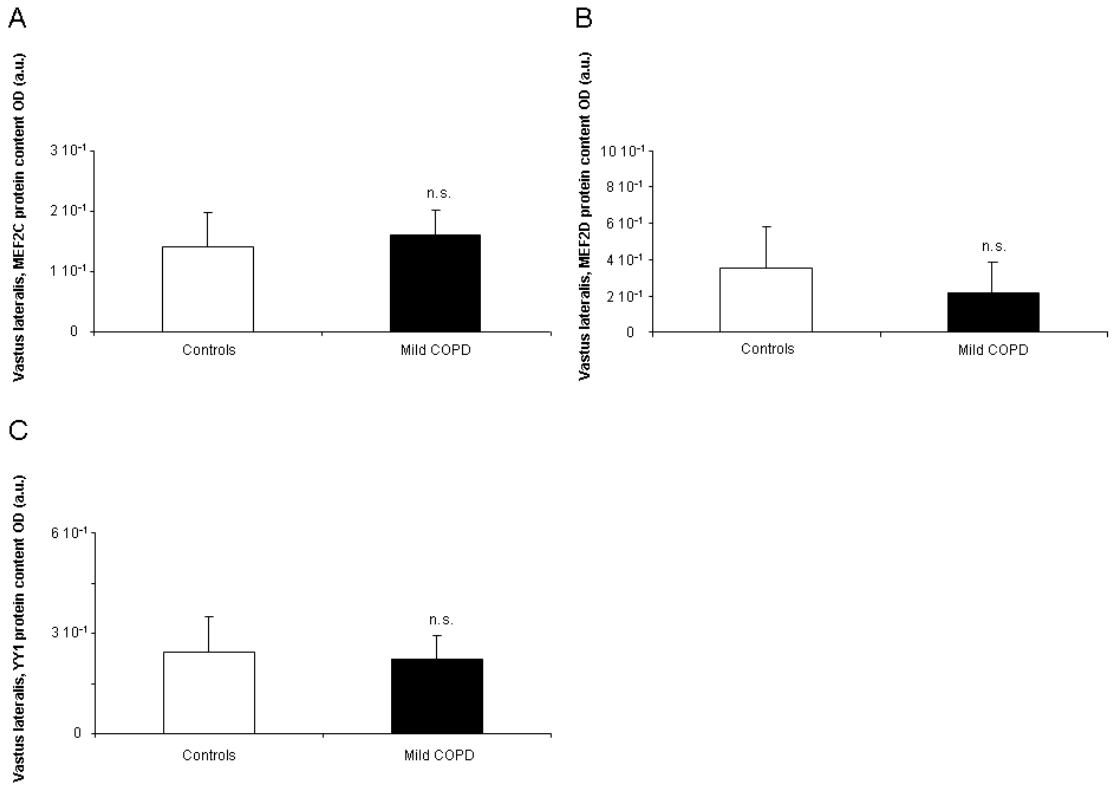

Figure 41. Myogenic transcription factors. Mean values and standard deviation. **A.** Protein levels of MEF2C in vastus lateralis of COPD and control subjects. **B.** Protein levels of MEF2D in vastus lateralis of COPD and control subjects. **C.** Protein levels of YY1 in vastus lateralis of COPD and control subjects

Statistical significance: n.s., non-significant between COPD patients and healthy controls.

4.2.4- Expression of SUMO. The mRNA expression levels of SUMO2 and SUMO3 did not differ between patients and controls in the vastus lateralis (Figure 42).

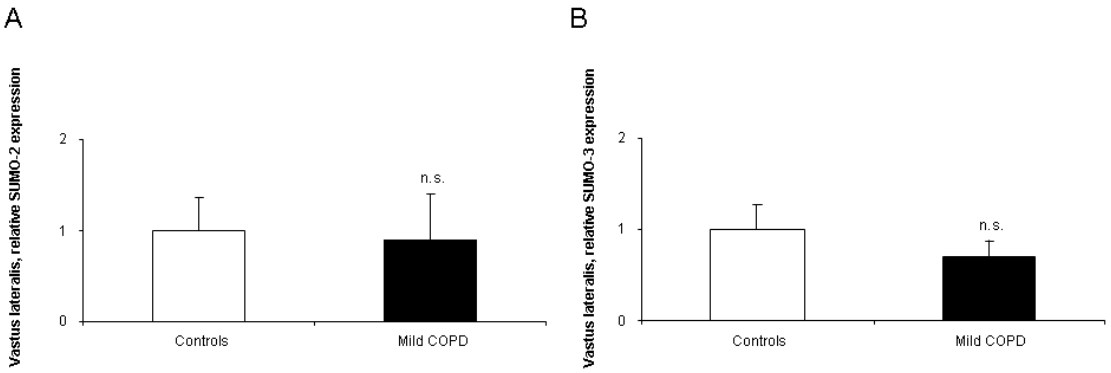

Figure 42. SUMO expression. Mean values and standard deviation (relative expression). **A.** SUMO-2 expression in vastus lateralis of COPD and control subjects. **B.** SUMO-3 expression in vastus lateralis of COPD and control subjects.
Statistical significance: n.s., non-significant between COPD patients and healthy controls.

4.3- Muscle structure

Fiber type composition. In the limb muscles, no significant differences were observed in either fiber type proportions or sizes between patients and controls (Table 16 and Figure 43).

	Controls N= 13	**Mild COPD N= 13**
Muscle fiber type composition		
Type I fibers, %	41 (6)	39 (7)
Type II fibers, %	59 (6)	61 (7)
Type I fibers, CSA (μm^2)	2736 (867)	2543 (604)
Type II fibers, CSA (μm^2)	3010 (939)	2758 (578)

Table 16. Fiber type composition in vastus lateralis muscle of all study subjects.
Values are expressed as mean (standard deviation).

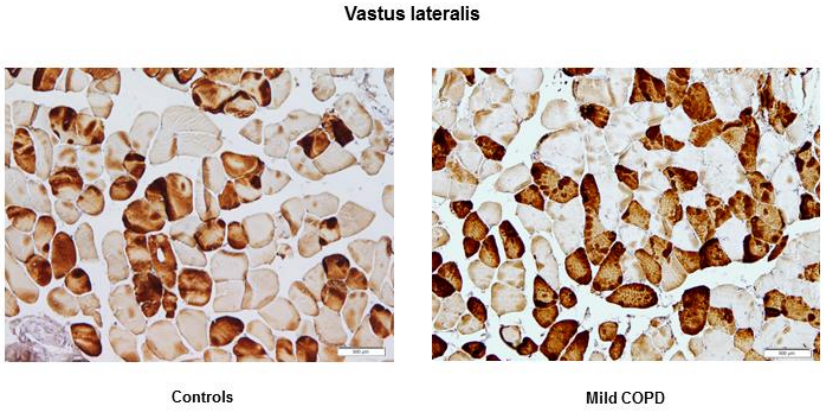

Figure 43. Muscle fiber type composition. Representative immunohistochemical preparations corresponding to the staining of type II fibers in the vastus lateralis of a healthy control subject (left panel) and a patient with mild COPD (right panel).

5- Summary of main findings

5.1- Study #1

In patients compared to control subjects:

Body weight and muscle function

Both groups of cachectic patients, LC and COPD, showed a reduction in body composition parameters as well as reduced exercise capacity and lower-limb muscle strength.

In vastus lateralis muscles of patients with LC cachexia and COPD cachexia:

Redox Balance

Protein oxidation and antioxidants levels were increased.

Inflammation

Levels of proinflamatory cytokines and growth factors were higher.

Signaling pathways

The signaling pathways NF-kB p65 and FoXO-3 were activated (phosphorylated).

Proteolytic systems

Protein levels of markers of the ubiquitin-proteasome system and total ubiquitinated proteins were increased.

Total protein oxidation and total ubiquitin levels were positively correlated.

Proteins susceptible to be degraded

Muscle myosin and creatine kinase protein contents were reduced.

Muscle structure

Type II fiber size was smaller.

Muscle structural and ultrastructural abnormalities (sarcomere disruptions) were increased.

In blood of patients with LC cachexia and COPD cachexia:

Redox Balance

Protein carbonylation and superoxide anion levels were increased.

Inflammation

Proinflamatory cytokines and growth factors levels were greater.

5.2- Study #2

In patients compared to control subjects:

Body weight and muscle function

COPD patients exhibited mild-to-severe airflow limitation, decreased exercise capacity and reduced both lower-limb and respiratory muscle function.

In the diaphragms of patients with different degrees of airflow obstruction:

MicroRNAs expression

Expression of myomiRs was downregulated.

Histone modifications

Histone deacetylase 4 (HDAC4) content was increased.

Myogenic transcription factors

Myocyte enhance factor 2C (MEF2C) levels were greater.

Expression of SUMO

Levels of SUMO expression did not differ.

Muscle structure

No differences were observed in either fiber type composition or size between patients and controls.

5.3- Study #3

In patients compared to control subjects:

Body weight and muscle function

All groups of COPD patients, either moderate or severe, showed impaired lung function and airflow limitation.

All groups of study patients showed decreased exercise capacity and lower-limb muscle strength.

Muscle-wasted severe COPD patients exhibited reduced BMI and FFMI compared to controls, moderate and non-wasted severe COPD patients.

In vastus lateralis muscles of patients with moderate and severe COPD and different body composition:

MicroRNAs expression

Moderate COPD patients showed greater levels of myomiR-1 than control subjects.

Non-wasted severe COPD patients showed an upregulation of muscle-enriched microRNAs compared to control subjects and also increased levels of miR-206 and -486 compared to moderate COPD patients.

Muscle-wasted severe COPD patients showed a downregulation of all muscle-enriched microRNAs compared to non-wasted severe COPD patients.

In all severe COPD patients, body composition parameters (BMI and FFMI) positively correlated with expression levels of microRNAs miR-133, -206, -486, and -29b.

Histone modifications

Only muscle-wasted severe COPD patients showed an increase in total acetylated proteins compared to controls, moderate, and non-wasted severe COPD patients.

Histone deacetylase levels of HDAC3 and SIRT-1 were also decreased in severe muscle-wasted COPD patients compared to both controls and non-wasted severe COPD patients.

In all severe COPD patients, levels of histone deacetylase SIRT1 positively correlated with levels of miR-133, -206, -486, -181a and HDAC3.

Myogenic transcription factors

No differences were observed in levels of the different myogenic transcription factors analyzed.

Expression of SUMO

Levels of SUMO expression did not differ between groups.

Muscle structure

Proportions of type II fibers were greater in both groups of severe COPD patients.

The size of type II fibers was smaller in the muscle-wasted severe COPD group of patients compared to both control subjects and non-wasted severe COPD patients.

5.4- Study #4

In patients compared to control subjects:

Body weight and muscle function

COPD patients exhibited mild airflow obstruction and decreased both exercise capacity and muscle strength.

In vastus lateralis muscles of patients with mild COPD:

MicroRNAs expression

MyomiR-1 expression was upregulated.

miR-1 expression positively correlated with lung function (FEV_1) and muscle strength (QMVC).

Histone modifications

Histone deacetylase 4 (HDAC4) content was increased.

Myogenic transcription factors

No differences were observed in levels of myogenic transcription factors

Expression of SUMO

SUMO expression levels did not differ.

Muscle structure

No differences were observed in either fiber type composition or size between patients and controls.

DISCUSSION AND CONCLUSIONS

1- Discussion

Clinical characteristics of the study subjects

As reported in previous studies (31, 32, 40, 43, 113-115, 132, 134), all COPD patients either undergoing thoracotomy (study #2) or limb muscle biopsies (studies #1,3 and 4) exhibited mild, moderate, and severe airflow obstruction according to both the GOLD and Spanish guidelines (26, 111, 116, 141). Additionally, severe COPD patients also showed air trapping together with functional signs of severe emphysema. Exercise capacity as measured by cycloergometry and walking test, and muscle strengths, of both respiratory (only assessed in study #2) and limb muscles, were also impaired in all groups of patients. Moreover, patients with lung cancer cachexia (study #1) also showed signs of mild-to-moderate airflow limitation probably due to the existing links between COPD and LC (146-152). The reduced exercise tolerance and muscle function that exhibited LC cachectic patients was though to a lesser extent than in COPD cachectic patients, probably due to the shorter disease progression in the former patients. Aside from the anthropometric features, from clinical and functional stand-points, no differences were observed in lung function, exercise intolerance or muscle function parameters between non-wasted and muscle-wasted severe COPD patients (study #3). This is a relevant feature which suggests that most of the findings encountered in the muscles of these two groups of severe patients seem to be rather related to their body and muscle mass composition than to the degree of the airflow limitation. No differences were found between controls and any of the study group of patients with respect to their smoking history (amount of smoked cigarettes). Patients from all four studies were either active smokers or ex-smokers. In order to avoid the interference of smoking history with the study results, control subjects had a similar smoking history to that reported in the patients except for study #1, in which control subjects were mostly ex-smokers or non-smokers to prevent that oxidants contained in the cigarette smoke (43, 153) could interfere into the molecular results, especially in those regarding redox balance.

As also previously reported (154-157) signs of chronic illness were also detected in the blood of all groups of patients, and especially in those with muscle wasting (studies #1 and #3), as shown by increased levels of inflammatory parameters including CRP, fibrinogen, and GSV compared to levels in the healthy controls. Additionally, in both

groups of cachectic patients from study #1, reduced levels of albumin were found decreased compared to controls thus evidencing the presence of nutritional depletion.

Muscle structure and ultrastructure

Interestingly, in the present thesis, muscle structure abnormalities and morphometry have been explored for the first time in muscles of cancer cachectic patients (study #1). Specifically, the degree of muscle abnormalities was similar between LC and COPD cachectic patients and comparable to previously reported data in COPD (115). Importantly, the size of fast-twitch fibers was reduced in the three groups of patients with muscle wasting (in both groups of severe COPD, studies #1 and #3; and in the LC group, study #1) compared to both control subjects and non-wasted severe COPD patients (this latter comparison only assessed in study #3). These results are also in accordance with previous reports (38, 115), in which the size of type II fibers was consistently smaller in two distinct models of cachexia. Taken together, these findings suggest that fast-twitch rather than slow-twitch fibers are more prone to degradation in those conditions. Limb-muscles fiber type composition and size did not significantly differ between mild and moderate COPD patients and healthy controls (studies #4 and #3, respectively). Reduced proportions of fiber type I and consequently, increased proportions of fiber type II were observed in the limb muscles of severe COPD patients (studies #1 and #3). These results are in line with previous findings of our group (3, 4) and others (158-160) in which has been demonstrated that a shift in fiber type composition towards a lower resistant phenotype takes places in limb muscles of COPD patients of advanced stages of severity (161). Interestingly, significant positive associations were also found between proportions and size of slow- and fast-twitch fibers and body composition parameters when both groups of patients with severe COPD (non-wasted and muscle-wasted) were analyzed together (study #3). These findings suggest that the amount of slow-and the size of fast-twitch fibers may rely on the nutritional status of the patients as previously shown in other muscles (162).

A relevant novel finding is the increased number of muscle fiber areas with sarcomere damage, as assessed by electron microscopy, detected in limb muscles from both lung cancer and COPD cachectic patients (study #1). Previous studies have also reported the presence of ultrastructural signs of sarcomere disruption and loss of thick filaments in critical illness myopathy (163), in the diaphragm of COPD patients exposed to increased respiratory loads (130, 131), and in other neurological or myofibrilar pathologies (137, 164, 165). In view of the study findings, we can conclude

that loss of the normal sarcomere architecture, especially of the thick filaments, may partly account for the decreased quadriceps muscle function observed in both groups of cachectic patients (study #1). Additionally, enhanced sarcomere disruption could also be explained by the reduced protein content of contractile myosin and creatine kinase enzyme detected in limb muscles of LC and COPD cachectic patients (study #1). In line with this, reduced myosin-actin cross bridge formation and altered kinetics have been recently shown in patients with cancer cachexia (155). Also, the significant negative correlation found between sarcomere damage and myosin protein loss supports such a conclusion.

Importantly, despite that total respiratory muscle force was not reduced in the patients, the specific assessment of diaphragm strength showed a significant reduction of this parameter in that group compared to values detected in the control subjects (study #2). The degree of diaphragm muscle dysfunction seen in the patients may not be sufficiently relevant to induce a significant clinical impact at rest, but it could certainly have implications during exercise and exacerbations. In line with these findings, proportions and sizes of the diaphragm muscle fibers did not differ between patients and control subjects (study #2). It is likely that changes taking place in muscle structure towards a more fatigue-resistant phenotype require a more drastic loss in muscle strength of the diaphragm, which is, in turn, directly related to the degree of the airway obstruction. In the present investigation (study #2), most of the patients exhibited mild and moderate airflow limitation, while only three patients had severe COPD. In previous studies from our group (31, 40) and others (166-168) as patients exhibited a more severe COPD, respiratory muscle strength and diaphragm force parameters were more significantly reduced. Moreover, in those investigations (31, 40, 166-168) a fiber-type switch towards a more resistant phenotype was also observed in the diaphragm of the severe COPD patients. In fact, in the present study, the negative correlation encountered between the degree of the airway obstruction as measured by FEV1 and the proportions of the slow-twitch fibers in the diaphragm further support these conclusions.

Biological mechanisms involved in muscle dysfunction and mass loss

Redox balance and inflammation

Previous reports (40, 115, 128, 132, 134) have consistently shown that enhanced levels of protein oxidation take place within respiratory and limb muscles of patients with severe COPD irrespective of body composition. In the current investigation (study #1), we confirm again that proteins undergo substantial oxidation in limb muscles (40, 115, 128, 132, 134) and blood of severe COPD cachectic patients (128, 134), and in the same compartments of the lung cancer cachectic patients (169). Besides, protein oxidation levels detected in limb muscles of both groups of cachectic patients together and in COPD patients separately inversely correlated with their body composition (both BMI and FFMI parameters) as previously reported in severe COPD patients (113). These observations indicate that oxidative stress may play a relevant role in the process of muscle wasting in patients with severe diseases such as advanced COPD and lung cancer cachexia. Other interesting findings of study #1 are the rise in mitochondrial and cytosolic isoforms of SOD and SOD enzyme activity, but not catalase, observed in the limb muscles of both groups of cachectic patients. These results suggest that superoxide anion is probably a major player in the oxidative stress cascade of cachectic muscles. Indeed, its levels were significantly increased in the blood of both groups of cachectic patients.

A significant rise in inflammatory cytokines such as IL-1beta and interferon-gamma was detected in muscles of both COPD and cancer cachectic patients, while systemic levels of interferon-gamma, VEGF, and TGF-beta were also increased in the same patients (study #1). Additionally, blood levels of IL-1 beta were higher in COPD cachectic patients. Taken together, these findings are in agreement with previous reports, in which systemic inflammation was suggested to be a mediator of muscle wasting in advanced malignancies (169, 170). As also shown in previous investigations (32, 43, 50, 115), inflammatory cell infiltration was not a major event in the limb muscles of the study patients. These findings suggest that circulating inflammatory cells are likely to be the main source of increased levels of proinflammatory cytokines, especially in blood compartments of both groups of cachectic patients. In fact, the significant rise observed in systemic levels of superoxide anion production further supports this conclusion.

Ubiquitin-proteasome system and redox-sensitive signaling pathways

In line with a previous report (115), in the current study #1, total protein ubiquitination levels were significantly higher in muscles of cachectic patients regardless of the underlying condition. Furthermore, a positive correlation was found between total levels of protein ubiquitination and MDA-protein adducts in each cachectic patient group and when analyzed altogether. This suggests that the oxidative modifications induced by the toxic lipid aldehyde MDA on muscle proteins may render them more susceptible to catabolism in either advanced COPD or lung cancer patients. However, precise identification on to what extent oxidized functional or structural proteins are more prone to degradation in muscles of patients with severe cachexia remains an open question. Moreover, hypoxia could also play a role in enhanced proteolysis in COPD cachectic muscles as shown by the inverse correlation found between PaO_2 and muscle protein ubiquitination and between diffusion capacity and muscle p-FoxO3 levels in these patients. Future investigations should specifically aim at investigating these relevant questions.

Other interesting findings of study #1 are the rise in muscle-specific E3 ligases MURF-1 and atrogin-1 levels encountered in the muscles of both groups of cachectic patients. These findings are in agreement with previous results obtained from both cancer cachexia experimental models (171-173) and severe COPD patients (114, 115, 138-140). To our knowledge, the increase in protein content of E3 ligases MURF-1 and atrogin-1 observed in limb muscles of cancer cachectic patients would also represent a novel finding in the investigation.

Identification of the upstream signaling regulation of muscle protein loss, partly mediated by the ubiquitin-proteasome system, in patients with either COPD or lung cancer cachexia is of interest, since it may offer insight into new therapeutic targets. Phosphorylated levels of transcription factors such as NF-κB p65, I-κB-alpha, FoxO-3 and that of the MAPK p38 significantly differed in muscles of both groups of cachectic patients from those in healthy controls. These are novel findings that lead to the conclusion that FoxO3 and NF-κB p65 transcription factors are the main signaling pathways involved in muscle protein loss in cachectic patients bearing two different respiratory conditions. In fact, these results are in line with previous reports in which activated FoxO-1, FoxO-3 and NF-κB transcription factors were also shown to actively participate in enhanced protein catabolism in experimental models of cachexia and in atrophying muscles of patients exposed to mechanical ventilation and COPD (114, 115, 135, 138-140, 144, 174-177). Nonetheless, protein levels of the cell signaling

pathway AMPK were similar between patients and controls, suggesting that this pathway does not seem to be involved in muscle protein catabolism in cachectic patients.

Protein levels of the myogenic transcriptor factor myogenin were reduced in limb muscles of all cachectic patients compared to the controls (study #1). These results are in agreement with previous reports, in which myogenin content was decreased in peripheral muscles of COPD patients with normal and altered body composition (115) and in the diaphragms of mice with experimental emphysema (126). As myogenin plays a relevant role in processes involving muscle mass maintenance and repair, it would be possible to conclude that these mechanisms may be altered in limb muscles of COPD and lung cancer cachectic patients. Indeed, a similar degree of muscle structural abnormalities was observed in both groups of cachectic patients.

Levels of the potent muscle mass regulator myostatin did not differ between any group of cachectic patients and the controls (study #1). These findings are in line with a recent report, in which myostatin levels were shown to be similar between COPD patients with and without cachexia and healthy controls (115). However, myostatin levels were increased in respiratory and limb muscles of patients with COPD in other reports (139, 140, 178). Differences in study design, disease severity, and body composition may account for the discrepancies between studies.

Epigenetic events

As far as we are concern, the present thesis is the first to report data on epigenetic regulation in diaphragm muscles of patients with a wide range of COPD severity (study #2) as well as in the lower limb muscles of patients with mild COPD (study #4) and also with severe COPD and atrophy (study #3).

Interestingly, in the present investigation (study #2), expression of the miR-1, -133, and -206 was downregulated in the diaphragm of patients with mild-to-moderate and severe COPD, whereas the expression of miR-486, -27a, -29b, and -181a did not differ between patients and controls. In COPD, the inspiratory loads to which the respiratory muscle is continuously exposed may be a major player accounting for this specific pattern of microRNA expression. Aside from the classic transcription factors, muscle-specific microRNAs play a relevant role in the regulation of muscle development and repair after injury by targeting different pathways (82, 109, 179). While miR-1 and -206 promote cell differentiation and innervation (82, 109, 179, 180), miR-133 induces myoblast proliferation by inhibiting myotube formation (82, 109, 179). In line with the

findings reported in the current study, the expression of miR-1 and -133 was also downregulated in response to muscle overload in an experimental model of hypertrophy (181). A likely explanation to account for all these results is that the decreased expression of miR-1 and -133 may promote adaptation to overload by eliminating the posttranscriptional repression of genes and pathways involved in muscle growth such as insulin-like growth factor (IGF)-1 and serum response factor (SRF). Hence, downregulation of muscle-specific microRNAs, which are part of one of the most ancient microRNA clusters, may play a crucial role in adaptation to overload in the diaphragm muscle of patients with moderate COPD.

In contrast, the lower limb muscles of mild and moderate COPD patients did not show any significant differences in microRNA expression except for miR-1, which was upregulated in both mild and moderate COPD patients compared to control subjects (studies #4 and #3, respectively). As such, miR-1 promotes myotube formation and participates in the innervation process of the myofibers. Moreover, miR-1 may also exert its actions on the muscle fibers through several mechanisms such as the insulin-like growth factor (IGF)-1 signal transduction cascade (182) or through induction of HDAC4 expression, which may further promote muscle cell proliferation and differentiation (82, 109, 182). Indeed protein levels of HDAC4 were also found increased in vastus lateralis of mild COPD patients compared to healthy controls (study #4). Moreover, in the limb muscle of these mild COPD patients, significant correlations were also found between miR-1 levels and the expression of miR-486 and miR-133, which are highly involved in muscle proliferation and differentiation. These observations may also indicate that in skeletal muscles, microRNAs possibly operate in a network fashion in order to ensure a continuous muscle repair process after injury, at least in patients with well-preserved body composition. In addition, significant positive correlations were found between miR-1 expression levels in the lower limb muscle of mild COPD patients and the degree of the airway obstruction as measured by FEV_1 and the force generated by the quadriceps muscle (study #4). Again these findings reinforce the concept that miR-1 is likely to be involved in the maintenance of muscle mass and function in COPD at early stages of the disease.

Importantly, the expression of all the myomiRs (miR-1, -133, and -206), and that of miR-486, -27a, -29b, and -181a was upregulated in the vastus lateralis of patients with severe COPD and preserved body composition compared to healthy controls (study #3). In addition, levels of miR-206 and -486 were also greater in this group of severe COPD patients than in moderate COPD patients (study #3). Nonetheless, expression

levels of all muscle-enriched microRNAs analyzed were significantly decreased in muscle-wasted severe COPD patients when compared to non-wasted severe COPD patients but not to control subjects (study #3). Moreover, among all the severe patients as a group, significant positive correlations were found between miR-133, -206, -486, and -29a and both BMI and FFMI. Indeed, as seen in graphs depicted in the results section of study #3 (page 103-104, Figures 29 and 30), patients exhibiting the greatest impairment in body composition and muscle structural atrophy (dark dots) were those showing the lowest expression of muscle-enriched microRNAs in their vastus lateralis. Although a cause-effect relationship cannot be established from these findings, it could be hypothesized that these microRNAs may regulate processes other than myogenesis in skeletal muscles of severe COPD patients. Hence, it is likely that genes involved in anabolic pathways (protein synthesis), enhanced catabolism, and signaling pathways are also targeted by muscle-enriched microRNAs in severe COPD, thus influencing body weight and muscle mass loss. Future research should focus on the elucidation of these downstream targets.

In line with current findings, spaceflight and hindlimb suspension models of atrophy also resulted in a downregulation of muscle-enriched microRNAs in limb muscles of rodents (183, 184). Specifically, the expression of miR-206 was downregulated in skeletal muscles of the exposed mice (183). Moreover a pioneering study conducted on limb muscles of severe COPD and relatively impaired body composition also showed a downregulation of miR-1 among the different microRNAs analyzed (109). Furthermore, in that study, miR-1 and -499 expression levels were also positively associated with FFMI and proportions of type I fibers among the severe patients (109). In keeping with our findings, a recent investigation from the same authors (108) demonstrated that expression levels of myomiRs including miR-1 were upregulated in the blood of patients with severe COPD and relatively preserved muscle mass. The authors concluded that skeletal muscles from the lower limbs would probably be the main source of increased plasma levels of myomiRs in those patients (108). Taken together, all these findings imply the existence of a myomiR network that may orchestrate muscle mass maintenance and fiber type composition events in muscles of patients with advanced COPD.

Hyperacetylation of proteins may participate in the process of muscle wasting through several mechanisms such as that of transcription factors and nuclear cofactors, by rendering proteins more prone to catabolism by ubiquitin-ligase activity of several HATs, and by dissociation of proteins from cellular chaperones (94). Among

several HATs, the nuclear cofactor p300 has been shown to regulate muscle differentiation and wasting in several experimental in vivo and in vitro models (99, 185). In the present thesis, no differences were found in p300 expression levels between controls and any group of COPD patients analyzed, in neither respiratory (study #2) and limb muscles (studies #3 and #4). However, differences between study models may account for such discrepancies. Importantly, protein acetylation also relies on histone deacetylase activity. Again in several experimental models of muscle wasting (99, 185), levels of HDAC3, HDAC6, and SIRT-1 were shown to be decreased in muscles. In keeping with this, levels of HDAC3 and SIRT-1 were also reduced in the limb muscles of the muscle-wasted severe COPD patients compared to healthy controls and non-wasted severe COPD patients (study #3), while those of HDAC6 did not significantly differ between groups in any of the study muscles. These findings suggest that lower expression of HDAC3 and SIRT1 are probably the most relevant contributors to the increased hyperacetylation levels encountered in the limb muscles of the muscle-wasted severe COPD patients (study #3).

Interestingly, it was also previously shown (109) that protein levels of HDAC4 were rather increased in the vastus lateralis of severe COPD patients. In the current investigation, no differences were observed in HDAC4 levels in limb muscles between moderate or any group of severe COPD patients and controls (study #3). Differences in disease severity, physical activity (all study subjects were sedentary), biological methodologies employed to detect HDAC4 levels, or body composition may account for discrepancies between studies.

Nonetheless, in agreement with those results previously reported in patients with preserved body composition (109), in the current studies, HDAC4 protein levels were shown to be increased in the vastus lateralis of mild COPD patients and in diaphragm of COPD patients compared to healthy controls (studies #4 and #2, respectively). Indeed, the interaction between HDAC4 and miR-1, actually being this last also found upregulated in vastus lateralis of mild and in diaphragm of COPD patients, was suggested to contribute to muscle mass maintenance, probably through insulin-like growth factor (IGF)-1 signaling (109, 186). Taken together, these findings suggest that HDAC4 expression is likely to be upregulated in the muscles of patients with relatively preserved body composition and muscle mass, regardless of the airway obstruction. They may also indicate that HDAC4 probably plays a major role in muscle repair and mass maintenance in patients with a well-preserved muscle compartment. Whether miR-1 and HDAC4 may drive the maintenance of muscle mass in respiratory and limb

muscles of patients with COPD remains to be elucidated though it could be an interesting question for future research.

The transcription factors myocyte enhancer factor (MEF)2 and Yin Yang (YY)1 seem to play a relevant role in muscle development, metabolic adaptation, and in the determination of muscle fiber type (187). Interestingly, in the current studies, only levels of MEF2C were found increased in diaphragm muscles of COPD patients compared to control subjects (study #2). No differences were observed in vastus lateralis of any study group of COPD patients (studies #3 and #4) with respect to MEF2 isoform or YY1. It is likely that in COPD, the adaptive potential is still preserved in the main respiratory muscle, at least through MEF2C upregulation and generally reduced in limb muscles of patients.

Sarcopenia and muscle wasting could be partly the result of the premature senescence of satellite cells, which ultimately would lead to decreased growth and poor repair potential. Interestingly, accumulation of SUMO ligases has been proposed to participate in the etiology of premature senescence of primary myogenic cultured cells (188), and other models (189, 190). Furthermore, premature satellite cell senescence through SUMO ligases among other mechanisms also seems to underlie the pathophysiology of muscular dystrophies (191). In the present thesis, expression levels of SUMO-2 and -3 did not differ between any group of patients and controls in neither diaphragm (study #2) nor vastus lateralis muscles (studies #3 and #4), thus suggesting that premature senescence may not be a relevant mechanism of muscle dysfunction and wasting in respiratory and limb muscles of COPD patients.

2- Study limitations

A first limitation in the current thesis has to do with the relatively small number of cancer cachectic patients recruited for the purpose of study #1. However, on the basis of the relatively “invasive” nature of the study, conducted on patients bearing a very severe condition (lung cancer), we felt discouraged to recruit a greater number of these patients. Furthermore, as statistical significance was reached on the basis of 10 patients with lung cancer cachexia, we believe that this number was adequate to answer the specific study questions. Besides, small numbers of patients were recruited in a previous study conducted on cachectic patients bearing different types of malignancies (155).

A second limitation refers to the fact that most of lung cancer patients (7 out of 10) also had mild-to-moderate COPD. Indeed, COPD has been consistently demonstrated to be a risk factor for lung cancer (146, 192-194). Hence, it could be speculated that the findings encountered in the cachectic lung cancer patients could be largely attributed to COPD rather than to cancer-induced muscle loss. However, we believe that COPD *per se* has had little or no influence on the biological findings observed in the lung cancer cachectic patients for several reasons: 1) reported findings so far have shown no significant differences in the cellular or molecular markers analyzed in the study in muscles of patients with mild-to-moderate COPD compared to healthy controls (31, 40, 195), and 2) body and muscle mass loss, exercise capacity and muscle function impairments were less severely affected in the cancer cachectic patients than in COPD, probably due to the shorter disease progression in the former patients. Moreover, these observations also lead to the conclusion that in cancer cachexia, the underlying biological mechanisms may take place very early in the course of the ongoing muscle wasting process as findings shared strong similarities with those detected in advanced COPD.

A third potential limitation in the present thesis is related to the use of sedentary individuals as the healthy controls in all studies. This explains the relatively low proportions of slow-twitch fibers observed within the limb muscles of the control subjects. Nevertheless, we reasoned that physical activity might influence to a great extent redox balance, signaling pathways, and the expression of the different epigenetic markers analyzed herein. As patients were all sedentary, this was, indeed, our major argument to specifically recruit healthy sedentary individuals as the control group. Finally, it should also be mentioned that in nine studies included in the meta-

analysis conducted by Gosker *et al* (196), severe COPD patients exhibited greater proportions of slow-twitch fibers (ranging from 34% to 44%) in their vastus lateralis than in other published reports, suggesting that discrepancies may also exist among patients with severe COPD.

A fourth limitation may have to do with the fact that smoking history in studies #2, #3, and #4 was similar between the COPD groups of patients and the healthy controls. However, we purposely recruited non-COPD control subjects who had a similar smoking history in order to avoid potential biases inherent to differences in smoking loads among the study groups.

A fifth limitation of the current thesis is that diaphragm muscle biopsies from the study subjects were obtained during thoracotomy because of localized lung lesions, the gold standard technique to obtain diaphragm specimens from different populations. Although lung volume reduction surgery also makes it possible to obtain diaphragm specimens, only very severe COPD patients undergo that type of surgery, thus, making the study of mild-to-moderate patients or control subjects impossible. Therefore, diagnostic-therapeutic thoracotomy is the only approach available for studying moderate and mild COPD and normal lung function subjects. Accordingly, subjects recruited for the purpose of the study #2 shares a common morbidity: the presence of a small and localized lung neoplasm. Nevertheless, we do not believe that this condition has made any significant contribution to the results obtained in the analyses of the diaphragm muscles, since extremely restrictive criteria were employed to properly select the population, and subjects showing either nutritional abnormalities, signs of chronic inflammation, or paraneoplastic syndromes, were systematically excluded. Therefore, we consider all the findings reported in the study #2 to be rather associated with COPD.

A sixth limitation in the current thesis has to do with the fairly small number of subjects studied in the study #4. However, on the basis of the relatively “invasive” nature of this investigation, with patients with very mild or mild COPD patients and healthy controls undergoing a muscle biopsy from the vastus lateralis, we felt discouraged to recruit more patients and controls for the purpose of this investigation. Moreover, as abovementioned in the corresponding methods section of study #4 (page 70), the sample size of both patient and control populations was calculated on the basis of formerly published studies by our group and other investigators, where similar physiological and biological approaches were used in both mild COPD patients and healthy control subjects (31, 32, 40, 43, 50, 113, 115, 128, 195, 197). Therefore, it is

reasoned herein that the relatively small number of mild COPD patients and controls included was sufficient to achieve our objectives.

3- Concluding remarks

Oxidative stress seems to regulate muscle wasting and atrophy, which particularly takes place in fast-twitch fibers, in patients with cachexia of two distinct highly prevalent conditions. Contractile myosin loss and ultrastructural abnormalities such as enhanced sarcomere disruption are characteristic phenotypic features of the cachectic muscles in both types of patients. Moreover, the ubiquitin-proteasome system signaled by the redox-sensitive NF-κB and FoxO-3 pathways seem to be relevant mechanisms of muscle atrophy in these patients.

Epigenetic mechanisms seem to differentially and tightly regulate muscle activity and mass maintenance in respiratory and limb muscles of COPD patients. In the main respiratory muscle of COPD patients with a wide range of disease severity and normal body composition, muscle-specific microRNAs were downregulated while HDAC4 and MEF2C levels were upregulated. Peripheral muscles of COPD patients and especially of those with severe airflow limitation exhibited a rise in muscle-enriched microRNAs expression. Furthermore, in those patients, muscle mass loss specifically seems to determine a differential epigenetic profile, regardless of the clinical characteristics and airway obstruction. These findings suggest that epigenetic events, which already take place in mild COPD patients, act as biological adaptive mechanisms to better overcome the continuous inspiratory loads imposed to the respiratory system as well as an attempt to counterbalance the underlying mechanisms that alter muscle function and mass.

REFERENCES

1. Zierath JR, Hawley JA. Skeletal muscle fiber type: influence on contractile and metabolic properties. PLoS Biol. 2004 Oct;2(10):e348.

2. Jones D RJ, de Haan A. . Skeletal Muscle from Molecules to Movement. 1 ed2004.

3. A M. Skeletal Muscle: Form and Function: Human Kinetics Publishers; 1996.

4. Tortora G DB. Principles of Anatomy and Physiology. 12th ed2009.

5. Bentzinger CF, Wang YX, Rudnicki MA. Building muscle: molecular regulation of myogenesis. Cold Spring Harb Perspect Biol. 2012 Feb;4(2).

6. Huh MS, Smid JK, Rudnicki MA. Muscle function and dysfunction in health and disease. Birth Defects Res C Embryo Today. 2005 Sep;75(3):180-92.

7. Pownall ME, Gustafsson MK, Emerson CP, Jr. Myogenic regulatory factors and the specification of muscle progenitors in vertebrate embryos. Annu Rev Cell Dev Biol. 2002;18:747-83.

8. Hasty P, Bradley A, Morris JH, Edmondson DG, Venuti JM, Olson EN, et al. Muscle deficiency and neonatal death in mice with a targeted mutation in the myogenin gene. Nature. 1993 Aug 5;364(6437):501-6.

9. Barreiro E, Hussain SN. Protein carbonylation in skeletal muscles: impact on function. Antioxid Redox Signal. 2010 Mar;12(3):417-29.

10. College O. Anatomy and Physiology 2013.

11. Gea J, Barreiro E. [Update on the mechanisms of muscle dysfunction in COPD]. Arch Bronconeumol. 2008 Jun;44(6):328-37.

12. Koeppen B SB. Berne & Levy Physiology. 6th ed: Mosby Elsevier.

13. Ratnovsky A, Elad D, Halpern P. Mechanics of respiratory muscles. Respir Physiol Neurobiol. 2008 Nov 30;163(1-3):82-9.

14. Gea J, Agusti A, Roca J. Pathophysiology of muscle dysfunction in COPD. J Appl Physiol (1985). 2013 May;114(9):1222-34.

15. Schiaffino S, Reggiani C. Fiber types in mammalian skeletal muscles. Physiol Rev. 2011 Oct;91(4):1447-531.

16. Scott W, Stevens J, Binder-Macleod SA. Human skeletal muscle fiber type classifications. Phys Ther. 2001 Nov;81(11):1810-6.

17. Lowry CV, Kimmey JS, Felder S, Chi MM, Kaiser KK, Passonneau PN, et al. Enzyme patterns in single human muscle fibers. J Biol Chem. 1978 Nov 25;253(22):8269-77.

18. Polla B, D'Antona G, Bottinelli R, Reggiani C. Respiratory muscle fibres: specialisation and plasticity. Thorax. 2004 Sep;59(9):808-17.

19. Kim HC, Mofarrahi M, Hussain SN. Skeletal muscle dysfunction in patients with chronic obstructive pulmonary disease. Int J Chron Obstruct Pulmon Dis. 2008;3(4):637-58.

20. Seymour JM, Spruit MA, Hopkinson NS, Natanek SA, Man WD, Jackson A, et al. The prevalence of quadriceps weakness in COPD and the relationship with disease severity. Eur Respir J. 2010 Jul;36(1):81-8.

21. Sakuma K, Yamaguchi A. Sarcopenia and cachexia: the adaptations of negative regulators of skeletal muscle mass. J Cachexia Sarcopenia Muscle. 2012 Jun;3(2):77-94.

22. Fanzani A, Conraads VM, Penna F, Martinet W. Molecular and cellular mechanisms of skeletal muscle atrophy: an update. J Cachexia Sarcopenia Muscle. 2012 Sep;3(3):163-79.

23. Tisdale MJ. Cachexia in cancer patients. Nat Rev Cancer. 2002 Nov;2(11):862-71.

24. von Haehling S, Anker SD. Cachexia as major underestimated unmet medical need: facts and numbers. Int J Cardiol. 2012 Nov 29;161(3):121-3.

25. Fearon K, Strasser F, Anker SD, Bosaeus I, Bruera E, Fainsinger RL, et al. Definition and classification of cancer cachexia: an international consensus. Lancet Oncol. 2011 May;12(5):489-95.

26. Rabe KF, Hurd S, Anzueto A, Barnes PJ, Buist SA, Calverley P, et al. Global strategy for the diagnosis, management, and prevention of chronic obstructive pulmonary disease: GOLD executive summary. Am J Respir Crit Care Med. 2007 Sep 15;176(6):532-55.

27. Leidinger P, Keller A, Borries A, Huwer H, Rohling M, Huebers J, et al. Specific peripheral miRNA profiles for distinguishing lung cancer from COPD. Lung Cancer. 2011 Oct;74(1):41-7.

28. Wust RC, Degens H. Factors contributing to muscle wasting and dysfunction in COPD patients. Int J Chron Obstruct Pulmon Dis. 2007;2(3):289-300.

29. Nathell L, Nathell M, Malmberg P, Larsson K. COPD diagnosis related to different guidelines and spirometry techniques. Respir Res. 2007;8:89.

30. Caron MA, Debigare R, Dekhuijzen PN, Maltais F. Comparative assessment of the quadriceps and the diaphragm in patients with COPD. J Appl Physiol (1985). 2009 Sep;107(3):952-61.

31. Barreiro E, de la Puente B, Minguella J, Corominas JM, Serrano S, Hussain SN, et al. Oxidative stress and respiratory muscle dysfunction in severe chronic obstructive pulmonary disease. Am J Respir Crit Care Med. 2005 May 15;171(10):1116-24.

32. Barreiro E, Schols AM, Polkey MI, Galdiz JB, Gosker HR, Swallow EB, et al. Cytokine profile in quadriceps muscles of patients with severe COPD. Thorax. 2008 Feb;63(2):100-7.

33. Fox KM, Brooks JM, Gandra SR, Markus R, Chiou CF. Estimation of Cachexia among Cancer Patients Based on Four Definitions. J Oncol. 2009;2009:693458.

34. MacDonald N, Easson AM, Mazurak VC, Dunn GP, Baracos VE. Understanding and managing cancer cachexia. J Am Coll Surg. 2003 Jul;197(1):143-61.

35. Muscaritoli M, Bossola M, Aversa Z, Bellantone R, Rossi Fanelli F. Prevention and treatment of cancer cachexia: new insights into an old problem. Eur J Cancer. 2006 Jan;42(1):31-41.

36. Oglesby IK, McElvaney NG, Greene CM. MicroRNAs in inflammatory lung disease--master regulators or target practice? Respir Res. 2010;11:148.

37. Donohoe CL, Ryan AM, Reynolds JV. Cancer cachexia: mechanisms and clinical implications. Gastroenterol Res Pract. 2011;2011:601434.

38. Marin-Corral J, Fontes CC, Pascual-Guardia S, Sanchez F, Olivan M, Argiles JM, et al. Redox balance and carbonylated proteins in limb and heart muscles of cachectic rats. Antioxid Redox Signal. 2010 Mar;12(3):365-80.

39. Barreiro E, de la Puente B, Busquets S, Lopez-Soriano FJ, Gea J, Argiles JM. Both oxidative and nitrosative stress are associated with muscle wasting in tumour-bearing rats. FEBS Lett. 2005 Mar 14;579(7):1646-52.

40. Marin-Corral J, Minguella J, Ramirez-Sarmiento AL, Hussain SN, Gea J, Barreiro E. Oxidised proteins and superoxide anion production in the diaphragm of severe COPD patients. Eur Respir J. 2009 Jun;33(6):1309-19.

41. Grimsrud PA, Xie H, Griffin TJ, Bernlohr DA. Oxidative stress and covalent modification of protein with bioactive aldehydes. J Biol Chem. 2008 Aug 8;283(32):21837-41.

42. Hussain SN, Matar G, Barreiro E, Florian M, Divangahi M, Vassilakopoulos T. Modifications of proteins by 4-hydroxy-2-nonenal in the ventilatory muscles of rats. Am J Physiol Lung Cell Mol Physiol. 2006 May;290(5):L996-1003.

43. Barreiro E, Peinado VI, Galdiz JB, Ferrer E, Marin-Corral J, Sanchez F, et al. Cigarette smoke-induced oxidative stress: A role in chronic obstructive pulmonary disease skeletal muscle dysfunction. Am J Respir Crit Care Med. 2010 Aug 15;182(4):477-88.

44. Agusti A, Edwards LD, Rennard SI, MacNee W, Tal-Singer R, Miller BE, et al. Persistent systemic inflammation is associated with poor clinical outcomes in COPD: a novel phenotype. PLoS One. 2012;7(5):e37483.

45. Gea J BE, Orozco-Levi M. Systemic inflammation in COPD. Clin Pubm Med 2009;16:233-24.

46. Wouters EF. Local and systemic inflammation in chronic obstructive pulmonary disease. Proc Am Thorac Soc. 2005;2(1):26-33.

47. Montes de Oca M, Torres SH, De Sanctis J, Mata A, Hernandez N, Talamo C. Skeletal muscle inflammation and nitric oxide in patients with COPD. Eur Respir J. 2005 Sep;26(3):390-7.

48. Debigare R, Cote CH, Maltais F. Peripheral muscle wasting in chronic obstructive pulmonary disease. Clinical relevance and mechanisms. Am J Respir Crit Care Med. 2001 Nov 1;164(9):1712-7.

49. Tisdale MJ. Biology of cachexia. J Natl Cancer Inst. 1997 Dec 3;89(23):1763-73.

50. Barreiro E, Ferrer D, Sanchez F, Minguella J, Marin-Corral J, Martinez-Llorens J, et al. Inflammatory cells and apoptosis in respiratory and limb muscles of patients with COPD. J Appl Physiol (1985). 2011 Sep;111(3):808-17.

51. Tisdale MJ. Molecular pathways leading to cancer cachexia. Physiology (Bethesda). 2005 Oct;20:340-8.

52. Chung KF, Marwick JA. Molecular mechanisms of oxidative stress in airways and lungs with reference to asthma and chronic obstructive pulmonary disease. Ann N Y Acad Sci. 2010 Aug;1203:85-91.

53. Berridge MJ. Cell signalling. A tale of two messengers. Nature. 1993 Sep 30;365(6445):388-9.

54. Kramer HF, Goodyear LJ. Exercise, MAPK, and NF-kappaB signaling in skeletal muscle. J Appl Physiol (1985). 2007 Jul;103(1):388-95.

55. McClung JM, Judge AR, Powers SK, Yan Z. p38 MAPK links oxidative stress to autophagy-related gene expression in cachectic muscle wasting. Am J Physiol Cell Physiol. 2010 Mar;298(3):C542-9.

56. Johns N, Stephens NA, Fearon KC. Muscle wasting in cancer. Int J Biochem Cell Biol. 2013 Oct;45(10):2215-29.

57. Birkenkamp KU, Coffer PJ. Regulation of cell survival and proliferation by the FOXO (Forkhead box, class O) subfamily of Forkhead transcription factors. Biochem Soc Trans. 2003 Feb;31(Pt 1):292-7.

58. Glauser DA, Schlegel W. The emerging role of FOXO transcription factors in pancreatic beta cells. J Endocrinol. 2007 May;193(2):195-207.

59. Costelli P, Muscaritoli M, Bonetto A, Penna F, Reffo P, Bossola M, et al. Muscle myostatin signalling is enhanced in experimental cancer cachexia. Eur J Clin Invest. 2008 Jul;38(7):531-8.

60. Han HQ, Zhou X, Mitch WE, Goldberg AL. Myostatin/activin pathway antagonism: molecular basis and therapeutic potential. Int J Biochem Cell Biol. 2013 Oct;45(10):2333-47.

61. Elkina Y, von Haehling S, Anker SD, Springer J. The role of myostatin in muscle wasting: an overview. J Cachexia Sarcopenia Muscle. 2011 Sep;2(3):143-51.

62. Fulco M, Sartorelli V. Comparing and contrasting the roles of AMPK and SIRT1 in metabolic tissues. Cell Cycle. 2008 Dec;7(23):3669-79.

63. Richter EA, Ruderman NB. AMPK and the biochemistry of exercise: implications for human health and disease. Biochem J. 2009 Mar 1;418(2):261-75.

64. White JP, Baynes JW, Welle SL, Kostek MC, Matesic LE, Sato S, et al. The regulation of skeletal muscle protein turnover during the progression of cancer cachexia in the Apc(Min/+) mouse. PLoS One. 2011;6(9):e24650.

65. Lecker SH, Solomon V, Mitch WE, Goldberg AL. Muscle protein breakdown and the critical role of the ubiquitin-proteasome pathway in normal and disease states. J Nutr. 1999 Jan;129(1S Suppl):227S-37S.

66. Baumeister W, Walz J, Zuhl F, Seemuller E. The proteasome: paradigm of a self-compartmentalizing protease. Cell. 1998 Feb 6;92(3):367-80.

67. Costelli P, De Tullio R, Baccino FM, Melloni E. Activation of Ca(2+)-dependent proteolysis in skeletal muscle and heart in cancer cachexia. Br J Cancer. 2001 Apr 6;84(7):946-50.

68. Hasselgren PO, Fischer JE. Muscle cachexia: current concepts of intracellular mechanisms and molecular regulation. Ann Surg. 2001 Jan;233(1):9-17.

69. Debigare R, Marquis K, Cote CH, Tremblay RR, Michaud A, LeBlanc P, et al. Catabolic/anabolic balance and muscle wasting in patients with COPD. Chest. 2003 Jul;124(1):83-9.

70. Gomes-Marcondes MC, Tisdale MJ. Induction of protein catabolism and the ubiquitin-proteasome pathway by mild oxidative stress. Cancer Lett. 2002 Jun 6;180(1):69-74.

71. Tisdale MJ. Mechanisms of cancer cachexia. Physiol Rev. 2009 Apr;89(2):381-410.

72. Orlowski M, Wilk S. Ubiquitin-independent proteolytic functions of the proteasome. Arch Biochem Biophys. 2003 Jul 1;415(1):1-5.

73. Jackson SP, Durocher D. Regulation of DNA damage responses by ubiquitin and SUMO. Mol Cell. 2013 Mar 7;49(5):795-807.

74. Wang Y, Shankar SR, Kher D, Ling BM, Taneja R. Sumoylation of the basic helix-loop-helix transcription factor sharp-1 regulates recruitment of the histone methyltransferase G9a and function in myogenesis. J Biol Chem. 2013 Jun 14;288(24):17654-62.

75. Geoffroy MC, Hay RT. An additional role for SUMO in ubiquitin-mediated proteolysis. Nat Rev Mol Cell Biol. 2009 Aug;10(8):564-8.

76. Hay RT. SUMO: a history of modification. Mol Cell. 2005 Apr 1;18(1):1-12.

77. Gareau JR, Lima CD. The SUMO pathway: emerging mechanisms that shape specificity, conjugation and recognition. Nat Rev Mol Cell Biol. 2010 Dec;11(12):861-71.

78. Sandri M. Autophagy in health and disease. 3. Involvement of autophagy in muscle atrophy. Am J Physiol Cell Physiol. 2010 Jun;298(6):C1291-7.

79. Penna F, Costamagna D, Pin F, Camperi A, Fanzani A, Chiarpotto EM, et al. Autophagic degradation contributes to muscle wasting in cancer cachexia. Am J Pathol. 2013 Apr;182(4):1367-78.

80. Sandri M. Autophagy in skeletal muscle. FEBS Lett. 2010 Apr 2;584(7):1411-6.

81. Scherz-Shouval R, Shvets E, Fass E, Shorer H, Gil L, Elazar Z. Reactive oxygen species are essential for autophagy and specifically regulate the activity of Atg4. EMBO J. 2007 Apr 4;26(7):1749-60.

82. Barreiro E, Sznajder JI. Epigenetic regulation of muscle phenotype and adaptation: a potential role in COPD muscle dysfunction. J Appl Physiol (1985). 2013 May;114(9):1263-72.

83. Baar K. Epigenetic control of skeletal muscle fibre type. Acta Physiol (Oxf). 2010 Aug;199(4):477-87.

84. Sartorelli V, Juan AH. Sculpting chromatin beyond the double helix: epigenetic control of skeletal myogenesis. Curr Top Dev Biol. 2011;96:57-83.

85. Kouzarides T. Chromatin modifications and their function. Cell. 2007 Feb 23;128(4):693-705.

86. Dawson MA, Kouzarides T. Cancer epigenetics: from mechanism to therapy. Cell. 2012 Jul 6;150(1):12-27.

87. Bannister AJ, Kouzarides T. Regulation of chromatin by histone modifications. Cell Res. 2011 Mar;21(3):381-95.

88. McKinsey TA, Zhang CL, Olson EN. Control of muscle development by dueling HATs and HDACs. Curr Opin Genet Dev. 2001 Oct;11(5):497-504.

89. Dyson MH, Rose S, Mahadevan LC. Acetyllysine-binding and function of bromodomain-containing proteins in chromatin. Front Biosci. 2001 Aug 1;6:D853-65.

90. Giordani L, Puri PL. Epigenetic control of skeletal muscle regeneration: Integrating genetic determinants and environmental changes. FEBS J. 2013 Sep;280(17):4014-25.

91. Pahlich S, Zakaryan RP, Gehring H. Protein arginine methylation: Cellular functions and methods of analysis. Biochim Biophys Acta. 2006 Dec;1764(12):1890-903.

92. Dekker FJ, Haisma HJ. Histone acetyl transferases as emerging drug targets. Drug Discov Today. 2009 Oct;14(19-20):942-8.

93. Clayton AL, Hazzalin CA, Mahadevan LC. Enhanced histone acetylation and transcription: a dynamic perspective. Mol Cell. 2006 Aug 4;23(3):289-96.

94. Alamdari N, Aversa Z, Castillero E, Hasselgren PO. Acetylation and deacetylation--novel factors in muscle wasting. Metabolism. 2013 Jan;62(1):1-11.

95. Grewal SI, Jia S. Heterochromatin revisited. Nat Rev Genet. 2007 Jan;8(1):35-46.

96. de Ruijter AJ, van Gennip AH, Caron HN, Kemp S, van Kuilenburg AB. Histone deacetylases (HDACs): characterization of the classical HDAC family. Biochem J. 2003 Mar 15;370(Pt 3):737-49.

97. Kwon HS, Ott M. The ups and downs of SIRT1. Trends Biochem Sci. 2008 Nov;33(11):517-25.

98. Zschoernig B, Mahlknecht U. SIRTUIN 1: regulating the regulator. Biochem Biophys Res Commun. 2008 Nov 14;376(2):251-5.

99. Alamdari N, Smith IJ, Aversa Z, Hasselgren PO. Sepsis and glucocorticoids upregulate p300 and downregulate HDAC6 expression and activity in skeletal muscle. Am J Physiol Regul Integr Comp Physiol. 2010 Aug;299(2):R509-20.

100. McKinsey TA, Zhang CL, Olson EN. Signaling chromatin to make muscle. Curr Opin Cell Biol. 2002 Dec;14(6):763-72.

101. Rao PK, Kumar RM, Farkhondeh M, Baskerville S, Lodish HF. Myogenic factors that regulate expression of muscle-specific microRNAs. Proc Natl Acad Sci U S A. 2006 Jun 6;103(23):8721-6.

102. Natanek SA, Riddoch-Contreras J, Marsh GS, Hopkinson NS, Man WD, Moxham J, et al. Yin Yang 1 expression and localisation in quadriceps muscle in COPD. Arch Bronconeumol. 2011 Jun;47(6):296-302.

103. Guller I, Russell AP. MicroRNAs in skeletal muscle: their role and regulation in development, disease and function. J Physiol. 2010 Nov 1;588(Pt 21):4075-87.

104. Williams AH, Liu N, van Rooij E, Olson EN. MicroRNA control of muscle development and disease. Curr Opin Cell Biol. 2009 Jun;21(3):461-9.

105. Zacharewicz E, Lamon S, Russell AP. MicroRNAs in skeletal muscle and their regulation with exercise, ageing, and disease. Front Physiol. 2013;4:266.

106. Krutzfeldt J, Stoffel M. MicroRNAs: a new class of regulatory genes affecting metabolism. Cell Metab. 2006 Jul;4(1):9-12.

107. Ge Y, Chen J. MicroRNAs in skeletal myogenesis. Cell Cycle. 2011 Feb 1;10(3):441-8.

108. Donaldson A, Natanek SA, Lewis A, Man WD, Hopkinson NS, Polkey MI, et al. Increased skeletal muscle-specific microRNA in the blood of patients with COPD. Thorax. 2013 Dec;68(12):1140-9.

109. Lewis A, Riddoch-Contreras J, Natanek SA, Donaldson A, Man WD, Moxham J, et al. Downregulation of the serum response factor/miR-1 axis in the quadriceps of patients with COPD. Thorax. 2012 Jan;67(1):26-34.

110. Miravitlles M, Calle M, Soler-Cataluna JJ. Clinical phenotypes of COPD: identification, definition and implications for guidelines. Arch Bronconeumol. 2012 Mar;48(3):86-98.

111. Miravitlles M, Soler-Cataluna JJ, Calle M, Molina J, Almagro P, Antonio Quintano J, et al. Spanish Guideline for COPD (GesEPOC). Update 2014. Arch Bronconeumol. 2014;50 Suppl 1:1-16.

112. Vestbo J, Hurd SS, Agusti AG, Jones PW, Vogelmeier C, Anzueto A, et al. Global strategy for the diagnosis, management, and prevention of chronic obstructive pulmonary disease: GOLD executive summary. Am J Respir Crit Care Med. 2013 Feb 15;187(4):347-65.

113. Barreiro E, Rabinovich R, Marin-Corral J, Barbera JA, Gea J, Roca J. Chronic endurance exercise induces quadriceps nitrosative stress in patients with severe COPD. Thorax. 2009 Jan;64(1):13-9.

114. Doucet M, Russell AP, Leger B, Debigare R, Joanisse DR, Caron MA, et al. Muscle atrophy and hypertrophy signaling in patients with chronic obstructive pulmonary disease. Am J Respir Crit Care Med. 2007 Aug 1;176(3):261-9.

115. Fermoselle C, Rabinovich R, Ausin P, Puig-Vilanova E, Coronell C, Sanchez F, et al. Does oxidative stress modulate limb muscle atrophy in severe COPD patients? Eur Respir J. 2012 Oct;40(4):851-62.

116. Miravitlles M, Soler-Cataluna JJ, Calle M, Molina J, Almagro P, Quintano JA, et al. Spanish COPD Guidelines (GesEPOC): pharmacological treatment of stable COPD. Spanish Society of Pulmonology and Thoracic Surgery. Arch Bronconeumol. 2012 Jul;48(7):247-57.

117. Jett JR, Schild SE, Kesler KA, Kalemkerian GP. Treatment of small cell lung cancer: Diagnosis and management of lung cancer, 3rd ed: American College of Chest Physicians evidence-based clinical practice guidelines. Chest. 2013 May;143(5 Suppl):e400S-19S.

118. Kozower BD, Larner JM, Detterbeck FC, Jones DR. Special treatment issues in non-small cell lung cancer: Diagnosis and management of lung cancer, 3rd ed: American College of Chest Physicians evidence-based clinical practice guidelines. Chest. 2013 May;143(5 Suppl):e369S-99S.

119. Coin A, Sergi G, Minicuci N, Giannini S, Barbiero E, Manzato E, et al. Fat-free mass and fat mass reference values by dual-energy X-ray absorptiometry (DEXA) in a 20-80 year-old Italian population. Clin Nutr. 2008 Feb;27(1):87-94.

120. Steiner MC, Barton RL, Singh SJ, Morgan MD. Bedside methods versus dual energy X-ray absorptiometry for body composition measurement in COPD. Eur Respir J. 2002 Apr;19(4):626-31.

121. Roca J, Burgos F, Barbera JA, Sunyer J, Rodriguez-Roisin R, Castellsague J, et al. Prediction equations for plethysmographic lung volumes. Respir Med. 1998 Mar;92(3):454-60.

122. Roca J, Rodriguez-Roisin R, Cobo E, Burgos F, Perez J, Clausen JL. Single-breath carbon monoxide diffusing capacity prediction equations from a Mediterranean population. Am Rev Respir Dis. 1990 Apr;141(4 Pt 1):1026-32.

123. Roca J, Sanchis J, Agusti-Vidal A, Segarra F, Navajas D, Rodriguez-Roisin R, et al. Spirometric reference values from a Mediterranean population. Bull Eur Physiopathol Respir. 1986 May-Jun;22(3):217-24.

124. Coronell C, Orozco-Levi M, Mendez R, Ramirez-Sarmiento A, Galdiz JB, Gea J. Relevance of assessing quadriceps endurance in patients with COPD. Eur Respir J. 2004 Jul;24(1):129-36.

125. Swallow EB, Reyes D, Hopkinson NS, Man WD, Porcher R, Cetti EJ, et al. Quadriceps strength predicts mortality in patients with moderate to severe chronic obstructive pulmonary disease. Thorax. 2007 Feb;62(2):115-20.

126. Fermoselle C, Sanchez F, Barreiro E. [Reduction of muscle mass mediated by myostatin in an experimental model of pulmonary emphysema]. Arch Bronconeumol. 2011 Dec;47(12):590-8.

127. Fagan JM, Ganguly M, Tiao G, Fischer JE, Hasselgren PO. Sepsis increases oxidatively damaged proteins in skeletal muscle. Arch Surg. 1996 Dec;131(12):1326-31; discussion 31-2.

128. Rodriguez DA, Kalko S, Puig-Vilanova E, Perez-Olabarria M, Falciani F, Gea J, et al. Muscle and blood redox status after exercise training in severe COPD patients. Free Radic Biol Med. 2012 Jan 1;52(1):88-94.

129. Macgowan NA, Evans KG, Road JD, Reid WD. Diaphragm injury in individuals with airflow obstruction. Am J Respir Crit Care Med. 2001 Jun;163(7):1654-9.

130. Orozco-Levi M, Gea J, Lloreta JL, Felez M, Minguella J, Serrano S, et al. Subcellular adaptation of the human diaphragm in chronic obstructive pulmonary disease. Eur Respir J. 1999 Feb;13(2):371-8.

131. Orozco-Levi M, Lloreta J, Minguella J, Serrano S, Broquetas JM, Gea J. Injury of the human diaphragm associated with exertion and chronic obstructive pulmonary disease. Am J Respir Crit Care Med. 2001 Nov 1;164(9):1734-9.

132. Couillard A, Maltais F, Saey D, Debigare R, Michaud A, Koechlin C, et al. Exercise-induced quadriceps oxidative stress and peripheral muscle dysfunction in patients with chronic obstructive pulmonary disease. Am J Respir Crit Care Med. 2003 Jun 15;167(12):1664-9.

133. Crul T, Testelmans D, Spruit MA, Troosters T, Gosselink R, Geeraerts I, et al. Gene expression profiling in vastus lateralis muscle during an acute exacerbation of COPD. Cell Physiol Biochem. 2010;25(4-5):491-500.

134. Koechlin C, Couillard A, Simar D, Cristol JP, Bellet H, Hayot M, et al. Does oxidative stress alter quadriceps endurance in chronic obstructive pulmonary disease? Am J Respir Crit Care Med. 2004 May 1;169(9):1022-7.

135. Levine S, Nguyen T, Taylor N, Friscia ME, Budak MT, Rothenberg P, et al. Rapid disuse atrophy of diaphragm fibers in mechanically ventilated humans. N Engl J Med. 2008 Mar 27;358(13):1327-35.

136. Ottenheijm CA, Heunks LM, Li YP, Jin B, Minnaard R, van Hees HW, et al. Activation of the ubiquitin-proteasome pathway in the diaphragm in chronic obstructive pulmonary disease. Am J Respir Crit Care Med. 2006 Nov 1;174(9):997-1002.

137. Ottenheijm CA, Lawlor MW, Stienen GJ, Granzier H, Beggs AH. Changes in cross-bridge cycling underlie muscle weakness in patients with tropomyosin 3-based myopathy. Hum Mol Genet. 2011 May 15;20(10):2015-25.

138. Plant PJ, Brooks D, Faughnan M, Bayley T, Bain J, Singer L, et al. Cellular markers of muscle atrophy in chronic obstructive pulmonary disease. Am J Respir Cell Mol Biol. 2010 Apr;42(4):461-71.

139. Testelmans D, Crul T, Maes K, Agten A, Crombach M, Decramer M, et al. Atrophy and hypertrophy signalling in the diaphragm of patients with COPD. Eur Respir J. 2010 Mar;35(3):549-56.

140. Vogiatzis I, Simoes DC, Stratakos G, Kourepini E, Terzis G, Manta P, et al. Effect of pulmonary rehabilitation on muscle remodelling in cachectic patients with COPD. Eur Respir J. 2010 Aug;36(2):301-10.

141. Rieger-Reyes C, Garcia-Tirado FJ, Rubio-Galan FJ, Marin-Trigo JM. Classification of Chronic Obstructive Pulmonary Disease Severity According to the New Global Initiative for Chronic Obstructive Lung Disease 2011 Guidelines: COPD Assessment Test Versus Modified Medical Research Council Scale. Arch Bronconeumol. 2013 Nov 20.

142. Livak KJ, Schmittgen TD. Analysis of relative gene expression data using real-time quantitative PCR and the 2(-Delta Delta C(T)) Method. Methods. 2001 Dec;25(4):402-8.

143. Barreiro E, Galdiz JB, Marinan M, Alvarez FJ, Hussain SN, Gea J. Respiratory loading intensity and diaphragm oxidative stress: N-acetyl-cysteine effects. J Appl Physiol (1985). 2006 Feb;100(2):555-63.

144. Hussain SN, Mofarrahi M, Sigala I, Kim HC, Vassilakopoulos T, Maltais F, et al. Mechanical ventilation-induced diaphragm disuse in humans triggers autophagy. Am J Respir Crit Care Med. 2010 Dec 1;182(11):1377-86.

145. Remels AH, Gosker HR, Langen RC, Schols AM. The mechanisms of cachexia underlying muscle dysfunction in COPD. J Appl Physiol (1985). 2013 May;114(9):1253-62.

146. Skillrud DM, Offord KP, Miller RD. Higher risk of lung cancer in chronic obstructive pulmonary disease. A prospective, matched, controlled study. Ann Intern Med. 1986 Oct;105(4):503-7.

147. Abal Arca J, Parente Lamelas I, Almazan Ortega R, Blanco Perez J, Toubes Navarro ME, Marcos Velazquez P. [Lung cancer and COPD: a common combination]. Arch Bronconeumol. 2009 Oct;45(10):502-7.

148. Barreiro E. [Chronic obstructive pulmonary disease and lung cancer]. Arch Bronconeumol. 2008 Aug;44(8):399-401.

149. Kuller LH, Ockene J, Meilahn E, Svendsen KH. Relation of forced expiratory volume in one second (FEV1) to lung cancer mortality in the Multiple Risk Factor Intervention Trial (MRFIT). Am J Epidemiol. 1990 Aug;132(2):265-74.

150. Mannino DM, Aguayo SM, Petty TL, Redd SC. Low lung function and incident lung cancer in the United States: data From the First National Health and Nutrition Examination Survey follow-up. Arch Intern Med. 2003 Jun 23;163(12):1475-80.

151. Nomura A, Stemmermann GN, Chyou PH, Marcus EB, Buist AS. Prospective study of pulmonary function and lung cancer. Am Rev Respir Dis. 1991 Aug;144(2):307-11.

152. Tockman MS, Anthonisen NR, Wright EC, Donithan MG. Airways obstruction and the risk for lung cancer. Ann Intern Med. 1987 Apr;106(4):512-8.

153. Cantin AM. Cellular response to cigarette smoke and oxidants: adapting to survive. Proc Am Thorac Soc. 2010 Nov;7(6):368-75.

154. Op den Kamp CM, Langen RC, Minnaard R, Kelders MC, Snepvangers FJ, Hesselink MK, et al. Pre-cachexia in patients with stages I-III non-small cell lung cancer: systemic inflammation and functional impairment without activation of skeletal muscle ubiquitin proteasome system. Lung Cancer. 2012 Apr;76(1):112-7.

155. Toth MJ, Miller MS, Callahan DM, Sweeny AP, Nunez I, Grunberg SM, et al. Molecular mechanisms underlying skeletal muscle weakness in human cancer: reduced myosin-actin cross-bridge formation and kinetics. J Appl Physiol (1985). 2013 Apr;114(7):858-68.

156. Man WD, Kemp P, Moxham J, Polkey MI. Skeletal muscle dysfunction in COPD: clinical and laboratory observations. Clin Sci (Lond). 2009 Oct;117(7):251-64.

157. Gagnon P, Lemire BB, Dube A, Saey D, Porlier A, Croteau M, et al. Preserved function and reduced angiogenesis potential of the quadriceps in patients with mild COPD. Respir Res. 2014;15:4.

158. Gosker HR, Kubat B, Schaart G, van der Vusse GJ, Wouters EF, Schols AM. Myopathological features in skeletal muscle of patients with chronic obstructive pulmonary disease. Eur Respir J. 2003 Aug;22(2):280-5.

159. Jobin J, Maltais F, Doyon JF, LeBlanc P, Simard PM, Simard AA, et al. Chronic obstructive pulmonary disease: capillarity and fiber-type characteristics of skeletal muscle. J Cardiopulm Rehabil. 1998 Nov-Dec;18(6):432-7.

160. Whittom F, Jobin J, Simard PM, Leblanc P, Simard C, Bernard S, et al. Histochemical and morphological characteristics of the vastus lateralis muscle in patients with chronic obstructive pulmonary disease. Med Sci Sports Exerc. 1998 Oct;30(10):1467-74.

161. Eliason G, Abdel-Halim S, Arvidsson B, Kadi F, Piehl-Aulin K. Physical performance and muscular characteristics in different stages of COPD. Scand J Med Sci Sports. 2009 Dec;19(6):865-70.

162. Kelsen SG, Ference M, Kapoor S. Effects of prolonged undernutrition on structure and function of the diaphragm. J Appl Physiol (1985). 1985 Apr;58(4):1354-9.

163. Danon MJ, Carpenter S. Myopathy with thick filament (myosin) loss following prolonged paralysis with vecuronium during steroid treatment. Muscle Nerve. 1991 Nov;14(11):1131-9.

164. Selcen D, Engel AG. Myofibrillar myopathies. Handb Clin Neurol. 2011;101:143-54.

165. Welvaart WN, Paul MA, van Hees HW, Stienen GJ, Niessen JW, de Man FS, et al. Diaphragm muscle fiber function and structure in humans with hemidiaphragm paralysis. Am J Physiol Lung Cell Mol Physiol. 2011 Aug;301(2):L228-35.

166. Levine S, Bashir MH, Clanton TL, Powers SK, Singhal S. COPD elicits remodeling of the diaphragm and vastus lateralis muscles in humans. J Appl Physiol (1985). 2013 May;114(9):1235-45.

167. Levine S, Kaiser L, Leferovich J, Tikunov B. Cellular adaptations in the diaphragm in chronic obstructive pulmonary disease. N Engl J Med. 1997 Dec 18;337(25):1799-806.

168. Polkey MI, Kyroussis D, Hamnegard CH, Mills GH, Green M, Moxham J. Diaphragm strength in chronic obstructive pulmonary disease. Am J Respir Crit Care Med. 1996 Nov;154(5):1310-7.

169. Fortunati N, Manti R, Birocco N, Pugliese M, Brignardello E, Ciuffreda L, et al. Pro-inflammatory cytokines and oxidative stress/antioxidant parameters characterize the bio-humoral profile of early cachexia in lung cancer patients. Oncol Rep. 2007 Dec;18(6):1521-7.

170. Argiles JM, Busquets S, Lopez-Soriano FJ. Anti-inflammatory therapies in cancer cachexia. Eur J Pharmacol. 2011 Sep;668 Suppl 1:S81-6.

171. Busquets S, Figueras MT, Fuster G, Almendro V, Moore-Carrasco R, Ametller E, et al. Anticachectic effects of formoterol: a drug for potential treatment of muscle wasting. Cancer Res. 2004 Sep 15;64(18):6725-31.

172. Argiles JM, Lopez-Soriano FJ. The ubiquitin-dependent proteolytic pathway in skeletal muscle: its role in pathological states. Trends Pharmacol Sci. 1996 Jun;17(6):223-6.

173. Costelli P, Muscaritoli M, Bossola M, Penna F, Reffo P, Bonetto A, et al. IGF-1 is downregulated in experimental cancer cachexia. Am J Physiol Regul Integr Comp Physiol. 2006 Sep;291(3):R674-83.

174. Cai D, Frantz JD, Tawa NE, Jr., Melendez PA, Oh BC, Lidov HG, et al. IKKbeta/NF-kappaB activation causes severe muscle wasting in mice. Cell. 2004 Oct 15;119(2):285-98.

175. Camps C, Iranzo V, Bremnes RM, Sirera R. Anorexia-Cachexia syndrome in cancer: implications of the ubiquitin-proteasome pathway. Support Care Cancer. 2006 Dec;14(12):1173-83.

176. Sandri M, Sandri C, Gilbert A, Skurk C, Calabria E, Picard A, et al. Foxo transcription factors induce the atrophy-related ubiquitin ligase atrogin-1 and cause skeletal muscle atrophy. Cell. 2004 Apr 30;117(3):399-412.

177. Sandri M, Lin J, Handschin C, Yang W, Arany ZP, Lecker SH, et al. PGC-1alpha protects skeletal muscle from atrophy by suppressing FoxO3 action and atrophy-specific gene transcription. Proc Natl Acad Sci U S A. 2006 Oct 31;103(44):16260-5.

178. Man WD, Natanek SA, Riddoch-Contreras J, Lewis A, Marsh GS, Kemp PR, et al. Quadriceps myostatin expression in COPD. Eur Respir J. 2010 Sep;36(3):686-8.

179. Perdiguero E, Sousa-Victor P, Ballestar E, Munoz-Canoves P. Epigenetic regulation of myogenesis. Epigenetics. 2009 Nov 16;4(8):541-50.

180. Nakajima N, Takahashi T, Kitamura R, Isodono K, Asada S, Ueyama T, et al. MicroRNA-1 facilitates skeletal myogenic differentiation without affecting osteoblastic

and adipogenic differentiation. Biochem Biophys Res Commun. 2006 Dec 1;350(4):1006-12.

181. McCarthy JJ, Esser KA. MicroRNA-1 and microRNA-133a expression are decreased during skeletal muscle hypertrophy. J Appl Physiol (1985). 2007 Jan;102(1):306-13.

182. Elia L, Contu R, Quintavalle M, Varrone F, Chimenti C, Russo MA, et al. Reciprocal regulation of microRNA-1 and insulin-like growth factor-1 signal transduction cascade in cardiac and skeletal muscle in physiological and pathological conditions. Circulation. 2009 Dec 8;120(23):2377-85.

183. Allen DL, Bandstra ER, Harrison BC, Thorng S, Stodieck LS, Kostenuik PJ, et al. Effects of spaceflight on murine skeletal muscle gene expression. J Appl Physiol (1985). 2009 Feb;106(2):582-95.

184. McCarthy JJ, Esser KA, Peterson CA, Dupont-Versteegden EE. Evidence of MyomiR network regulation of beta-myosin heavy chain gene expression during skeletal muscle atrophy. Physiol Genomics. 2009 Nov 6;39(3):219-26.

185. Sadoul K, Boyault C, Pabion M, Khochbin S. Regulation of protein turnover by acetyltransferases and deacetylases. Biochimie. 2008 Feb;90(2):306-12.

186. Chen LF, Greene WC. Regulation of distinct biological activities of the NF-kappaB transcription factor complex by acetylation. J Mol Med (Berl). 2003 Sep;81(9):549-57.

187. Potthoff MJ, Wu H, Arnold MA, Shelton JM, Backs J, McAnally J, et al. Histone deacetylase degradation and MEF2 activation promote the formation of slow-twitch myofibers. J Clin Invest. 2007 Sep;117(9):2459-67.

188. Andreou AM, Tavernarakis N. SUMOylation and cell signalling. Biotechnol J. 2009 Dec;4(12):1740-52.

189. Bischof O, Dejean A. SUMO is growing senescent. Cell Cycle. 2007 Mar 15;6(6):677-81.

190. Bischof O, Schwamborn K, Martin N, Werner A, Sustmann C, Grosschedl R, et al. The E3 SUMO ligase PIASy is a regulator of cellular senescence and apoptosis. Mol Cell. 2006 Jun 23;22(6):783-94.

191. Kudryashova E, Kramerova I, Spencer MJ. Satellite cell senescence underlies myopathy in a mouse model of limb-girdle muscular dystrophy 2H. J Clin Invest. 2012 May 1;122(5):1764-76.

192. Angulo M, Lecuona E, Sznajder JI. Role of MicroRNAs in lung disease. Arch Bronconeumol. 2012 Sep;48(9):325-30.

193. Roca-Ferrer J, Pujols L, Agusti C, Xaubet A, Mullol J, Gimferrer JM, et al. [Cyclooxigenase-2 levels are increased in the lung tissue and bronchial tumors of patients with chronic obstructive pulmonary disease]. Arch Bronconeumol. 2011 Dec;47(12):584-9.

194. Ruano-Ravina A, Perez Rios M, Fernandez-Villar A. Lung cancer screening with low-dose computed tomography after the National Lung Screening Trial. The debate is still open. Arch Bronconeumol. 2013 Apr;49(4):158-65.

195. van den Borst B, Slot IG, Hellwig VA, Vosse BA, Kelders MC, Barreiro E, et al. Loss of quadriceps muscle oxidative phenotype and decreased endurance in patients with mild-to-moderate COPD. J Appl Physiol (1985). 2013 May;114(9):1319-28.

196. Gosker HR, Zeegers MP, Wouters EF, Schols AM. Muscle fibre type shifting in the vastus lateralis of patients with COPD is associated with disease severity: a systematic review and meta-analysis. Thorax. 2007 Nov;62(11):944-9.

197. Slot IG, van den Borst B, Hellwig VA, Barreiro E, Schols AM, Gosker HR. The muscle oxidative regulatory response to acute exercise is not impaired in less advanced COPD despite a decreased oxidative phenotype. PLoS One. 2014;9(2):e90150.